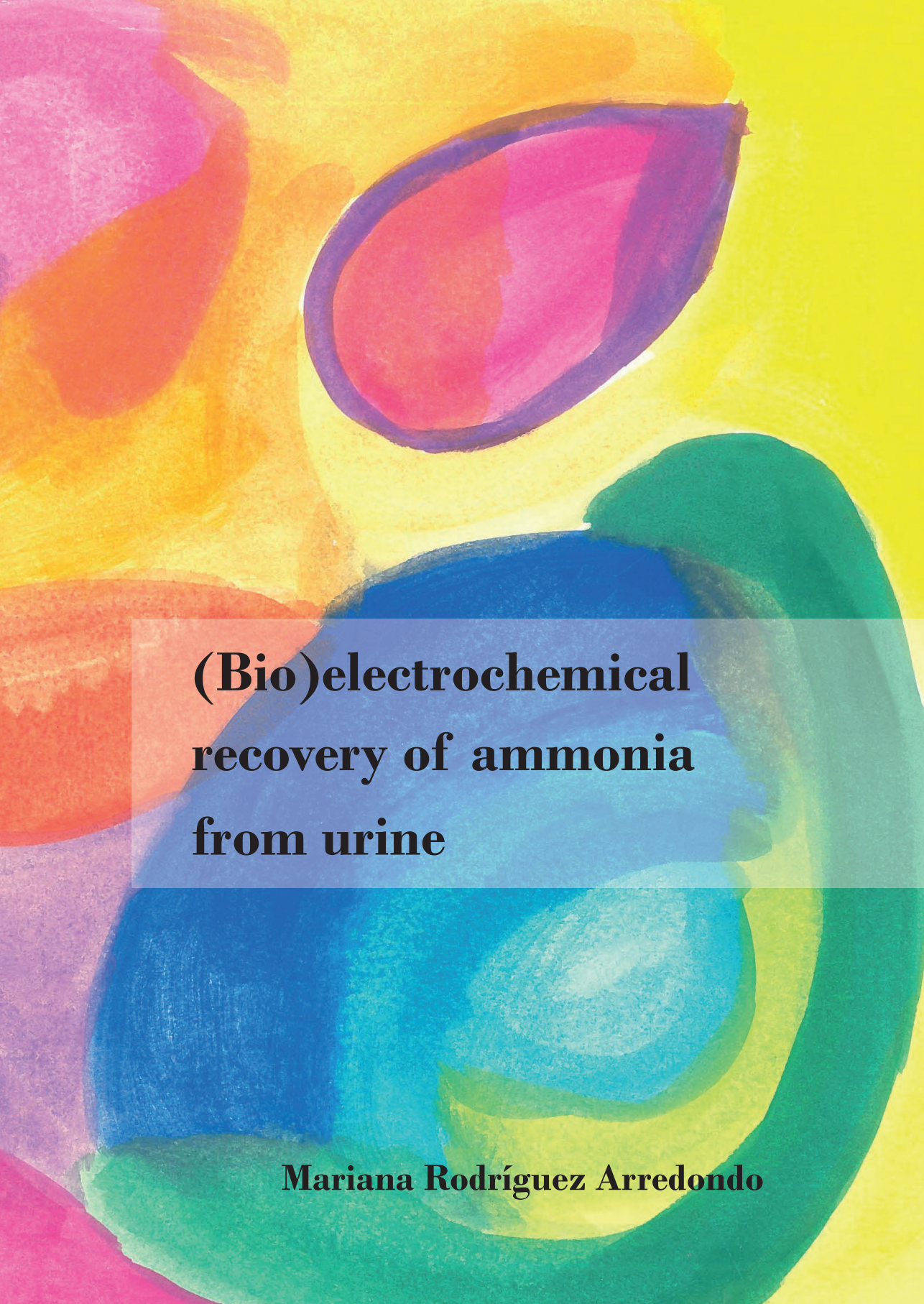

(Bio)electrochemical recovery of ammonia from urine

Mariana Rodríguez Arredondo

(Bio)electrochemical recovery of ammonia from urine

Mariana Rodríguez Arredondo

Thesis committee

Promotor
Prof. Dr C.J.N. Buisman
Professor of Biological Recovery and Reuse Technology
Wageningen University & Research

Co-promotors
Dr A. ter Heijne
Assistant professor, Environmental Technology
Wageningen University & Research

Dr P. Kuntke
Scientific project manager
Wetsus- European Centre of Excellence for Sustainable Water Technology, Leeuwarden

Other members
Prof. Dr J. van der Gucht, Wageningen University & Research
Prof. Dr M. Alves, University of Minho, Portugal
Dr J. Kretzschmar, German Biomass Research Center (DBFZ), Germany
Dr P. van den Brink, Evides Industriewater, Rotterdam

This research was conducted under the auspices of the Graduate School for Socio-Economic and Natural Sciences of the Environment (SENSE)

(Bio)electrochemical recovery of ammonia from urine

Mariana Rodríguez Arredondo

Thesis

submitted in fulfilment of the requirements for the degree of doctor
at Wageningen University
by the authority of the Rector Magnificus,
Prof. Dr A.P.J. Mol,
in the presence of the
Thesis Committee appointed by the Academic Board
to be defended in public
on Friday 4 October 2019
at 3:30 p.m. in De Kanselarij, Leeuwarden.

Mariana Rodríguez Arredondo
(Bio)electrochemical recovery of ammonia from urine
172 pages.

PhD thesis, Wageningen University, Wageningen, The Netherlands (2019)
With references, with summary in English

ISBN 978-94-6395-076-3
DOI https://doi.org/10.18174/497889

A mis padres

Table of contents

CHAPTER 1.	**General introduction**	**9**
1.1	Ammonia production: drawbacks and environmental impact	10
1.2	Ammonia removal from wastewater	13
1.3	We need to look for alternatives: Recovery instead of removal	14
1.4	(Bio)electrochemical systems: A novel alternative for the recovery of ammonia	17
1.5	Aim and thesis outline	27
CHAPTER 2.	**Bioelectrochemical systems for nitrogen removal and recovery from wastewater**	**31**
2.1	Introduction	32
2.2	The influence of humans on the nitrogen cycle: Biological, chemical, and physical processes	33
2.3	Bioelectrochemical systems for ammonium removal and recovery	37
2.4	Ammonia recovery from urine in an MFC and MEC	43
2.5	Economic analysis for ammonia recovery from urine in an MFC and MEC	47
2.6	Challenges in bioelectrochemical systems for nitrogen recovery	50
CHAPTER 3.	**Load ratio determines the ammonia recovery and energy input of an electrochemical system**	**55**
3.1	Introduction	56
3.2	Materials and methods	58
3.3	Results and discussion	63
3.4.	Conclusions	71
3.5	Supporting information	73
CHAPTER 4.	**Hydrogen gas recycling for energy efficient ammonia recovery in electrochemical systems**	**81**
4.1	Introduction	82
4.2	Materials and methods	84
4.3	Results and discussion	87
4.4	Implication	92
4.5	Supporting information	94

CHAPTER 5. The concept of load ratio applied to bioelectrochemical systems for ammonia recovery **103**
5.1 Introduction 104
5.2 Materials and methods 106
5.3 Results and discussion 110
5.4 Supporting information 118

CHAPTER 6. General discussion and future perspectives **125**
6.1 TAN recovery in (B)ES: State-of-the-art and limitations of the load ratio concept 126
6.2 Urine in (B)ES: opportunities and obstacles 134
6.3 Future perspectives and recommendations 143

References 146
Summary 160
List of publications 163
Acknowledgements 164

CHAPTER 1

General introduction

This thesis describes the use of (bio)electrochemical systems to recover ammonia from nitrogen-rich wastewaters, with a focus on urine. The aim of this thesis is to improve the understanding on the transport of total ammonia nitrogen (TAN; the sum of NH_3 and NH_4^+), as well as to optimize the TAN removal and recovery in (bio)electrochemical systems.

In this introduction, we first show the impact that the industrial production of ammonia has had on the nitrogen cycle, and briefly discuss how nitrogen is removed in wastewater treatment plants (WWTPs). Later, we explain the need for technologies that focus on recovering (instead of removing) ammonia from wastewaters, in order to close the nitrogen cycle in a sustainable way. Next, we propose the use of (bio)electrochemical systems for TAN recovery from nitrogen-rich wastewaters and explain the basic concepts to describe their performance. Afterwards, we focus on the recovery of TAN from urine by means of (bio)electrochemical systems and its challenges. Finally, we describe the thesis outline.

Context

The threats of water scarcity, climate change and depletion of non-renewable resources (such as fossil fuels) are linked to the impact of anthropogenic activities brought about by the rapid growth in human population over the last century. The rapid growth in human population has resulted in an increased demand for resources such as water and food. The widespread application of synthetically produced fertilizers has allowed to sustain the growing demand for food. However, the production and use of synthetic nitrogen fertilizers results in not only a significant use of energy in the form of fossil fuels, but also in soil degradation and the pollution of air, groundwater and surface water.

1.1 Ammonia production: drawbacks and environmental impact

Nitrogen, an essential element for all living organisms, is made available to plants by converting inert atmospheric nitrogen (N_2) to more reactive forms, such as ammonia (NH_3) or nitrate (NO_3^-). This process is called nitrogen fixation and can be carried out naturally or artificially. Natural, biological nitrogen fixation takes place when atmospheric N_2 is reduced to NH_3 by certain prokaryotes (i.e. diazotrophs) via nitrogenase, an enzyme complex [1, 2]. Artificial nitrogen fixation, on the other hand, occurs mostly via the Haber-Bosch process.

The invention of the Haber-Bosch process was a collaboration between Fritz Haber and Carl Bosch. Fritz Haber successfully synthesized ammonia from N_2 and hydrogen (H_2) in 1908, and only four years later, his laboratory setup had been upscaled to an industrial level by Carl Bosch [3, 4].

Around 80% of the ammonia produced globally by the Haber-Bosch process is used for the production of synthetic nitrogen fertilizers [4–6]. The role of the Haber-Bosch process in our modern agriculture is so crucial that, by 2008, almost half of the world's population was sustained by food produced with synthetic nitrogen fertilizers [3].

The production of ammonia via the Haber-Bosch process is energetically very demanding: it consumes 1-2% of the global energy supply [3, 6–9] and accounts for 3-5% of the global natural gas consumption [10]. N_2 is widely available in the atmosphere, where it accounts for 78% of all gases, but it is inert and very stable due to the strong triple bond shared by the two nitrogen atoms [9, 11, 12]. The nitrogen bond needs to be split up in order to reduce N_2 to bioavailable NH_3, which requires a catalyst, high temperatures and pressures (α-iron or ruthenium catalyst, 350–550 °C, 150–350 atm [13]). Furthermore, the H_2 used in the Haber-Bosch process is mostly obtained from fossil fuels (mainly natural gas (72%) and coal (22%) [6]), which makes the process energy-intensive and results in emissions of large amounts of CO_2. In the Netherlands, for example, the CO_2 emissions from ammonia production account for 2% of all greenhouse gas emissions [14].

Even though the Haber-Bosch process has been optimized by using novel catalysts [11] or hydrogen produced by more sustainable processes (such as by water electrolysis [7]), its use of fossil fuels is currently the most economical and mature option [6, 15].

Consequences of our intervention on the nitrogen cycle

The introduction of the Haber-Bosch process significantly increased the amount of biologically available nitrogen on Earth, causing an imbalance in the nitrogen cycle (Figure 1.1). Nowadays, over half of the nitrogen received by the world's crops comes from synthetic nitrogen fertilizers, so the amount of global nitrogen fixation has doubled [4]. This has led to an accumulation of reactive nitrogen in natural ecosystems, resulting in severe environmental consequences.

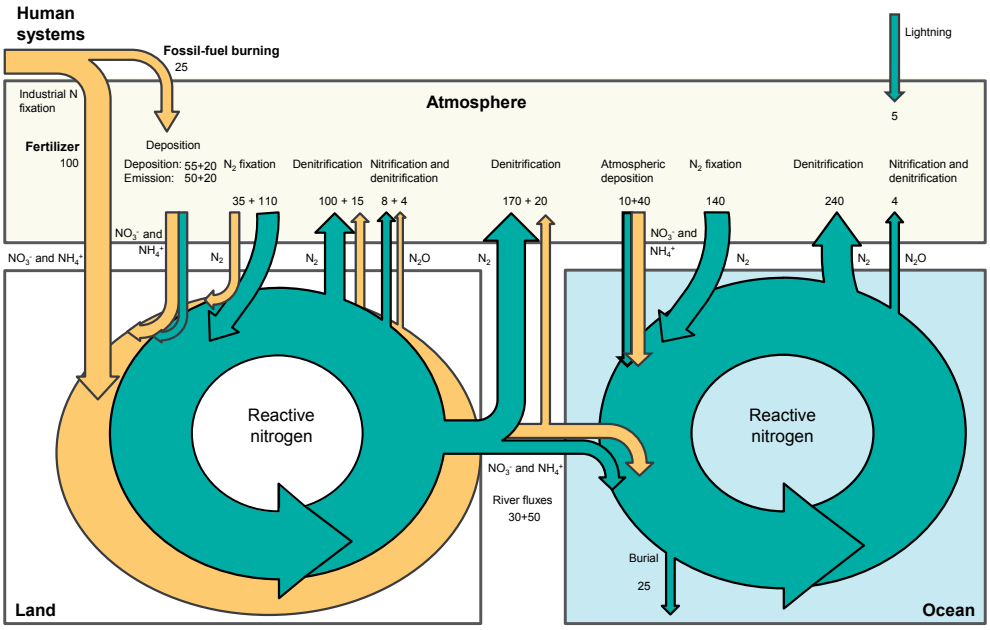

Figure 1.1. Representation of the global nitrogen cycle. Green arrows depict natural fluxes and yellow arrows the anthropogenic disturbances. The major processes in which inert N_2 is transformed to reactive nitrogen forms (NO_3^-, NH_4^+, N_2O), and vice versa, are shown. Values are presented in Mt N per year and are based on estimations with data from the 1990s; many of the values have uncertainties of ±50% and larger. Adapted from [16].

A big proportion of the nitrogen applied globally on the field (50- 70%) is lost to the environment via volatilization, denitrification, leaching, and runoff [4, 17, 18]. These losses result in soil acidification and the pollution of air (via ammonia volatilization and nitrous oxide (N_2O) gas emissions) groundwater and surface water [4, 17, 19].

Runoff from the agricultural field can cause eutrophication in surface water bodies. Eutrophication is caused by an excessive growth of aquatic plants and algae due to a high concentration of nutrients (mainly nitrogen and phosphorous) in the water. The excessive growth of aquatic plants and algae can result in oxygen depletion, triggering the loss of biodiversity (such as the extinction of fish species and the death of coral reefs) and the emergence of harmful algal blooms which pose risks to human health [20, 21].

1.2 Ammonia removal from wastewater

1.2.1 Why do we need to remove it?

Apart from volatilization, denitrification, leaching, and runoff from agriculture, nitrogen also ends up in the environment via the discharge of wastewater. As plants are consumed by animals and humans, some of the nitrogen used to fertilize them ends up in animal and human excreta, which can be partly found in sewage. Estimations show that, on average, 15-30% of the nitrogen from fertilizers applied in agriculture ends up in wastewater [22, 23]. Nitrogen from wastewater can enter surface waters by means of sewer overflows, discharge of untreated sewage, or effluent from wastewater treatment plants (WWTPs). In order to decrease the risk of eutrophication of receiving water bodies, it is of crucial importance to remove nitrogen from wastewater.

1.2.2 The drawbacks of current technologies for the removal of ammonia from wastewater

From the total nitrogen entering surface waters in the Netherlands in 2004, around 13% (14 401 tonnes N) came from the effluent of wastewater treatment plants [24, 25]. In the European Union, nitrogen in wastewater needs to be removed down to a concentration of 10-15 mg N L^{-1} (depending on the capacity of the WWTP) before discharge into water bodies sensitive to eutrophication [26]. There are several ways to remove N from wastewater (see Chapter 2 of this thesis), but most conventional WWTPs remove it by subsequent biological nitrification and denitrification [27].

The nitrification/denitrification process can remove nitrogen to low concentrations, but it has four disadvantages: 1) ammonia is converted back to N_2, so it cannot be directly reused; 2) it is energy-intensive; 3) produces large amounts of sludge; and 4) it results in N_2O emissions.

The nitrification/denitrification process is one of the most energy-intensive processes for wastewater treatment plants because it requires aeration for the nitrification step (to oxidize ammonia to nitrate by *Nitrosomonas* and *Nitrobacter*) and a carbon source for the denitrification step (to reduce nitrate to N_2 by a variety of denitrifiers) [28–30]. Most of the energy consumed in wastewater treatment plants is used for aeration, accounting for 45 to 75% of the total energy demand [28–33]. Furthermore, the aerobic treatment of wastewater results in the production of large amounts of sludge [34], and its handling and disposal is another costly aspect for WWTPs [35].

Another drawback of the nitrification/denitrification process is that nitrous oxide can be formed in both the nitrification and denitrification steps. The N_2O emissions from wastewater treatment plants are not considered as high compared to the total emissions

(they represent about 3% of the anthropogenic N_2O emissions [36]). However, the greenhouse gas potential of N_2O is 300 times that of CO_2 [37], which is why its contribution to the total greenhouse gas footprint of WWTPs (expressed on CO_2 equivalents) can be as high as 78% [31].

Alternative N removal technologies have been developed to reduce the energy use and operational costs of the conventional nitrification/denitrification process, such as SHARON/Anammox (see Chapter 2). These technologies, however, still rely on converting usable, reactive forms of nitrogen back to nitrogen gas. Therefore, to reuse the ammonia in wastewater, two steps would be needed: 1) the removal of ammonia as N_2, and 2) the reduction of N_2 back to NH_3 via the Haber-Bosch process.

To summarize, both the conventional processes to produce NH_3 and remove TAN from wastewaters result in:

a) Heavy use of non-renewable energy in the form of fossil fuels
b) Significant operational costs to WWTPs
c) Pollution in the form of greenhouse gas emissions (CO_2 and N_2O)
d) Low resource efficiency, as much of the produced reactive nitrogen is re-processed to N_2 instead of recovered and recycled

1.3 We need to look for alternatives: Recovery instead of removal

1.3.1 Why to recover ammonia instead of removing it?

Recovering TAN directly from wastewater would create a shortcut in the nitrogen cycle, while energy and resources would be saved by circumventing the conversion of NH_3 to N_2 and then back to NH_3. Therefore, this would result in reduced energy consumption and greenhouse gas emissions associated with both its production and removal processes. In the Netherlands, for example, around 16% of the synthetic nitrogen fertilizer production could be replaced if all the nitrogen entering WWTPs would be recovered [38].

The recovery of TAN is energetically more efficient when treating nitrogen-rich wastewater streams with concentrations higher than 1 g TAN L^{-1} [15, 38], as in the case of urine [39], municipal digestate [40], reject water from the anaerobic digestion of sludge [41–43], dairy manure [44], pig slurry [45–49] and landfill leachate [50].

1.3.2 Current technologies for ammonia recovery

Several techniques have been developed to recover ammonia from nitrogen-rich wastewaters (Figure 1.2). While they can be separated in physico-chemical and electrochemical, some of them overlap, such as electrodialysis and capacitive deionization.

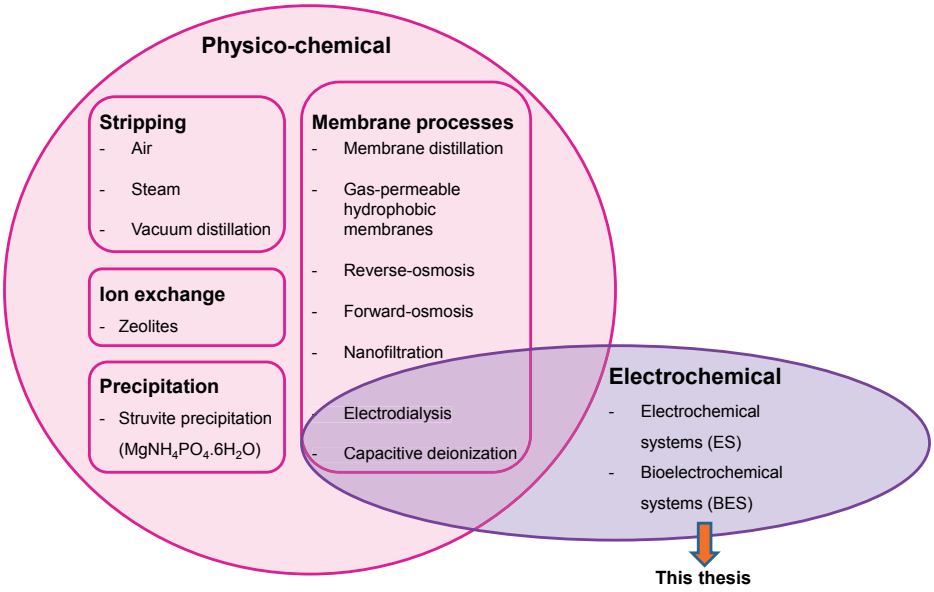

Figure 1.2. Different techniques for the recovery of TAN from nitrogen-rich wastewater streams (based on [38, 51]). The recovery by nitrogen incorporation into biomass (such as microalgae cultivation) has been excluded in this overview. This thesis involves the use of electrochemical and bioelectrochemical systems.

Currently, many of these techniques require high inputs of energy and chemicals to achieve high TAN recovery efficiencies, and some of them produce a low-purity product [39, 52]. Membrane processes such as reverse osmosis, nanofiltration, electrodialysis, or capacitive deionization, for example, mainly concentrate or reduce the volume of the wastewater stream, so that another process such as air stripping is needed to obtain a purer product [49, 53–55]. Furthermore, they require a solution with a low pH to keep the TAN as ammonium (NH_4^+) and prevent volatilization of NH_3. Ion-exchange processes such as the use of zeolites to recover NH_4^+ also require a pH between 6 and 7 to perform optimally [56], as well as brine or caustics for the regeneration of the zeolite, and an additional step to recover TAN from them. Zeolites could also be used directly as soil conditioner after NH_4^+ adsorption, but their adsorption is not selective for NH_4^+ [57].

From the techniques in Figure 1.2, stripping and struvite precipitation are the most established and applied on larger scales [38]. Recovering nitrogen by stripping or struvite precipitation results in a liquid solution of ammonium salts (e.g. $(NH_4)_2SO_4$, NH_4NO_3) or a phosphate mineral (magnesium ammonium phosphate, or MAP), respectively. Both can be used as fertilizers [58]. Due to the high solubility of ammonia, stripping requires the application of heat, aeration or vacuum, and caustics to raise the pH of the wastewater to > 9.3 [58, 59], which results in a relatively high energy consumption (Table 1.1). To recover

TAN from wastewater by struvite precipitation, addition of caustics (for pH adjustment), magnesium salts and phosphate (to achieve an equimolar ratio of Mg^{2+}:NH_4^+:PO_4^{3-}), might be needed [60]. Urine, for example, contains much more nitrogen than phosphorous and magnesium: by adding magnesium all the phosphate can be recovered, but this would only result in a TAN recovery of around 3% [39]. Therefore, a considerable addition of phosphate, a finite resource, would be needed to fully recover the nitrogen from urine by MAP precipitation. For this reason, struvite precipitation is better suited for the recovery of phosphorous than for recovery of nitrogen.

TAN chemistry

Ammonium (NH_4^+) and ammonia (NH_3) are a weak acid and weak base, respectively. Their equilibrium is defined by the following equation:

$$NH_4^+ \leftrightharpoons NH_3\,(g) + H^+ \qquad \text{Equation 1.1}$$

The equilibrium is dependent on pH and temperature. In dilute aqueous solutions and at standard temperature (298.15 K), the acid dissociation constant of NH_4^+ is 5.6 E-10, so its pKa is 9.25. This means that both nitrogen species will have the same molar concentration at pH 9.25. A pH lower than 9.25 results in a higher concentration of NH_4^+, while a pH higher than 9.25 will result in a higher concentration of NH_3. At the same time, higher temperatures shift the equilibrium towards NH_3, while lower temperatures shift the equilibrium towards NH_4^+. When trying to recover TAN as a gas, in the form of NH_3, higher pH and temperatures are favorable.

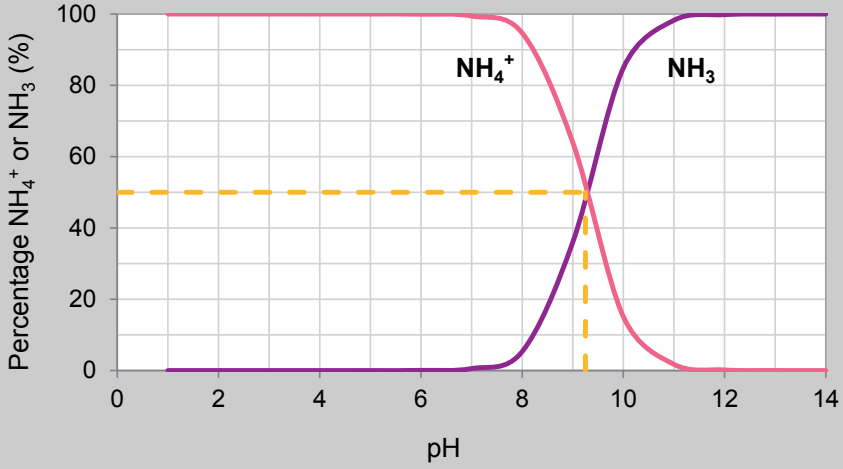

Table 1.1. Energy requirements* of conventional processes for the production, removal or recovery of TAN (based on [58])

	MJ kg_N^{-1}	kWh kg_N^{-1}
Ammonia production		
Haber-Bosch[1]	37-45	10-13
Ammonia removal		
Nitrification/denitrification[2]	14-87	4-24
SHARON/Anammox	5-6	1-2
Ammonia recovery		
Nitrification/denitrification + Haber-Bosch	51-132	14-37
SHARON/Anammox + Haber-Bosch	42-51	12-14
Stripping (air)	32	9
Struvite precipitation[3]	81	23

* Energy demand for the production of necessary chemicals (such as H_2SO_4, NaOH, CaO, etc.) is taken into account.

[1] Values based on best available technologies from natural gas (lower value) and coal (higher value)

[2] Lower value is calculated without additional carbon source, higher value with methanol as carbon source

[3] Struvite precipitation taking into account addition of magnesium salts and phosphate to recover all nitrogen from urine (no pH adjustment).

Both stripping and struvite precipitation values from Table 1.1 are based on the recovery of ammonia from urine [58]. However, other nitrogen-rich streams, such as reject water from a municipal WWTP, have similar requirements [38].

The use of electrochemical systems (ES) and bioelectrochemical systems (BES) for the recovery of TAN from wastewaters has been investigated over the past few years [40, 43, 61, 62]. These systems have been proposed as a sustainable alternative to conventional processes because they have the potential to recover energy from wastewaters while recovering TAN.

In this thesis, we explore the use of (B)ES for the recovery of ammonia from nitrogen-rich wastewaters, with a focus on urine.

1.4 (Bio)electrochemical systems: A novel alternative for the recovery of ammonia

(Bio)electrochemical systems ((B)ESs) are technologies that make use of electrodes where oxidation and reduction reactions take place. In BESs, reactions at one or both electrodes are catalyzed by electrochemically active microorganisms, while in ESs purely electrochemical reactions take place, usually catalyzed by noble metal electrodes. During

the last decades BESs have gained attention for their potential to recover energy and/or valuable products from wastewaters: energy in the form of electricity [63], fuels and chemicals such as hydrogen, acetic acid, and methane [35, 64, 65], and resources that would otherwise be regarded as pollutants, such as heavy metals and nutrients [66, 67]. ESs have also gained increased attention due to their ability to degrade a wide range of contaminants at ambient temperature and pressure, their modular design and their small footprint [68].

Depending on their configuration, these systems can remove or recover nitrogen (an overview of the nitrogen removal and recovery mechanisms in BES can be found in Chapter 2). The focus of this thesis is the recovery and not the removal of TAN using (B)ESs.

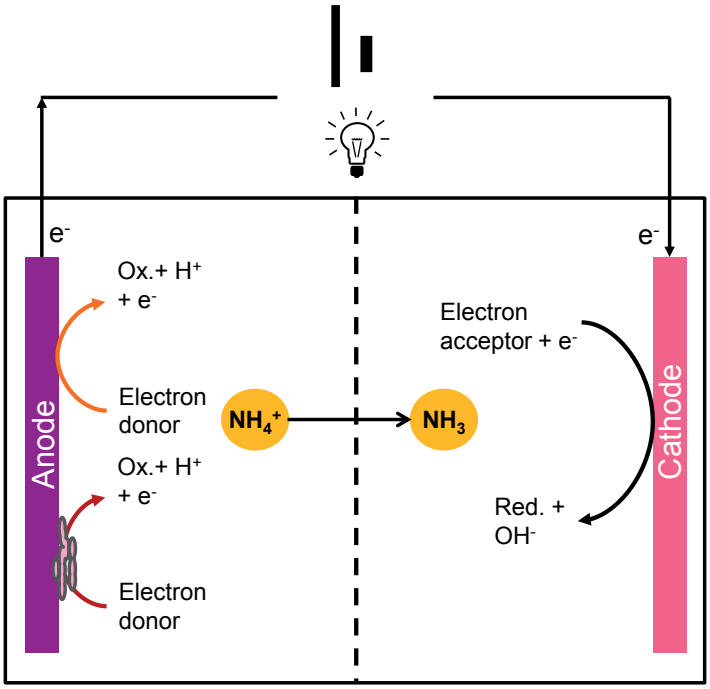

Figure 1.3. Schematic view of (bio)electrochemical systems for TAN recovery. In a bioelectrochemical system, the anode oxidation is catalyzed by microorganisms (red arrow). In an electrochemical system (orange arrow) the oxidation is usually catalyzed by noble metal electrodes. The electric current induces NH_4^+ (and other positively charged ions, such as Na^+ and K^+) migration from the anode to the cathode compartment through a cation exchange membrane, to maintain charge neutrality. (B)ESs for TAN recovery can generate electricity (light bulb) or require energy input to drive the reactions (external power source).

Figure 1.3 shows a typical (B)ES for TAN recovery, with the anode and cathode compartments separated by a cation exchange membrane (CEM). In (B)ESs two half-reactions take place:

an oxidation reaction (at the anode) and a reduction reaction (at the cathode). During oxidation, an electron donor is oxidized and electrons are transferred to the anode, which is connected to the cathode via an external circuit. While electrons flow from anode to cathode, positively charged ions (such as NH_4^+, Na^+, and K^+) migrate from the anode to the cathode compartment through a membrane, to maintain charge neutrality. Once at the cathode, the electrons reduce an electron acceptor.

The advantage of TAN recovery by (B)ESs compared to the conventional methods for TAN recovery is that the electrical current allows for 1) the concentration of TAN at the cathode and 2) the production of caustics at the cathode, which means that TAN is converted to NH_3 in situ. (B)ESs can then be coupled with conventional recovery methods, such as stripping, without the need for caustics addition [54, 69].

Classification of (B)ESs for the recovery of TAN

(B)ESs for TAN recovery can be classified based on their catalyst type (biotic/abiotic) and energy balance (power input/output), as shown in Figure 1.4. Electrolysis cells (ECs) and microbial electrolysis cells (MECs) require power input (energy needs to be invested to drive a non-spontaneous reaction), whereas fuel cells (FCs) and microbial fuel cells (MFCs) generate electricity (energy is harvested).

Bioelectrochemical systems (i.e. MFCs and MECs) are seen as a sustainable, attractive technology because the microorganisms involved are self-regenerating, and using them as catalysts allows for the use of non-noble, inexpensive electrodes and the operation of the system at mild conditions (neutral pH, mesophilic temperatures and ambient pressure) [67, 70]. One of the advantages of BESs is that they can produce renewable energy or chemicals from organic waste materials. At the anode, microorganisms usually catalyze the oxidation of an organic substrate (the electron donor, often represented as acetate) to bicarbonate, protons, and electrons (Table 1.2, reaction 1). Therefore, these systems depend on organic matter for current production.

Electrochemical systems (i.e. ECs and FCs) commonly make use of noble metal electrodes to catalyze both reactions at the electrodes, although the use of non-noble metal electrodes for wastewater treatment has been increasingly reported over the recent years [68, 71]. At the anode, usually inorganic substrates, such as water or hydrogen (Table 1.2, reactions 2 and 3), are oxidized. These systems are seen as more stable and predictable than BESs because they do not rely on microorganisms, which are more sensitive to changes in pH and loading rates. Electrochemical systems for the recovery of TAN usually require a higher energy input compared to BESs, because they oxidize water instead of organic matter (Table 1.2).

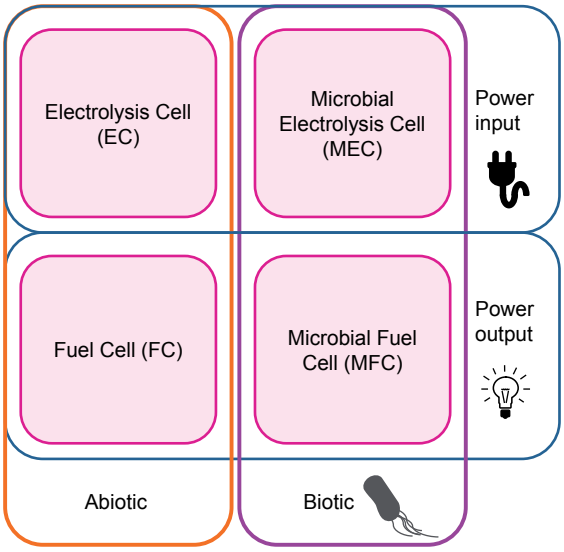

Figure 1.4. Classification of (bio)electrochemical systems used for the recovery of TAN (based on [62]).

Table 1.2. Standard (E^0) and conditional (E) electrode potentials for the typical oxidation and reduction reactions occurring in (B)ESs for the recovery of TAN, as well as the thermodynamic cell voltage (E_{cell}) for the complete reaction in each system. All potentials are reported versus normal hydrogen electrode (NHE). The conditional potentials were calculated using the Nernst equation assuming a temperature of 298.15 K, a partial pressure of 1 atm for H_2 and O_2, pH of 7 and acetate and bicarbonate concentrations of 0.005 M (based on [62, 63])

Anode oxidation reaction			**E^0 (V)**	**E_{anode} (V)**
(1)	Acetate oxidation	$CH_3COO^- + 4H_2O \rightarrow 2CHO^-_3 + 9H^+ + 8e^-$	0.187	-0.296
(2)	Oxygen evolution	$2H_2O \rightarrow O_2 + 4H^+ + 4e^-$	1.229	0.815
(3)	Hydrogen oxidation	$H_2 \rightarrow 2H^+ + 2e^-$	0.000	-0.414
Cathode reduction reaction			**E^0 (V)**	**$E_{cathode}$ (V)**
(4)	Oxygen reduction	$O_2 + 4e^- + 2H_2O \rightarrow 4OH^-$	0.401	0.815
(5)	Hydrogen evolution	$2H_2O + 2e^- \rightarrow H_2 + 2OH^-$	-0.828	-0.414

System	**Reactions involved**	**E_{cell} ($E_{cathode}$-E_{anode}) (V)**
MFC	(1) + (4)	1.111
MEC	(1) + (5)	-0.118
EC	(2) + (5)	-1.229
EC	(3) + (5)	0.000

Whether a (B)ES will generate electricity (MFC) or require energy input (MEC and EC) depends on the combination of the oxidation and reduction reactions occurring in it, which are shown in Table 1.2.

Thermodynamic aspects of the (B)ES for ammonia recovery

The theoretical energy input or output of a (B)ES is determined by the difference between the electrode potentials. In Table 1.2 typical oxidation and reduction reactions used in (B) ESs for the recovery of TAN are shown together with their standard (E^0) and conditional (E) electrode potentials.

The electrode potentials can be calculated from the Gibbs free energy of the reaction. The Gibbs free energy of a reaction (represented by Eq. 1.2) in a dilute system, such as in (B)ESs, can be calculated according to Eq. 1.3

$$v_A A + v_B B \rightarrow v_C C + v_D D \qquad \text{Equation 1.2}$$

$$\Delta G = \Delta G^0 + RTln \left\{ \frac{[C]^{v_C} [D]^{v_D}}{[A]^{v_A} [B]^{v_B}} \right\} \qquad \text{Equation 1.3}$$

where ΔG (J) is the Gibbs free energy of the reaction at specified conditions, ΔG^0 (J) is the Gibbs free energy of the reaction at standard conditions (298 K, 1 atm of 1 M for all species in the reaction), R is the universal gas constant (8.314 J mol^{-1} K^{-1}), T is the temperature (K), [i] is the concentration in mol L^{-1} of species i and v_i is the stoichiometric coefficient of species i. In the case of electrochemical half reactions, the reaction needs to be written as a reduction reaction. A negative Gibbs free energy means that the reaction occurs spontaneously, while a positive Gibbs free energy means that energy needs to be applied for the reaction to occur.

The electrode potential for the anodic and cathodic reactions in a (B)ES is related to the Gibbs free energy according to

$$E = - \frac{\Delta G}{nF} \qquad \text{Equation 1.4}$$

Where n is the number of mole electrons (mol e-) transferred in the reaction, F is the Faraday constant (96485 C mole e^{-1}) and E (V) the electrode potential at which the reaction occurs. Combining equations 1.3 and 1.4 leads to the Nernst equation (Eq. 1.5), which is used to calculate the electrode potentials of the reactions occurring in a (B)ES.

$$E = E^0 - \frac{RT}{nF} \ln \left\{ \frac{[C]^{\nu_C} [D]^{\nu_D}}{[A]^{\nu_A} [B]^{\nu_B}} \right\}$$ Equation 1.5

The conditional electrode potential for the oxidation of acetate, for example (Table 1.2, reaction 1), is calculated as follows:

$$E_{anode} = E^0_{anode} - \frac{RT}{nF} \ln \left\{ \frac{[CH_3 COO^-]^1}{[HCO_3^-]^2 [H^+]^9} \right\}$$

$$E_{anode} = 0.187 - \frac{8.314*298.15}{8*96485} \ln \left\{ \frac{[0.005]^1}{[0.005]^2 [10^{-7}]^9} \right\} = -0.296 \text{ V}$$

The difference between the cathode and anode electrode potentials is known as the thermodynamic cell voltage or electromotive force (E_{cell}, V). In an MFC, E_{cell} shows us the theoretical maximum output voltage, whereas in an MEC or an EC it shows us the minimum voltage that is required to drive the reactions. E_{cell} can be calculated from the potential of the reduction reaction at the cathode ($E_{cathode}$, V) and the potential of the oxidation reaction at the anode (E_{anode}, V) according to

$$E_{cell} = E_{cathode} - E_{anode}$$ Equation 1.6

A positive cell voltage indicates that the reaction occurs spontaneously (energy can be harvested), and a negative cell voltage indicates that energy needs to be invested for the reaction to proceed. For acetate oxidation combined with hydrogen evolution (an MEC), for example, the difference is -0.118 V (Table 1.2, MEC). The minus sign means that energy needs to be invested, and this is because the energy content of acetate is lower than that of hydrogen. For acetate oxidation combined with oxygen reduction (an MFC), for example, the difference is 1.1 V. This is the maximum theoretical cell voltage that can be delivered by the system.

In practice, due to different losses occurring in the system, the output voltage of an MFC is considerably lower, and the voltage that needs to be applied to an MEC or EC is considerably higher, than these theoretical values [72].

Important parameters to evaluate the performance of (B)ES studies for the recovery of TAN

- TAN **removal** efficiency (%): a measure of how much TAN was removed from the wastewater influent
- TAN **recovery** efficiency (%): a measure of how much TAN from the wastewater influent was recovered as a final product (absorbed in an acid, for example).
- TAN **transport** efficiency (%) (also called charge transfer efficiency or current efficiency): the contribution of NH_4^+ to the total charge transport across the membrane. In other words, which part of the current is used for NH_4^+ transport compared to the transport of all other cations.
- TAN **flux** over the membrane (gTAN m^{-2} d^{-1}) (also called TAN removal rate or TAN transport rate): the rate at which TAN was transported from the anode to the cathode compartment through the membrane with respect to the membrane area.
- Specific **energy input** (MJ kg_N^{-1} or kWh kg_N^{-1}) (also called specific energy demand): the amount of energy required to remove or recover TAN, per unit TAN.

Losses affecting the (B)ES performance

There are several losses occurring in (B)ESs that affect how much the actual voltage deviates from the thermodynamic cell voltage. The voltage losses can be classified into reversible and irreversible, and together affect the voltage efficiency of the system [72–75].

The reversible voltage loss is the part of the energy input that can be partly recovered. For example, the applied voltage used to drive the non-spontaneous production of hydrogen gas can be partly recovered in the form of hydrogen, which can be used later as a fuel [72, 75]. Irreversible energy losses are related to resistances in different parts of the cell, such as anode and cathode overpotentials (which include activation losses, catalyst deactivation, energy needed by the microorganisms to maintain their metabolism in the case of BES, resistance to the flow of electrons through the electrodes, concentration losses, etc.), ionic losses (resistance to the flow of ions through the electrolytes), transport losses (resistance to the flow of ions through the membrane) and the potential loss due to the development of a pH gradient between anode and cathode [63, 72]. Knowing what these losses are in order to minimize them is crucial to improve the energy efficiency of the system. Some of these losses will be reviewed in Chapters 3 and 4 of this thesis.

The coulombic efficiency (CE) is another important parameter to take into account for the energy efficiency of the system. The CE describes the percentage of the electrons present in the substrate that actually end up in the desired product. In BESs, for example, the coulombic efficiency is lower when there are other microbial processes that compete for the organic substrate to produce biomass and other undesired products (such as methane) instead of electricity. Especially problematic are other electron acceptors that are energetically more favourable to use than the anode, such as oxygen. In ESs, for example, reactions other than the desired one can occur, such as chloride oxidation at the anode instead of oxygen evolution. This can lead to the production of toxic compounds such as chlorine gas, chlorination byproducts and adsorbable organic halides (AOX) [71, 76].

The performance of (B)ESs can be negatively affected when treating real wastewaters due to their typically low conductivities and buffering capacity. Many real wastewaters have conductivities in the order of 1-2 mS cm^{-1}, which lead to considerable ionic losses [70, 77]. Furthermore, the low buffering capacity of most wastewaters (5-10 mM) is not enough to prevent the acidification of the anolyte due to the proton production in the anode compartment, which can affect and eventually inactivate the microorganisms in a BES [77].

1.4.1 Ammonia recovery from urine: From waste to resource by using (B)ES

As mentioned previously, a high proportion of the nitrogen input from fertilizers ends up in wastewater via animal and human excreta. Currently, wastewater is collected and treated in centralized systems, where nutrients contained in human excreta are diluted more than 100 times before reaching wastewater treatment plants [27]. In these centralized systems, domestic wastewater streams of very different nature (such as the wastewater from the shower and the one from the toilet) are mixed. A way to promote recovery instead of removal from wastewater is to collect and treat the household wastewater streams separately. The concept of separation at source, or new sanitation, is based on the separate collection of domestic wastewater streams to enable a more efficient recovery of resources such as nutrients and water. It also promotes decentralized treatment to reuse resources locally, aiming towards a circular economy [15, 20, 78].

Within the separation at source scheme, domestic wastewater streams can be separated into grey water (wastewater from the shower or bath, sinks, and laundry), black water (toilet water, containing faeces and urine) and rainwater. Solid kitchen waste is sometimes included in the separated streams [15]. Black water can be further separated into brown water (faeces and flush water) and yellow water (urine).

From all the domestic wastewater streams, urine contains most of the nitrogen (around 80%) (Figure 1.5) and around 50% of the phosphorous, and represents only 1% of the volume [15, 27]. Urine can be collected by the use of urine-diverting toilets or waterless urinals, preventing the dilution of the nutrients with high volumes of potable water [27, 79]. It is estimated that 60% of the total nitrogen load to a wastewater treatment plant could be reduced by collecting and treating urine separately [51], which could lead to considerable energy and environmental savings.

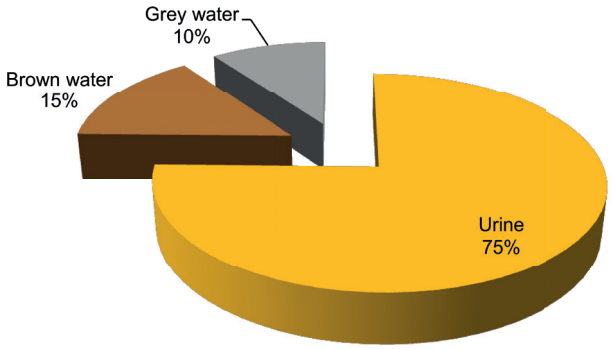

Figure 1.5. Percentage of nitrogen in different domestic wastewater streams. Urine contains most of the nitrogen, while it only represents 1% of the total volume (calculated from [15] by excluding solid kitchen waste). Brown water is comprised of faeces and flush water, while grey water contains wastewater from the shower or bath, sinks and laundry.

Urine characteristics

Human urine is a liquid produced by the kidneys and excreted from the body through the urethra [80]. It consists mostly of water, urea, inorganic salts, organic compounds and organic ammonium salts [81]. Its concentration of nutrients vary widely depending mainly on people's diet: a high consumption of meat and dairy, for example, results in a higher nitrogen concentration compared to plant-based diets. The total nitrogen concentration of undiluted urine can therefore vary widely, from as low as 2.3 to as high as 12.0 g L^{-1}, with an average of around 9 g L^{-1} [39, 80, 82]. This high nitrogen concentration makes urine a very suitable candidate for nitrogen recovery techniques.

Urea ($(NH_2)_2CO$) is the predominant constituent in the nitrogen excretion from the body, representing over 50% of the total solutes in urine [80]. The pH of fresh urine is around 6-7, but once out of the system, urea is hydrolysed by the bacterial enzyme urease (produced by many microorganisms present in wastewater) to ammonia and carbamate. Subsequently, carbamate is hydrolysed further to ammonia and bicarbonate (Equation 1.7 shows the overall reaction). This leads to a high buffering capacity and a pH increase.

$$(NH_2)_2 CO + 2H_2 O \rightarrow NH_3 + NH_4^+ + HCO_3^-$$ Equation 1.7

Stored urine, therefore, has a pH of around 9 (the pKa of NH_4^+/NH_3 is 9.25 at 25°C) [83]. The pH increase due to urea hydrolysis causes the spontaneous precipitation of minerals such as struvite, hydroxyapatite (HAP, $Ca_{10}(PO_4)_6(OH)_2$) and calcite ($CaCO_3$) [84], which is considered as favourable for the purpose of phosphorous recovery, and unfavourable in urine-collection systems because it can cause scaling and blockages.

Due to its high nutrient content, urine has the potential to be used as a fertilizer, and has been found to be efficient for many crops [85]. However, using urine as a fertilizer can be costly because it involves storage, transport (from urban areas to agricultural areas) and spreading of high volumes of liquid [86]. The transport of urine instead of urea in solid form, for example, would cost around 50 times more [77]. The loss of ammonia by evaporation during storage and spreading of urine is seen as another problematic aspect, along with its possible faecal cross-contamination [15, 57]. For this reason, using urine directly as fertilizer (after proper storage) would be more feasible for local, small-scale systems, such as for the household's own consumption. For larger-scale systems, other technologies for nitrogen recovery from urine are preferred [15, 38], such as the ones shown in Figure 1.2.

Urine, apart from being nitrogen-rich, has a high ionic conductivity (around 20 mS cm^{-1}) and a high buffering capacity (around 660 mM) [77], which makes it an attractive wastewater for the recovery of TAN by (B)ESs.

Recovery of TAN from urine by means of (B)ESs and its challenges

The proof of principle of TAN recovery from nitrogen-rich wastewaters by a (B)ES was first reported by Kuntke et al. (2011) [61] using an MFC. As shown in Section 1.4, TAN recovery by means of a (B)ES is based on the production of a stream concentrated in TAN and its in situ conversion to NH_3, using electrical current as the driving force. Subsequently, the NH_3 in this stream (the catholyte) can be recovered as a pure product by conventional recovery methods, such as stripping-absorption [40, 54].

Experimentally, however, the coupling of (B)ESs with conventional recovery methods for the recovery of TAN from the catholyte was not properly established, and low TAN recoveries were obtained [87].

In order to effectively recover TAN, it is crucial to successfully couple an efficient extraction method with the (B)ES. After the proof of principle of TAN recovery by a BES (which used a sacrificial potassium ferricyanide cathode system), subsequent studies involved a) an MFC treating urine where the NH_3 was stripped from the catholyte by aeration provided to the

cathode, and absorbed in boric acid [69] and b) an MEC treating urine where the NH_3 was passively stripped from the catholyte by the hydrogen produced at the cathode, and later absorbed in boric acid [87]. The latter study stressed the importance of coupling a proper NH_3 stripping process with the BES. The high NH_3 concentration in the catholyte due to insufficient TAN extraction caused the transport of NH_3 from the cathode compartment back into the anode compartment, which resulted in unstable removal rates and low TAN recoveries of around 30% [87].

Moreover, the operation of (B)ESs needed to be further optimized to allow for higher TAN recoveries, which depends on the effective transport of TAN from anode to cathode. Apart from continous extraction of NH_3 from the catholyte, this transport is dependent on several factors, such as current density, TAN loading rate, TAN concentration, and pH [40]. Many of these factors are interrelated, and their interdependence is not well understood. More insight into the factors affecting TAN recovery is crucial for further development of the technology.

Finally, achieving maximum TAN recovery at minimal energy input is essential for the application of this technology. Operating at high removal efficiencies usually comes with the trade-off of a high energy input. ESs, for example, can usually operate at higher removal rates than BESs, but require higher energy inputs [40, 88]. At the same time, MFCs can generate electricity, but operate at lower removal rates than MECs, which require an energy input (Rodriguez Arredondo et al 2015)[89]. It is therefore important to define the conditions in which (B)ESs can be operated optimally, which would allow for a better comparison between them.

1.5 Aim and thesis outline

The aim of this thesis is to improve the understanding on the transport of TAN, as well as to optimize the ammonia removal and recovery in (bio)electrochemical systems treating nitrogen-rich wastewaters, with a focus on urine.

In **chapter 2**, we present an overview of the nitrogen removal and recovery mechanisms in bioelectrochemical systems treating wastewaters, and review state-of-the-art research. In that same chapter, we provide an economic and energy analysis of the costs and revenues of treating urine with both an MFC and an MEC. In the analysis we discuss the limitations and main challenges of the technology and show that BES can be considered economically feasible when revenues of TAN recovery are taken into account.

Two of our objectives were to improve the ammonia extraction from the catholyte and to better understand the TAN transport in (B)ESs, and these are addressed in **chapter 3.** In this chapter, we coupled an electrochemical system with a gas-permeable hydrophobic membrane unit to study the influence of the interplay between the current density and the TAN loading rate on the TAN transport. We defined the load ratio (the ratio between the applied current density and the TAN loading rate) and developed a simple model to predict the nitrogen recovery in similar systems based on this load ratio.

Treating wastewaters electrochemically can be energy-intensive, so in **chapter 4** a more energy efficient electrochemical system for the recovery of TAN was developed. In this technology, the hydrogen gas produced at the cathode is reused as the electron donor in the anode, allowing for TAN recovery at high rates and low energy input.

The optimization of TAN recovery in a bioelectrochemical system was addressed in **chapter 5.** In this chapter, we tested the applicability of the load ratio concept developed in chapter 2 in a bioelectrochemical system treating real and synthetic urine. We evaluated the challenges of a system which depends on the biodegradation of organics for the recovery of TAN.

In **chapter 6,** a general discussion is presented about the recovery of TAN by the use of (bio)electrochemical systems, including the most recent studies in the field. We discuss why (bio)electrochemical systems for TAN recovery from urine have not been applied on a larger scale yet, based on the work performed in this thesis and on literature. Finally, we discuss the future perspectives and propose recommendations to bring this technology closer to application.

CHAPTER 2

Bioelectrochemical systems for nitrogen removal and recovery from wastewater

ABSTRACT

Removal of nitrogen compounds from wastewater is essential to prevent pollution of receiving water bodies (*i.e.* eutrophication). Conventional nitrogen removal technologies are energy intensive, representing one of the major costs in wastewater treatment plants. For that reason, innovations in nitrogen removal from wastewater focus on the reduction of energy use. Bioelectrochemical Systems (BESs) have gained attention as an alternative to treat wastewater while recovering energy and/or chemicals. The combination of electrodes and microorganisms has led to several methods to remove or recover nitrogen from wastewater via oxidation reactions, reduction reactions and/or transport across an ion exchange membrane. In this study, we give an overview of nitrogen removal and recovery mechanisms in BESs based on state-of-the-art research. Moreover, we show an economic and energy analysis of ammonium recovery in BESs and compare it with existing nitrogen removal technologies. We present an estimation of the conditions needed to achieve maximum nitrogen recovery in both a microbial fuel cell (MFC) and a microbial electrolysis cell (MEC). This analysis allows for a better understanding of the limitations and key factors to take into account for the design and operation of MFCs and MECs. Finally, we address the main challenges to overcome in order to scale up and put the technology in practice. Overall, the revenues from removal and recovery of nitrogen, together with the production of electricity in an MFC or hydrogen in an MEC, make ammonium recovery in BESs a promising concept.

This chapter has been published as: Rodríguez Arredondo M, Kuntke P, Jeremiasse AW, Sleutels THJA, Buisman CJN, ter Heijne A. Bioelectrochemical systems for nitrogen removal and recovery from wastewater. *Environ. Sci. Water Res. Technol.* 2015, *1* (1), 22-33.

Water impact
Nitrogen is an essential element for life. It is applied in reactive form (NH_3 or NO_3^-) as fertilizer on soils for growth of agricultural crops. The accumulation of reactive nitrogen in the environment causes environmental problems such as eutrophication and acidification. To decrease the accumulation of nitrogen in the environment, it needs to be removed from wastewaters before discharge on receiving water bodies. Classically, this is done using a combined aerobic and anaerobic treatment process in wastewater treatment plants (WWTPs). This process requires energy for aeration, which can constitute up to 60% of the total energy consumption of a WWTP, while nitrogen is lost. This review gives an overview on innovative nitrogen removal and recovery technologies based on bioelectrochemical systems (BESs). We show that BESs enable energy-efficient nitrogen removal and even recovery of useful nitrogen (ammonia) from wastewaters.

2.1 Introduction

Population growth has dramatically accelerated [90], fueled by developments during and following the industrial revolution. As of 2012, over 7 billion people live on earth [91]. As a result, the impact of human activities on the environment has reached a critical point, not just for humanity [92]. Three out of nine planetary boundaries - proposed thresholds for a 'safe operation space of humanity' - have been breached, namely climate change, biodiversity loss and nitrogen cycle [92].

Nitrogen is one of the elements essential for life. Most of the nitrogen is present in the atmosphere as inert N_2 gas, where it represents approximately 78% of the present gases. In its inert form, nitrogen is not available to most living organisms and needs to be converted to more reactive forms like nitrate (NO_3^-), nitrite (NO_2^-), ammonium (NH_4^+), and ammonia (NH_3). Natural nitrogen-fixation of inert N_2 to reactive NH_3 is carried out by some prokaryotes (*e.g. Azotobacter*, *Clostridium*, cyanobacteria, *Rhizobium*) using the nitrogenase enzyme [93]. This conversion is essential to provide the more reactive forms of nitrogen, as a nutrient for other living organisms.

Nowadays, humanity severely interferes with the natural nitrogen-cycle to provide fertilizers for agriculture. Large amounts (120-160 Mt yr^{-1}) of inert N_2 are transformed into NH_3 via the Haber-Bosch process [8, 92]; a value exceeding the total amount of N_2 fixed annually via natural terrestrial processes [92]. While this conversion of N_2 into reactive NH_3 is essential for fertilizer production and to increase food production, large part of this 'newly produced' nitrogen eventually ends up in the environment [94], where it accumulates and

leads to pollution of waterways, soils and atmosphere (acidification). One of the strategies to mitigate the effects of nitrogen on the environment is, amongst others, removal of nitrogen from domestic wastewater. In the current practice of wastewater treatment, alternating aerobic and anaerobic treatments are required to remove the dissolved nitrogen and to convert it to inert N_2 gas. The disadvantage of aerobic treatment is the considerable amount of energy required for aeration. Innovations in nitrogen removal from wastewater therefore focus on the reduction of energy use.

Bioelectrochemical Systems (BESs) offer clean and CO_2 neutral recovery of energy from wastewaters. The core of BESs are electrochemically active microorganisms, which can exchange electrons between electrodes and organic substances, to convert chemical energy into electrical energy, or the other way around [35, 63, 95–98]. This variety of conversions has led to research in many areas: from wastewater treatment for electricity production, and the production of chemicals, to conversion of electricity into methane or organic compounds. Alternatively, BESs have been proposed as a new treatment technology to remove nitrogen from wastewaters while producing electricity [61, 69]. Different types of nitrogen-based reactions have been reported at both anode and cathode. Recently, some of these reactions were addressed in a study about nutrient removal and recovery in BESs by Kelly and He (2014) [99].

The objective of our study is to give an overview of the state-of-the-art of research on nitrogen removal or recovery in BESs, and to compare these new processes to existing nitrogen removal technologies. Our economic analysis, that builds on previous work by Sleutels et al. (2012) [73], shows that ammonium recovery from urine is a promising concept for economical application of BESs, mainly because of the high revenues generated from removal and recovery of nitrogen.

2.2 The influence of humans on the nitrogen cycle: Biological, chemical, and physical processes

The Haber-Bosch process is the primary human-driven industrial conversion process of inert N_2 to NH_3. In this conversion, nitrogen gas reacts with hydrogen gas (H_2) according to (reaction 1, Figure 2.1):

$$N_2 + 3\,H_2 \rightarrow 2\,NH_3 \qquad (1)$$

The H_2 required for the Haber-Bosch process is produced via steam reforming of natural gas. Most of the industrially produced ammonia (~80 Mt N $year^{-1}$) is used as fertilizer in agriculture to enhance food production [8, 92]. Part of the ammonium is taken up by

the crops, but another part ends up in the environment, where they increase the risk of eutrophication of receiving water bodies, and adds to the pollution of the atmosphere.

Because of these adverse effects on the environment, reactive nitrogen compounds in wastewater were considered as pollutants, and the importance of removing or recovering nitrogen compounds from wastewater was recognized [100]. In wastewater, nitrogen is mostly present in the form of ammonium, and removal of ammonium in wastewater treatment plants mainly occurs via a two-step process [101]. During the first step, nitrification under aerobic conditions, ammonia is oxidized to nitrite by *Nitrosomonas* and subsequently nitrite is oxidized to nitrate by *Nitrobacter* according to (reaction 2, Figure 2.1):

I: $NH_4^+ + 1.5\ O_2 \rightarrow NO_2^- + H_2O + 2\ H^+$
II: $NO_2^- + ½\ O_2 \rightarrow NO_3^-$
Overall: $NH_4^+ + 2\ O_2 \rightarrow NO_3^- + H_2O + 2\ H^+$ (2)

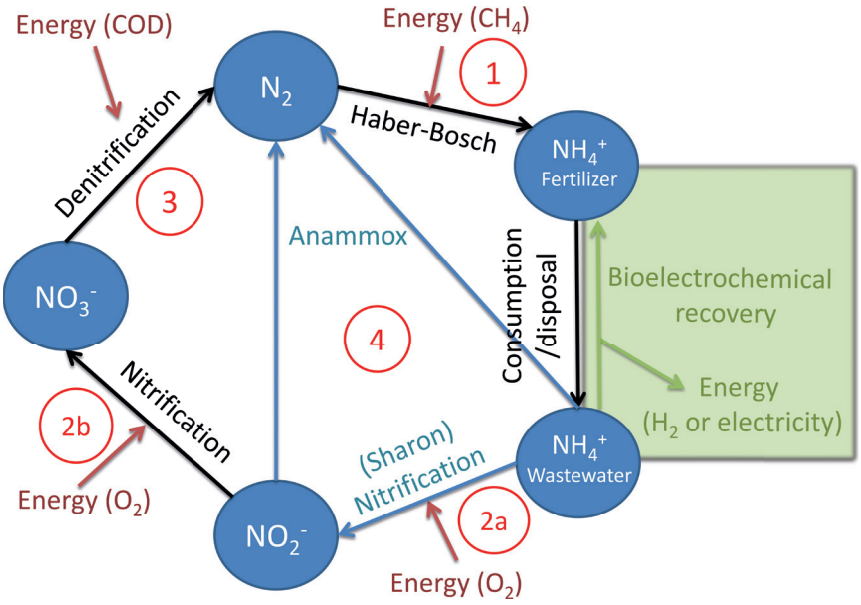

Figure 2.1. The nitrogen cycle in fertilizer production and wastewater treatment processes.

So for each mole of ammonium, 2 moles of oxygen are required for full oxidation to NO_3^-. During the second step, denitrification under anoxic conditions, nitrate is reduced to N_2 gas, for example by *Paracoccus denitrificans*, according to (reaction 3, Figure 2.1):

$2\ NO_3^- + COD \rightarrow N_2 + CO_2 + 2OH^- + H_2O$ (3)

The produced N_2 gas is released (or recycled) to the atmosphere.

The disadvantage of the conventional nitrification/denitrification reaction is that it requires considerable amounts of energy, because the wastewater needs to be aerated to supply oxygen for the conversion of ammonium to nitrate, and supply of electrons for denitrification in the form of COD (*e.g.* methanol) is required. The advantage of nitrification/denitrification is that nitrogen can be removed to low concentrations.

Anammox (anaerobic ammonium oxidation) has been proposed as a more energy efficient alternative to the conventional nitrification and denitrification process. Anammox relies on the biological conversion of ammonium and nitrite to N_2 gas by specialized bacteria (Planctomycete-like) [102]. First, part of the ammonium needs to be partially oxidized to nitrite in a pretreatment step. Therefore, Anammox is combined with, for example, the SHARON (Single reactor system for High-rate Ammonium Removal Over Nitrite) [103, 104] process. SHARON is a biological process in which ammonium is oxidized to nitrite (instead of a complete oxidation to nitrate). The oxidation to nitrite is possible due to the specific growth rates of nitrite oxidizing bacteria, ammonium oxidizing bacteria and the applied loading rate of the reactor. Another approach is the so-called CANON (Completely Autotrophic Nitrogen removal Over Nitrite) process, where the aerobic and anaerobic ammonium oxidizers symbiotically coexist. In the CANON process it is possible to perform aerobic and anaerobic ammonium oxidation simultaneously. Therefore, ammonium-oxidizing and Anammox bacteria cooperate [105]. The overall Anammox process can be described by (reaction 4, Figure 2.1):

$$\text{I: } NH_4^+ + 1.5\ O_2 \rightarrow NO_2^- + H_2O + 2\ H^+$$
$$\text{II: } NH_4^+ + NO_2^- \rightarrow N_2 + 2\ H_2O \qquad (4)$$

Because only half of the ammonium needs to be oxidized to nitrite and no addition of COD is required, the energy input for the Sharon/Anammox process is considerably lower than the energy input for conventional nitrification/denitrification [102, 103].

A recent study [106] reports a new process for the removal of nitrogen from wastewater: Coupled Aerobic-anoxic Nitrous Decomposition Operation (CANDO). CANDO consists of three steps: (1) partial nitrification of NH_4^+ to NO_2^- (by the SHARON process), (2) partial anoxic reduction of NO_2^- to N_2O and (3) decomposition or combustion of N_2O to nitrogen, oxygen and energy [106]. Even though pilot scale studies are needed, this process has the potential to lower oxygen demand and sludge production, as well as recover energy from nitrogen.

Recently, bioelectrochemical systems (BESs) have been investigated as an alternative to the conventional wastewater treatment processes, such as organic matter and nitrogen removal. A BES is an electrochemical cell which uses microorganisms to catalyse one or more reactions taking place on the electrodes. At the anode, anaerobic microorganisms can oxidize biodegradable organic matter to carbon dioxide, protons and electrons, which is often represented by the oxidation of acetate:

$$CH_3COO^- + 4\,H_2O \rightarrow 2\,HCO_3^- + 9\,H^+ + 8\,e^- \quad (5)$$

As the electrode can act as an electron acceptor, the produced electrons are transferred by the microorganisms to the anode, which is connected over an external circuit to the cathode where a reduction reaction takes place.

Depending on the cathode reaction, BESs can be divided in two types: galvanic and electrolytic cells. In galvanic cells, electricity is produced by coupling the anodic oxidation to the reduction of a suitable electron acceptor (*i.e.* O_2, Fe^{3+}, Cu^{2+}) [107–109]. These systems are called microbial fuel cells (MFCs). In electrolytic cells, electricity is needed to drive the reduction reaction at the cathode. In a so called microbial electrolysis cell (MEC) the anodic oxidation is coupled to reduction of protons to hydrogen gas [35, 63, 110, 111].

The cathodic reactions of an MFC (Oxygen Reduction Reaction, ORR) and an MEC (Hydrogen Evolution Reaction, HER) under neutral to alkaline pH conditions are given in reaction 6 and 7, respectively.

$$2\,H_2O + O_2 + 4\,e^- \rightarrow 4\,OH^- \quad (6)$$

$$2\,H_2O + 2\,e^- \rightarrow H_2 + 2\,OH^- \quad (7)$$

BESs are seen as a potential sustainable solution to treat wastewaters while at the same time producing energy and/or chemicals. Anode and cathode chambers are often separated by an ion exchange membrane to prevent mixing of the oxidation and reduction products [35, 63]. The ion exchange membrane allows for anions and/or cations to be transported to maintain electron neutrality of the electrochemical system.

BESs allow for energetically and chemically efficient ammonium recovery from wastewater. The organic matter in wastewater is oxidized at the anode by bacteria, while ammonium (present in the wastewater) is transported over a cation ion exchange membrane (CEM) to the cathode chamber, where the high catholyte pH allows for recovery in the form of ammonia. Therefore, no addition of caustics is required compared to other ammonia recovery technologies. This way, BESs can create a shortcut in the nitrogen cycle by

removing NH_3 from the wastewater, not by reduction to N_2 but by direct recovery in the form of NH_3 (Figure 2.1).

Ammonium recovery using an electrochemical cell (EC) was investigated by Desloover et al. (2012) [40]. Ammonium recovery from anaerobic digestate was investigated using an electrolysis cell, in which ammonium transported over a CEM was stripped from the catholyte by the produced hydrogen. The current, and thus the rate of ammonium transport, in such an abiotic system is not limited by the biological catalyzed anode reaction. Furthermore, the common limitation of high internal resistance in MFCs by the cathodic reaction (ORR), which is the result of the prevalent conditions found in MFCs (temperature, pH and oxygen concentration), is not found in such an EC. As a result, the reported ammonium transport rates (120 $g_N\ m^{-2}\ d^{-1}$) are significantly higher than reported in MFCs, whereas the ammonium transport accounted for approximately 40% of the overall charge transport over the membrane, similar to results found in BESs [61, 69]. Desloover et al. (2012) reported an energy demand of 5 kWh kg_N^{-1} (or 18 kJ g_N^{-1}) for ammonium recovery by an EC, which is lower than the reported energy demand of 9 kWh kg_N^{-1} (or 32.4 kJ g_N^{-1}) for conventional ammonia stripping [58]. However, they did not take into account the energy used for stripping and absorption. Finally, similar to the BES approach, no caustic is necessary to increase the pH at the cathode.

2.3 Bioelectrochemical systems for ammonium removal and recovery

As an alternative to conventional nitrogen removal processes, bioelectrochemical systems offer new advantages. Several nitrogen-based reactions in BESs, both at the anode and at the cathode, have been reported so far. In this section, we will give an overview of the reported ammonia removal and recovery mechanisms in BESs (Figure 2.2). The first mechanism of ammonium removal/recovery is based on active and passive transport through the ion exchange membrane, combined with acid/base equilibrium (1). NH_4^+ concentrations in wastewater are considerable: in urine > 4 g L^{-1} [39, 54, 112], and domestic waste water 0.04 g L^{-1} [101, 113]. Consequently, especially in highly concentrated wastewaters, NH_4^+ is the main ion transported through the membrane, either passively in its non-charged NH_3 form (1a), or actively in its charged NH_4^+ form (1b). In the catholyte, it can leave the system in the form of ammonia as the chemical equilibrium shifts from ammonium to ammonia because of the elevated pH in the cathode (1c). The second mechanism is reduction (denitrification) of nitrate to inert N_2 gas by microorganisms at the cathode (2a). In this case, nitrate needs to be formed first, for example via biological oxidation of ammonium by aeration (2b). Alternatively, ammonium can be converted into N_2 via Anammox, which is in principle independent of the cathode. The third mechanism that has been suggested occurs at the anode, where ammonium is directly converted

into nitrogen gas by microorganisms (3), but clear evidence is still lacking. The fourth mechanism is incorporation of ammonium in biomass during microbial growth in the anode (4) or in the cathode compartment.

Concerning the direct oxidation of ammonium to nitrogen gas at the anode (3), a study reports that ammonium is involved in electricity generation either directly as the anodic fuel or indirectly as substrates for nitrifiers to produce organic compounds for heterotrophs [114]. On the contrary, it was reported in the study of Kim et al. (2008) that ammonia removal, instead of being biologically oxidized at the anode to nitrogen gas, was mainly due to physicochemical factors, such as diffusion through the membrane and volatilization of ammonia due to pH increase at the cathode [115]. Zang et al. (2012) also reported that direct ammonia oxidation in the anode was not a source for electricity [116]. Cyclic voltammetry tests did not detect redox couples, nitrite and nitrate were not found and nitrifying or Anammox bacteria were not identified in the anode compartment [116]. In conclusion, the occurrence of direct oxidation of ammonium to nitrogen gas so far lacks solid proof.

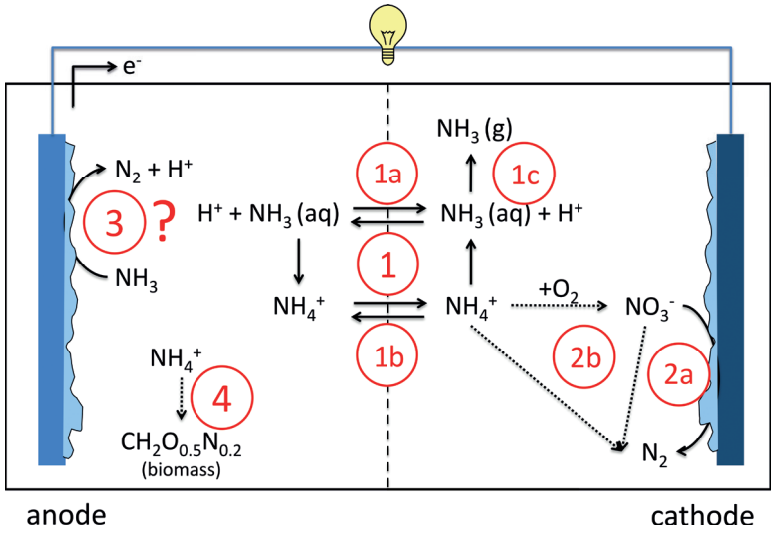

Figure 2.2 Overview of the ammonia removal mechanisms in an MFC. This figure is representative for BES in general. Ammonium can be transported through the membrane (1) either passively via diffusion of ammonia (1a) or actively via migration in the form of ammonium (1b). Ammonia can leave the system by evaporating into its gaseous form as a result of the elevated pH in the cathode (1c). At the cathode chamber, it can be (biologically) oxidized by oxygen and denitrified by microorganisms at the cathode (2a) or in solution (2b) – the dashed lines show processes that are independent of the electrodes. At the anode, it has been suggested that ammonia can directly be nitrified/denitrified to nitrogen gas by microorganisms, however, solid proof is still lacking (3). Finally, ammonium can be incorporated in biomass for growth (4), either in the anode or in the cathode chamber.

Table 2.1 gives an overview of the reported mechanisms for the removal and recovery of ammonium via routes 1 and 2, and their performance.

Table 2.1. Performance of the reported mechanisms for the removal and recovery of nitrogen in BESs

Reactor type	Type of wastewater	Removal mechanism	N concentration influent ($mg_N L^{-1}$)	Removal efficiency/rate (%) or ($g_N m^{-2} d^{-1}$)	Current density ($A m^{-2}$)	Reference
Single chamber MFC	Swine wastewater	Ammonia removal	188 ± 6	60%	0.5 mA[e]	[115]
Dual chamber MFC	Swine wastewater	Ammonia removal	219 ± 2	68%	0.5 mA[e]	[115]
Dual chamber MFC	Swine wastewater	Ammonia removal	219 ± 2	89%	0.3 mA[e]	[115]
Dual chamber MFC	Urine	Ammonia removal	4050	3.3 $g_N m^{-2} d^{-1}$	0.5	[69]
Dual chamber MFC	Urine	Ammonia removal	4050	9.7 $g_N m^{-2} d^{-1}$	2.7	[54]
Dual chamber MEC	Urine	Ammonia removal	700	162.18 $g_N m^{-2} d^{-1}$	14.7	[87]
Dual chamber MFC	Synthetic	Nitrate reduction	2615	146 $g_N m^{-3} d^{-1}$ [a]	35 A m^{-3} [a]	[117]
Dual chamber MFC	Synthetic	Nitrification coupled to nitrate reduction	88	410 $g_N m^{-3}$ NCC d^{-1} [b] 67.4 %	133 A m^{-3} [a]	[118]
Dual chamber MFC	Synthetic	Simultaneous nitrification and denitrification	41	94.1% TN[c] 104 $g_N m^{-3}$ TCV[d] d^{-1}	39.7 A m^{-3}	[119]
Dual cathode MFC	Synthetic	Nitrification and denitrification	30- 90	67-90% of TN[c] 14 $g_{TN} m^{-3} d^{-1}$	43 A m^{-3} [f]	[120]
Single chamber MFC	Synthetic	Simultaneous nitrification and denitrification	100	96.8%	3.6	[121]
Dual chamber MFC/MEC	Synthetic	Ammonia removal	3000	2.94 $g_N m^{-2} d^{-1}$	3.6	[122]
Dual chamber MFC/MEC	Synthetic	Ammonia removal	3000	8.5 $g_N m^{-2} d^{-1}$	3.6	[122]
Dual chamber MFC/MEC	Synthetic	Urea removal	4000	37.8 $g_N m^{-2} d^{-1}$	5	[122]

[a] Based on cathodic volume. [b] NCC: Net cathodic compartment. [c] TN: total nitrogen. [d] TCV: total compartment volume. Both cathode and anode have the same volume. [e] Insufficient data to determine current density. [f] based on anodic volume.

2.3.1 Diffusion and migration of NH_3 and NH_4^+

In a BES equipped with a CEM, ammonium (and other cations) can be transported from the anode to the cathode chamber by two processes: migration and diffusion. Transport by migration is induced by the electric field across the ion exchange membrane. Diffusional transport is induced by a concentration gradient across the ion exchange membrane. As a result of the production of hydroxyl ions in the ORR and HER, and the insufficient H^+ and OH^- transport over the CEM, the pH increases in the cathode chamber [72, 123, 124]. Therefore, ionic ammonium is transformed into volatile ammonia, which can be removed from the cathode compartment by NH_3 stripping with a suitable gas stream. Hence, one of the advantages of using BES for nitrogen recovery is that no additional caustics need to be added to increase the pH of the solution [69].

Kim et al. (2008) studied ammonia loss from swine wastewater in both single- and two-chambered MFCs [115]. An air-cathode was used in the single-chamber MFC, while both aerated phosphate buffer and ferricyanide were tested as catholyte in the two-chambered MFC. An ammonia removal of 60% was reached in 5 days in the single-chamber MFC (cathode exposed to air), while 68% was accomplished in 13 days when using ferricyanide as a catholyte in the two-chambered MFC. The authors concluded that main mechanism for this ammonia removal was ammonium transport (migration and diffusion) to the cathode with subsequent ammonia volatilization.

Exploiting this ammonia loss mechanism, future work of research groups focused on ammonia as a suitable proton shuttle for pH control in BESs and ammonium recovery by NH_3 stripping from the cathode [61, 69, 125]. Cord-Ruwisch et al. (2011) investigated the feasibility of more sustainable pH control in MFCs by proton shuttling from anode to cathode via ammonia addition to the anode chamber [125]. Their results showed that ammonium accounts for 90% of the ionic flux in the BES and that ammonia recovered from the cathode could be recycled to the anode. Further investigation by Cheng et al. (2013) demonstrated the feasibility of such ammonium recycle for anolyte pH control in an MEC also demonstrating a possible pathway for ammonia recovery from wastewater [126].

In domestic wastewater, most of the nitrogen (75%) originates from urine [127]. This nitrogen is excreted by humans in the form of urea ($(NH_2)_2CO$) [112], which is hydrolyzed to ammonia and carbamate by the enzyme urease [84, 128].

$$(NH_2)_2CO + H_2O \xrightarrow{\text{urease}} NH_2COOH + NH_3 \quad (8)$$

Subsequently, carbamate decomposition leads to the formation of ammonia and carbon dioxide:

$$NH_2COOH + H_2O \rightarrow NH_3 + H_2CO_3 \quad (9)$$

Ammonium recovery from urine in an MFC was first reported by Kuntke et al. (2011), where the authors investigated the feasibility of ammonium recovery in a two chamber MFC with a CEM using a sacrificial potassium ferricyanide cathode system [61]. The authors showed that ammonium concentrations up to 4 g_N L^{-1} did not affect the performance of the MFC and that total ammonium transport from anode to cathode accounted for up to 50% of the charge transport. Following up on this proof of principle, Kuntke et al. (2012) demonstrated and evaluated the feasibility of using a two chamber MFC with a gas diffusion cathode [69]. Here, the volatile ammonia was removed from the cathode chamber by the gas stream used for aeration and subsequently collected in a gas wash bottle containing an acid (boric acid). They reported an ammonium recovery rate of 3.3 g_N m^{-2} d^{-1} from urine with an energy yield of -3.46 kJ g_N^{-1} at a current density of 0.5 A m^{-2}. Later results presented by Kuntke et al. (2013) showed an ammonium recovery rate of 9.7 g_N m^{-2} d^{-1} from urine with an energy yield of -10 kJ g_N^{-1} at a current density of 2.6 A m^{-2} [54]. Following the work of Cheng et al., (2013) [126] and Desloover et al., (2012) [40], Kuntke et al. (2014) investigated simultaneous ammonium recovery and hydrogen production from urine in an MEC [87]. They achieved a stable ammonium removal rate of 162.2 g_N m^{-2} d^{-1} at a current density of 14.7 A m^{-2}, while a maximum removal rate of 173.3 g_N m^{-2} d^{-1} at a current density of 23.1 A m^{-2} was reported [87].

The consumed COD also represents a certain amount of energy. In this respect, it is interesting to compare the COD consumption for different nitrogen removal and recovery processes. Using an MFC or MEC, for each kg of N recovered, 0.57 kg of COD is required, assuming that each mole of COD corresponds to 4 moles of electrons, that the COD is converted into electricity at 100% Coulombic efficiency, that all cation transport occurs through NH_4^+, and that all NH_4^+ is recovered at the cathode. For nitrification/denitrification, theoretically, 2.86 kg COD is required for removal of 1 kg of N [129]. On the other hand, nitrification and Anammox require no COD at all.

2.3.2 Nitrification/denitrification at the cathode

The second part of Table 2.1 summarizes performances of systems that studied denitrification at the biocathode. Clauwaert et al. (2007) showed that complete denitrification could be performed by microorganisms in the cathode of an MFC [117]. Acetate was used as the electron donor in the biological anode, while nitrate as the electron acceptor in the biological cathode. Electricity production was thus coupled

to the reduction of nitrate to nitrogen gas by denitrifying microorganisms. Nitrate was removed at a rate of 146 g_N m^{-3} d^{-1}.

Virdis et al. (2008) coupled the anodic oxidation of organic matter and cathodic nitrate reduction in an MFC to an external nitrification reactor enabling the removal of ammonium from wastewater by nitrification and denitrification, while producing electricity. During their experiments, organics present in the anode influent containing ammonium were oxidized to produce electricity. The anode effluent containing ammonia was fed to an external biofilm reactor for nitrification followed by denitrification at the cathode [118]. The authors reported a removal rate of 0.41 kg_N m^{-3} Net Cathode Compartment d^{-1} and a removal efficiency of 67.4%.

Virdis et al. (2010) also used nitrate as an electron acceptor at the cathode of an MFC [119]. The system accomplished simultaneous nitrification and denitrification by optimising the oxygen supply in the aerated cathode chamber. The anode effluent was directed to the cathode through a loop connection to mitigate the pH increase in the cathode. Low levels of nitrate and ammonium in the effluent were accomplished (1 and 2 mg_N L^{-1}, respectively). The highest nitrogen removal efficiency obtained in this system was 94%.

Zhang and He (2012) also achieved high ammonia and total nitrogen removal efficiencies (96 and between 67 and 90%, respectively) by testing a tubular-dual cathode MFC, in which both anion and cation exchange membranes were used [120]. The design allowed for an anoxic inner cathode in which bioelectrochemical denitrification could take place and an aerobic outer cathode for the nitrification process, which shared the same anode. A final nitrate concentration of 3 mg_N L^{-1} was achieved in this system.

Finally, higher ammonia removal efficiencies compared to previous system were reached without the extra energy input of aeration by Yan et al. (2012) [121]. The MFC consisted of a single-chamber with an air cathode which was pre-enriched with a nitrifying biofilm. The cathode was especially prepared with partial positive charges to promote the nitrifying biofilm formation by using a diethylamine-functionalized polymer (DEA) as a catalyst binder instead of the conventional Nafion-type binder, and went through an enrichment period of 75 days. The MFC with the DEA binder had an ammonia removal efficiency of up to 97%, while with a Nafion binder (which also went through the pre-enrichment) it was 91%. The maximum total nitrogen efficiencies were between 75 and 95%, but nitrate concentrations of up to 30 mg L^{-1} were detected in the MFCs effluent. Furthermore, the enrichment process improved the maximum power densities of the MFCs regardless of the catalyst binder, while without the enrichment, power production was about 25% lower.

2.4 Ammonia recovery from urine in an MFC and MEC

Kuntke et al. (2013) proposed a full treatment concept for urine, in which ammonium is recovered using a BES [54] (Figure 2.3).

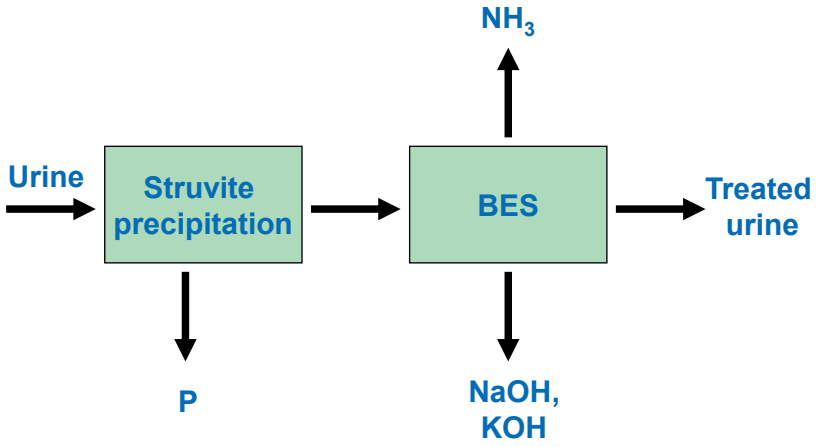

Figure 2.3. Proposed full treatment concept for urine, in which ammonium is recovered using a BES

The treatment concept includes phosphate recovery via struvite (also known as MAP, $MgNH_4PO_4.6H_2O$) precipitation as a pre-treatment step followed by a BES to recover energy and ammonia simultaneously. Notably, the recovered ammonia can be used either as a fertilizer or as an energy source, for example in a fuel cell [130]. In the proposed scheme, caustics can be obtained as by-product. The BES could be either an MFC for electricity production, or an MEC, in which case hydrogen would be produced instead of electricity. The advantage of using an MEC is that a voltage is applied that helps overcoming the internal resistances of the system and higher current densities can be achieved compared to an MFC. On the other hand, the advantage of an MFC is its electricity production, as applying a voltage in an MEC means an additional energy input.

In this section, we present an analysis of the potential energy recovery from urine, in the form of electricity or hydrogen, and ammonia, using a BES under different conditions. Urine, collected by separation toilets and water free urinals, has a COD and an ammonia concentration of 10 - 1.6 g_{COD} L^{-1} and 8.1 - 0.4 g_N L^{-1}, respectively [39]. In this case, to resemble the treatment concept shown in Figure 2.3, a urine supernatant after struvite precipitation with COD and NH_4-N concentrations of 4 g L^{-1} was used as a model, corresponding to earlier reported concentrations [69]. The typical pH difference observed in previous experiments performed in two-chambered BESs with urine is 6 (pH 7 in the anode and 13 in the cathode). This pH gradient means that a higher applied voltage would be required

in an MEC and a higher energy loss would be experienced in an MFC [73]. The effect of this gradient, which can be considered as an additional internal resistance, was included in the calculations. Furthermore, in this calculation, it was assumed that there is no energy input for the MFC, and the energy outputs come from electricity production and ammonia recovery. For MECs, the energy input consists of electricity or external power supply, and the energy outputs are hydrogen production and ammonia recovery. To calculate the theoretical energy output, the lower heating values (LHV) for both hydrogen and ammonia were used: -10817 J L^{-1} for hydrogen [131] and -18577 J g^{-1} for ammonia (adapted from Hacker et al. 2003 [132]) . For comparison, the values for both MFC and MEC are presented in units of kJ per gram of nitrogen recovered. The potential NH_4-N removal depends on both the coulombic efficiency of the system and the ammonium transport efficiency across the membrane. Therefore, the amount of removed ammonium from the anode compartment can be calculated based on assumptions for coulombic efficiency, loading rate and transport efficiency as will be described below.

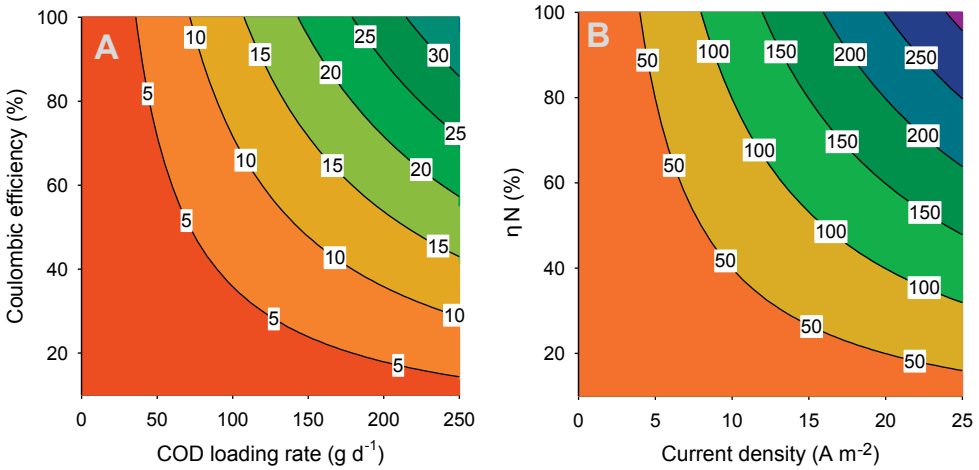

Figure 2.4. **(A)** Current density (A m^{-2}) as a function of the coulombic efficiency (%) and the loading rate (g d^{-1}) and **(B)** ammonium flux from anode to cathode (g d^{-1}) as a function of transport efficiency (%) and current density (A m^{-2}).

Figure 2.4A shows the theoretical current density (contour lines) as a function of the coulombic efficiency and the COD loading rate. The coulombic efficiency represents the amount of degraded COD that ends up in electricity, where one mole of COD corresponds with 4 moles of electrons, while the loading rate is the amount of COD that is added to the system per time unit. This figure shows that current density increases with increasing loading rate and increasing coulombic efficiency. In addition, the same current density can be achieved by combining a high loading rate and a low coulombic efficiency or *vice versa*.

In BESs, the produced charge (related to current) is equal to the amount of ions that are transported through the membrane. The transport efficiency (η N) represents the percentage of ammonium that is transported through the membrane compared to the total amount of ions transported. Thus, at a transport efficiency of 100%, all the transported charge through the system is in the form of ammonium. The overall ammonium flux increases with increasing current density and increasing ammonium transport efficiency. From the combination of Figures 2.4A and B, the total amount of ammonium that is transported from the anode compartment to the cathode compartment can be related to ammonium transport efficiency, coulombic efficiency, and COD loading rate. Here, it is assumed that 100% of the ammonia which is removed is also recovered. Clearly, to maximize the ammonium recovery, the BES needs to be operated at high coulombic efficiency and high loading rate (to achieve a high current density), in combination with high ammonium transport efficiency. These aspects will be further discussed in Section 2.6.

Reported values (Table 2.2) for MFCs and MECs for urine treatment are well in line with Figure 2.4A. In MFC mode, the COD loading rate was 286 g_{COD} m^{-2} d^{-1}, but not all COD was removed, while in the calculation for Figure 2.4, it is assumed that all COD is removed. Therefore, we compare the performance of the BES treating urine (Table 2.2) with Figure 2.4 based on COD removal rate. At 181 g_{COD} m^{-2} d^{-1}, and 10% coulombic efficiency, indeed the expected current from Figure 2.4A is below 5 A m^{-2} (measured value 2.6 A m^{-2}). In MEC mode, at a COD removal rate of 171 g_{COD} m^{-2} d^{-1}, and 96% coulombic efficiency, the expected current is between 20 and 25 A m^{-2}, matching well with the measured value. Now, the current can be linked with the N removal rate (Table 2.2) to determine the N transport efficiency. For the MFC, the N transport efficiency derived from Figure 2.4 is 30%, a value also reported in this study; for the MEC, it is 60%.

Table 2.2. Examples of current densities, coulombic efficiencies, COD loading and removal rates, internal resistances, and power outputs achieved in BES treating urine

	Microbial Fuel Cell	Microbial Electrolysis Cell
Current density (A m^{-2})	2.6 ± 0.1	23.1 ±1.15
COD loading rate (g_{COD} m^{-2} d^{-1})	285.7 ± 7.1	466.6 ± 14.0
COD removal rate (g_{COD} m^{-2} d^{-1})	180.9 ± 5.8	171.0 ±16.9
Coulombic efficiency (%)	10.4 ± 0.5	95.6 ±3.1
N removal rate (g_N m^{-2} d^{-1})	10	173.34 ± 18.07
Internal resistance (mΩ m^2)	95	43 ± 2.2
Reference	[33]	[39]

Figure 2.5A shows the energy yield for a scaled-up MEC treating urine for ammonia recovery, using the concept proposed by Kuntke et al. (2013) [54]. All calculations were performed for current densities from 0.5 to 25 A m^{-2} (normalized to the membrane surface area) and for high (200 mΩ m^2) and low (25 mΩ m^2) internal resistance. Negative values for energy recovery represent actual energy recovery. Figure 2.5A shows that systems with low internal resistance (25 mΩ m^2) can be used in the full current range to recover energy from urine. At high internal resistance though (200 mΩ m^2), operating in the low current density range (up to 13 A m^{-2}) is required to recover energy from the system. The reason for this is that at high internal resistance, the power input required to overcome the internal resistance to achieve a certain current density increases much faster than the recovery of energy in the form of hydrogen and ammonium. This can be seen in more detail in Figure 2.5B. Here, the effect of the different contributions to the total energy balance for a system with 200 mΩ m^2 internal resistance is shown. The input of electrical energy increases linearly with increasing internal resistance, as more energy is required to overcome the internal resistance at higher current density. The output energy (kJ g_N^{-1} recovered) in the form of H_2 and NH_3 in Figure 2.5B is independent of current density because it is normalized by the nitrogen recovered. The nitrogen recovered is directly related to the current density through the transport efficiency of ammonium. Overall, energy can only be recovered at high internal resistance when the electrical energy input is limited, and thus current density is lower than 13 A m^{-2}. These results show that achieving a low internal resistance in these systems is crucial to actually recover energy from urine, because low internal resistance leads to both high current density and low power consumption.

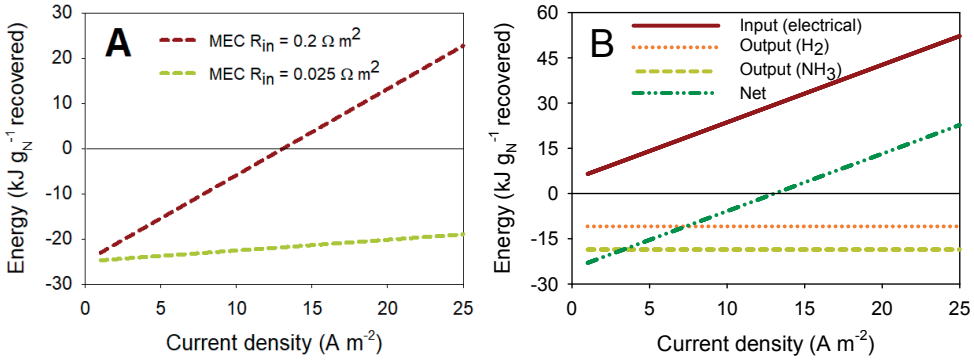

Figure 2.5 (A) Energy recovery in an MEC as a function of current density for high (200 mΩ m^2) and low (25 mΩ m^2) internal resistance. The energy recovery for an MFC is not shown since it is comparable to the MEC. Figure 2.5 **(B)** shows a more detailed overview of the energy input (electrical) and output (hydrogen and ammonia) for the MEC with an internal resistance of 200 mΩ m^2 as a function of current density.

The results of the analysis for an MFC are not shown here, but are comparable. The main difference is that the current range that can be achieved in the MFC is much smaller (3.5 A m^{-2}) compared to the MEC. In an MFC, the cell voltage is limited by the internal resistance. This internal resistance causes the cell voltage to decrease to short circuit conditions (0 V, reached at 3.5 A m^{-2} in our analysis). Currents higher than short circuit cannot be achieved in MFC mode, meaning that to achieve higher current densities, the MFC would operate as an MEC. Here, the applied voltage acts as a driving force for the reactions to proceed at high rate and thus, current densities higher than 3.5 A m^{-2} can be achieved. Although MFCs do not rely on the input of electrical energy to drive the reactions (applied voltage), this additional applied energy in MECs is recovered in the form of hydrogen. The recovered energy in the form of nitrogen is the same for both systems as it is directly correlated to the produced current. As a result, the energy balance for both MFC and MEC, at low current densities (< 3.5 A m^{-2}), is similar.

In the comparison shown above the energy required for pumping and stripping is not taken into account, because at this early stage of development no realistic estimations can be made in terms of flow rates required in scaled-up systems. Of course, these processes will negatively affect the energy recovery from urine.

2.5 Economic analysis for ammonia recovery from urine in an MFC and MEC

Sleutels et al. (2012) have shown an approach to determine the maximum internal resistance at which point it is still economically feasible to apply MFCs and MECs for the removal of COD from wastewater [73]. In this analysis, the costs (both operational and capital) and benefits of both systems for the treatment of COD in wastewaters were estimated. Here, we extend the analysis for the case that ammonium is recovered in an MFC or MEC. The economic value of the treatment of urine, products and by-products are presented in Table 2.3. Similar to the example of COD removal, the value for ammonia removal mainly originates from the fact that no additional treatment is required.

As an indication for feasibility of simultaneous ammonium recovery and wastewater treatment in MFCs and MECs, costs and benefits have been calculated for current densities in a range of 0 to 50 A m^{-2}. The results for the economic comparison for the removal of ammonia are shown in Figure 2.6A for MFCs and in Figure 2.6B for MECs. To study the effect of internal resistance, the analysis was done at both 25 and 200 mΩ m^2.

Table 2.3. Overview of the parameters used in the economic evaluation of MECs and MFCs as a treatment concept for wastewater

Parameter		Unit	Reference
Electricity	0.06	€ kWh^{-1}	[133]
Hydrogen	0.35	€ m^{-3}	[134]
Capital and operational costs	0.05	€ kg COD $removed^{-1}$	Calculated from [135]
COD removal	0.35	€ kg COD $removed^{-1}$	[136]
Ammonia removal efficiency	30	%	Based on [69]
Ammonia removal	1.63	€ kg of N $removed^{-1}$	[137]
pH difference between anode and cathode	6	-	Estimated from [138]
Applied voltage	1	V	-
Interest rate	6	%	-

The solid lines in Figure 2.6 represent the costs for the MFC and MEC consisting of both capital and operational costs. The dotted lines represent the revenues at high and low internal resistance and with and without N recovery. When revenues are higher than costs, the system becomes profitable. Clearly, when ammonium recovery is included in the economic analysis in addition to COD removal, the revenues increase for both MFC and MEC at both internal resistances (Figure 2.6A and B) compared to the situation without ammonium recovery. Both systems become profitable at almost all current densities, even at higher internal resistance.

The capital costs for both MFCs and MECs are similar since these systems have the same configuration and are constructed from the same materials. However, the capital costs decrease with increasing current density when expressed in € kg_{CODr}^{-1}, because the rate of COD removal increases at higher current densities. In contrast with the capital costs, the operational costs are different for MECs and MFCs. For MFCs, the operational costs are independent of current densities, while for MECs, the electrical energy input and thus the operational costs need to be increased to achieve a higher rate of hydrogen production. Therefore, the total costs for MECs have a minimum, determined by the current density and the internal resistance, and the total costs for MFCs decrease with increasing current density. For the MFC, low internal resistances are required to make production of electricity from wastewater economically attractive. Only at 25 mΩ m^2, the revenues become higher than the costs at current densities that have been achieved in MFCs so far (5-10 A m^{-2}). Like Sleutels et al (2012) reported before, hardly any MFCs so far have reached such a low internal resistance [73].

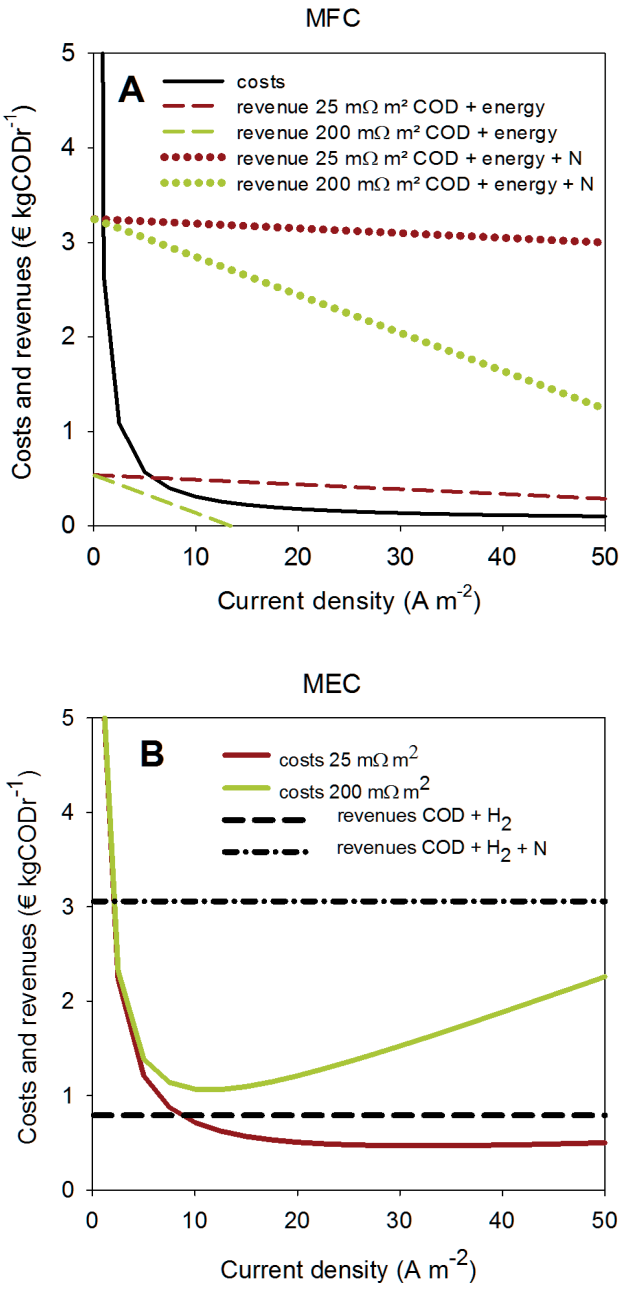

Figure 2.6. Comparison of the costs and revenues of ammonia recovery in an MFC **(A)** and in an MEC **(B)**. The costs and revenues are shown at different internal resistances of the system and with and without the recovery of ammonia

When the recovery of ammonia is taken into account, much higher internal resistances can be allowed for both systems at which the process is still economic; mainly because the savings for wastewater treatment that are reflected in the value of ammonia per kg of N removed. This means that for example, distances between electrodes can be allowed to be higher to still achieve higher revenue than cost, making scale-up of the systems easier. When ammonium recovery is taken into account the costs become relatively low compared to the revenue for both the MFC and the MEC. It should be noted however that, when locally produced, the production of electricity compared to hydrogen is probably more attractive.

These calculations show that the removal of ammonia in BESs gives a significant economic value in addition to the production of electricity in an MFC or hydrogen in an MEC, which leads to less stringent design criteria (*e.g.* in terms of internal resistance), and an easier road towards practical application. Kuntke et al. (2014) reported an internal resistance of 43 mΩ m^2 (Table 2.2) for urine treatment using an MEC with platinum coated titanium electrodes. The challenge now is to reach similar internal resistances with less expensive materials.

2.6 Challenges in bioelectrochemical systems for nitrogen recovery

In the previous sections, we have shown and compared the different processes for nitrogen removal and recovery in BESs. Although our analysis shows a promising prospect for application of ammonium recovery via membrane transport in an MFC or MEC, there are still several challenges to overcome before the technology can be applied in practice.

Most importantly, we need to optimize the ammonium recovery, and therefore the ammonium transport across the membrane. At present, the reported values for the ammonium removal efficiency from urine, *e.g.* the fraction of ammonium that is removed from urine, are around 30%. The removal of ammonium from the anode waste stream is dependent on several factors; most importantly (i) the concentration of ammonium in the wastewater, (ii) the removal of ammonium from the catholyte/cathode head space by stripping, (iii) the current density, (iv) the catholyte pH, (v) the type of membrane, and (vi) the equilibria of other ions at anode and cathode. Many of these factors are interrelated, *e.g.* the current density determines the catholyte pH [138] and is in turn dependent on the type of membrane and the ions present in solution [72]. These interactions should be studied in more detail to clarify how the removal efficiency and ammonium recovery can be improved. It has been shown that removing the ammonium/ammonia batch-wise from the catholyte by replenishing the catholyte results in higher ammonium removal rates [87]. In a continuous setup, removal of ammonium can be achieved by stripping,

where the soluble ammonia evaporates to gaseous ammonia by contact with a N_2 or H_2 gas stream, and subsequently absorbed in sulphuric acid, as has been done in the electrochemical ammonium recovery process [40]. Up until now such a system has not been tested and the performance of a BES connected to a stripper, and the maximum achievable ammonia recovery, needs to be determined. Another approach to understand the processes that determine ammonium transport is modelling. Dykstra et al. (2014) derived a one-dimensional steady state model of the urine MEC used by Kuntke et al. (2014) [139]. The model includes the transport of ions through the membrane and allowed to identify one of the main limiting factors of the system, which is the inert gas flow along the cathode. It was concluded that a higher N_2 flow or decreasing the pressure in the cathode chamber were needed to increase ammonia recovery. Modelling the system gave valuable insight and understanding of its performance. In urine, COD concentrations are approximately 10 g L^{-1}, and ammonium concentrations are approximately 9 g L^{-1}. Because ideally 0.57 kg of COD is required for the removal of 1 kg N, urine contains sufficient COD to recover all the ammonium, and no additional carbon source is required. In this ideal case, we assume that all the COD is converted into electrons and that ammonium is the single transported cation. Further experiments are needed to study which COD removal efficiency, coulombic efficiency, and nitrogen recovery can be achieved in a BES.

While all current nitrogen removal technologies require energy for the removal of nitrogen gas mainly through aeration, BESs, though not applied in practice yet, are a promising technology for energy efficient ammonia recovery. The main reason for the low energy requirement for MFCs and MECs, or even energy recovery, is the fact that no oxygen is required to oxidize the ammonium nitrate or nitrite. Instead, the movement of electrons from anode to cathode drives the transport and recovery of ammonium at the cathode.

The next step is to bring BESs in general, and also specifically for the application of nitrogen recovery, to a larger scale. A recent review article summarizes all the work performed until now on scaling-up of MFCs [140]. Their major observations are that in terms of design, both tubular and flat-plate systems still suffer from too high internal resistance. The main causes for these high internal resistances are that the electrode spacing is too high, electrode materials have limited conductivity, and contact between electrodes and current collectors is often not optimal. They point out that separators, like membranes, are crucial to obtain high treatment efficiency, although separators also increase the total internal resistance. Janicek et al. (2014) stress that waste streams with high organic concentrations are likely to generate higher performance [65], although the drawback is that COD removals are generally lower and as a result, treatment efficiencies are limited, when a single system is used. They conclude that pilot studies are essential to demonstrate the practical feasibility of BESs.

In 2013, Wetsus has set up a pilot BES at the water board of Fryslân located in Leeuwarden, the Netherlands in cooperation with partners from industry. The objective of this pilot experiment is to purify urine by removing the COD and ammonium, and recover energy in the form of hydrogen, in addition to ammonia gas. This installation consists of 4 flat-plate cells that are stacked in parallel with a total surface area of 0.16 m^2. With this pilot, we will demonstrate the feasibility of on-site treatment of urine and conversion into ammonium and hydrogen gas.

Acknowledgments

This work was performed in the cooperation framework of Wetsus, centre of excellence for sustainable water technology (www.wetsus.nl). Wetsus is co-funded by the Dutch Ministry of Economic Affairs and Ministry of Infrastructure and Environment, the European Union Regional Development Fund, the Province of Fryslân, and the Northern Netherlands Provinces. The authors like to thank the participants of the research theme "Resource Recovery" for the fruitful discussions and their financial support. This research has received funding from the European Union's Seventh Programme for research, technological development and demonstration under grant agreement No 308535.

CHAPTER 3

Load ratio determines the ammonia recovery and energy input of an electrochemical system

ABSTRACT

Complete removal and recovery of total ammonia nitrogen (TAN) from wastewaters in (bio) electrochemical systems has proven to be a challenge. The system performance depends on several factors, such as current density, TAN loading rate and pH. The interdependence among these factors is not well understood yet: insight is needed to achieve maximum ammonium recovery at minimal energy input. The aim of this study was to investigate the influence of current density and TAN loading rate on the recovery efficiency and energy input of an electrochemical cell (EC). We therefore defined the load ratio, which is the ratio between the applied current and the TAN loading rate. The system consisted of an EC coupled to a membrane unit for the recovery of ammonia. Synthetic wastewater, with TAN concentration similar to urine, was used to develop a simple model to predict the system performance based on the load ratio, and urine was later used to evaluate TAN transport in a more complex wastewater. High fluxes (up to 433 gN m^{-2} d^{-1}) and recovery efficiencies (up to 100%) were obtained. The simple model presented here is also suited to predict the performance of similar systems for TAN recovery, and can be used to optimize their operation.

This chapter has been published as: Rodríguez Arredondo M, Kuntke P, ter Heijne A, Hamelers HVM, Buisman CJN. Load ratio determines the ammonia recovery and energy input of an electrochemical system. *Water Res.* 2017, *111*, 330-337

3.1 Introduction

Nitrogen removal from wastewaters is necessary to prevent the pollution of receiving water bodies. Nitrogen, on the other hand, is an essential nutrient for plants, so it is used in the production of fertilizers to increase food production. Both the removal of nitrogen compounds from wastewater and their production are energy intensive [23, 58]. Energy use for the removal and production of nitrogen compounds can be reduced by recovering these from wastewater. In domestic wastewater, most of the nitrogen can be found in the form of ammonium (NH_4^+) or ammonia (NH_3), depending on the temperature and pH [141]. The combination of both NH_4^+ and NH_3 is referred to as total ammonia nitrogen (TAN). Direct recovery of TAN from wastewater can save resources by creating a shortcut in the nitrogen cycle: it accomplishes removal and eliminates the need of an artificial nitrogen fixation process [89].

(Bio)electrochemical systems ((B)ESs) have been proposed as an energy-efficient alternative to recover TAN from wastewater [40, 69, 77, 89]. These systems consist of two electrodes: an anode, where an oxidation reaction takes place, and a cathode, where reduction occurs. Energy from the wastewater can be recovered in the form of electricity or chemicals (such as H_2) depending on the cathodic reaction [35]. In bioelectrochemical systems (BESs), at least one of the reactions taking place at the electrodes is catalysed by microorganisms; while in electrochemical systems (ESs) all reactions are purely electrochemical and no microorganisms are involved. In the case of TAN recovery in ES, water electrolysis usually takes place, where oxygen is produced at the anode and H_2 is produced at the cathode.

The anode and cathode chambers of (B)ESs are often separated by an ion exchange membrane [35, 63]. When the electrons produced in the oxidation reaction flow through an external circuit from anode to cathode, ions in solution migrate through this ion exchange membrane to maintain electroneutrality [142]. In (B)ESs for the recovery of TAN, a cation exchange membrane (CEM) is used to allow the transport of NH_4^+ in the wastewater from anode to cathode. In the cathode chamber, the NH_4^+ removed from the wastewater is converted to volatile NH_3 due to the high pH of the catholyte (cathode electrolyte) [115]. To strip the NH_3 out of the catholyte effectively, an additional gas flow or stripping process is needed [87, 139]. The NH_3 is then recovered as gas or absorbed into an acid.

TAN has successfully been recovered from nitrogen-rich wastewaters (like anaerobic digestate or urine) by the combination of (bio)electrochemical systems with either stripping-absorption [40, 88] or gas-permeable hydrophobic membranes (TransMembraneChemiSorption, or TMCS) [143]. Complete TAN removal (how much TAN is removed from the wastewater) and recovery (how much TAN is recovered in the acid or

as gas) in these integrated systems, however, has proven to be a challenge. As examples, an ES coupled to a stripping-absorption unit treating urine obtained an average TAN removal efficiency of 75% and an average recovery efficiency of 57% [88]; while a BES coupled to a gas-permeable membrane unit obtained an average of 42% removal efficiency and a maximum recovery of 49% [143].

In order to be effectively recovered, TAN needs to be transported from anode to cathode. It has been shown that TAN transport across the CEM is determined by several factors, such as current density, TAN loading rate, pH and continuous removal of NH_3 from the cathode by the stripping or membrane unit [40, 61, 69]. The interdependence among these factors, however, is currently not well understood: insight is needed to achieve maximum TAN recovery at minimal energy input. In steady-state, NH_4^+ is the main charge carrier, since it is the only ion effectively removed from the catholyte (by stripping or any other means); however, at a certain point (limiting current density), the NH_4^+ gets depleted at the membrane surface (anode side), causing other ions to transport the charge. This phenomenon can cause the membrane potential, and therefore, the total energy input, to increase steeply. The limiting current density itself depends on, among others, the bulk concentration and the electrolyte flow rate [144]. Thus, both current density and loading rate can affect the system performance. We therefore defined the load ratio (L_N) as the ratio between the current density and TAN loading rate, in order to study its relation to TAN transport.

The aim of this study was to investigate the influence of current density and TAN loading rate on the TAN recovery efficiency and energy input of an electrochemical system. The system consisted of an electrochemical cell (EC) coupled to a TMCS unit for the recovery of ammonia. An EC was chosen instead of an MEC [143] to be able to work at high and constant currents, which is needed to study the effects of current in combination with TAN loading on TAN transport. Whereas the main difference between both systems is the anodic oxidation reaction (organic carbon source vs. water oxidation), other aspects are similar: hydrogen evolution reaction at the cathode [89, 99] and high pH at the cathode [145]. Synthetic wastewater, with TAN concentration similar to urine, was used to develop a simple model to predict the performance of the system based on the load ratio, and urine was later used to evaluate TAN transport in a more complex wastewater.

3.2 Materials and methods

3.2.1 Experimental setup

The experiments were performed in an EC coupled to a membrane module (TMCS unit) (Figure 3.1).

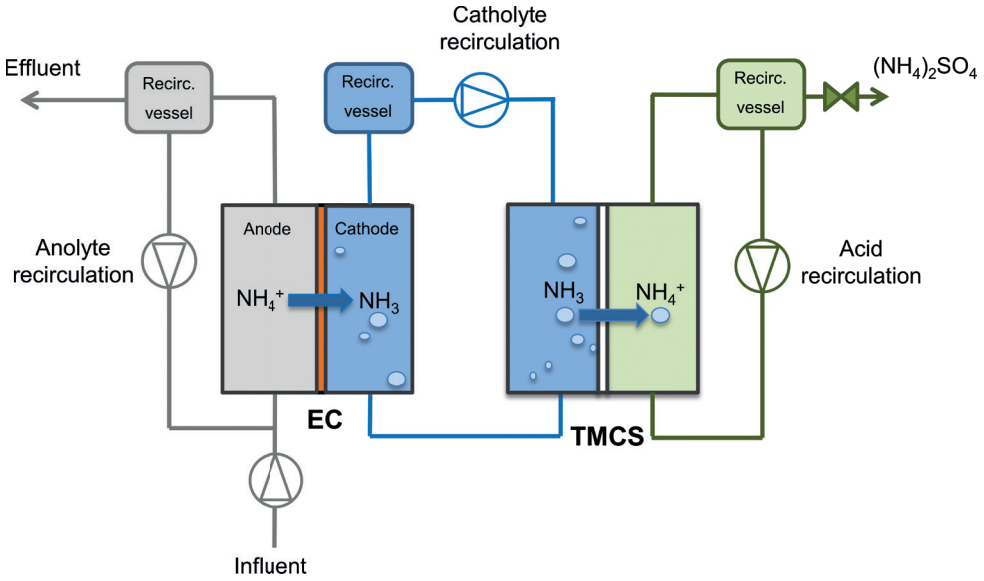

Figure 3.1. Schematic representation of experimental setup. EC= Electrochemical Cell; TMCS= TransMembrane ChemiSorption. There were two membranes in the system: a cation exchange membrane in the EC and a gas-permeable hydrophobic membrane in the TMCS unit.

The catholyte was recirculated via the TMCS unit for recovery of NH_3. The TMCS unit contains a tubular hydrophobic membrane through which ammonia (gas) can pass and then be absorbed by an acid. This configuration was chosen since it has been proven to effectively remove ammonia from the catholyte, facilitating the overall TAN removal and recovery [143].

The electrochemical cell consisted of two poly (methyl methacrylate) (PMMA) panels (21 cm x 21 cm) which encased the anode and the cathode. Titanium mesh electrodes with a 50 g m^{-2} platinum coating (Magneto Special Anodes, The Netherlands) were used as anode and cathode. The dimensions of the anode and cathode chambers are 10 cm x 10 cm x 0.2 cm. Anode and cathode chambers were separated by a cation exchange membrane (Nafion® 117, Ion Power GmbH, Germany) with a projected surface area of 0.01 m^2 (same as anode and cathode). The hydraulic volume of the anode chamber, including

the recirculation vessel, was 200 mL. The hydraulic volume of the cathode chamber, including the recirculation vessel and the volume encased in the TMCS unit, was 240 mL.

The TMCS unit used in this study consisted of a tubular polyproplylene membrane (pore size 200 nm, type Accurel PP V8/HF, CUT Membrane Technology GmbH, Germany) encased in a custom-made membrane module (Kuntke et al. 2016). The TMCS-membrane has an outer surface area of 0.04 m^2. It was operated in crossflow mode, with the catholyte on the inner and the acid on the outer side of the TMCS membrane.

Anode and cathode potential were measured versus reference electrodes (Ag/AgCl 3 M KCl, +0.2 V vs. NHE, QM711X, ProSense BV-QiS, Oosterhout, The Netherlands), which were placed in the respective electrolytes near the inlet of anode and cathode chambers. The reference electrodes were connected to a high impedance preamplifier (Ext-Ins technologies, Leeuwarden, The Netherlands). Electrical current was controlled by an external power supply (ES 030-5, Delta Elektronika BV, Zierikzee, The Netherlands).

Temperature and pH of both anolyte (anode electrolyte) and catholyte were measured by pH meters (Orbisint CPS11D sensor with Liquisys M COM 253 transmitter, Endress+Hauser BV, Naarden, The Netherlands) placed in each recirculation vessel. A data logger (Memograph M RSG40, Endress + Hauser BV, Naarden, The Netherlands) recorded each minute the anode and cathode potentials, cell voltage and anode and cathode pH.

Two peristaltic pumps (Masterflex L/S, Metrohm Applikon BV, Schiedam, The Netherlands) were used in the system: one to provide fresh anode medium continuously and the other to recirculate both anolyte and catholyte. A diaphragm pump (SIMDOS 10, KNF Flodos AG, Sursee, Switzerland) was used to recycle the acid through the TMCS unit.

3.2.2 System operation

The system was operated at room temperature (23.4 ± 1.1 °C). The anode chamber of the electrochemical cell had a continuous inflow of fresh medium (anolyte inflow rate), while both the cathode chamber and TMCS unit were operated in batch mode. All three liquids (anolyte, catholyte and acid) were recirculated over their respective chambers at 70 mL min^{-1}. Two anolyte inflow rates were used: 1.1 mL min^{-1} and 0.2 mL min^{-1}, resulting in an HRT of 3.0 and 16.7 h.

The effluent from the anode chamber was collected in a closed container sealed with a water lock. Both anode and cathode recirculation vessels had a vent to let the produced gasses escape.

Steady-state was defined as the situation in which anode and cathode pH, as well as anode and cathode potentials were stable. After taking two samples in steady-state, the experiment was finished.

3.2.3 Media composition

Two types of wastewater were used as anolyte during the experiments: a simplified synthetic wastewater and pre-treated human urine. The synthetic wastewater consisted of 13.7 g L^{-1} $(NH_4)_2CO_3$ and 4.6 g L^{-1} Na_2CO_3 (0.14 and 0.04 M, respectively). This composition was chosen to have similar concentrations of TAN and Na^+ compared to urine [69], but with only one competing cation (Na^+) to simplify the study of ammonium transport. Sodium was chosen as the competing cation due to its high predominance in urine. The pH of the synthetic wastewater was 9.3 ± 0.1. Urine was collected from the water-free urinals (Urimat®, Biocompact, Rotterdam, The Netherlands) installed in the male bathrooms of Wetsus (Leeuwarden, The Netherlands). The collected urine was stored in a tank for approximately 7 days, and later pre-treated by struvite precipitation and filtration to remove phosphate [87]. Struvite precipitation was performed at a molar ratio of 1.3:1 (Mg:P) using $MgCl_2.6H_2O$ as the magnesium source. After precipitation, the urine was filtered through a 10 µm cartridge filter (Van Borselen Filters, Zoetermeer, The Netherlands) to remove the struvite crystals. The urine was used in the experiments immediately after filtration (pH 9.2 ± 0.1). The composition of the pre-treated urine can be found in Table S3.1 (Supporting information).

The catholyte was a 0.09 M NaOH solution, in order to have the same sodium concentration in both anolyte and catholyte. One litre of 1M H_2SO_4 was used as the acid for absorption in the TMCS unit. The anode chamber, cathode chamber, and the TMCS unit were emptied completely and filled with fresh media before starting a new experiment.

3.2.4 Experimental plan

Eight experiments were performed with synthetic wastewater, as shown in Table 3.1. Two of these experiments were performed with no applied current (open circuit) to investigate TAN transport by diffusion. The other six experiments were performed to study TAN transport in dependence of applied current density. These six experiments resulted in three sets of conditions with respect to the applied current density: balanced TAN loading ("sufficient"), excess TAN loading ("excess") and insufficient TAN loading ("deficit"). These conditions are defined by the parameter load ratio (L_N), which is a relation between the applied current and the TAN loading rate (both expressed in A m^{-2}) (Equation 3.1):

$$L_N = \frac{j_{applied}}{C_{anolyte\ inflow,TAN} * Q_{anode} * \frac{F}{A_m}}$$ Equation 3.1

Where $j_{applied}$ is the applied current (A m^{-2}), $C_{anolyte\ inflow,\ TAN}$ is the molar concentration of TAN in the anolyte inflow (mol m^{-3}), Q_{anode} the anolyte inflow rate ($m^3\ s^{-1}$), F the Faraday constant (96485 C mol^{-1}) and A_m the surface area of the cation exchange membrane (0.01 m^2).

Therefore, a L_N lower than 1 means that there is more TAN than the current can transport ("excess"), whereas a L_N higher than 1 means that the TAN is limiting ("deficit"). A load ratio equal to zero describes open circuit experiments ($j_{applied}$ 0 A m^{-2}). A L_N of 1 describes a situation in which the TAN loading and the applied current are equal ("sufficient"). Due to variations in the TAN concentration, however, it is challenging to achieve a load ratio of exactly 1.0. Therefore, the load ratios close to 1 are also considered as "sufficient".

The synthetic wastewater experiments were used to study and model the TAN transport processes in the system. Afterwards, three experiments were performed with urine (Table 3.1) to evaluate TAN transport in a more complex mixture of ions and to observe how these results fit to the model obtained with synthetic wastewater. These three experiments were chosen based on the fact that the application of (B)ESs for the treatment of urine has the objective of achieving high TAN removal efficiencies and transport rates, which implies "sufficient" or "deficit" load ratios.

Table 3.1. Experiments performed in the study and their load ratio (L_N). Sufficient, deficit and excess refer to the TAN loading with respect to the applied current. Synthetic wastewater and urine were used as anolyte

	Q_{anode} = 0.2 mL min^{-1}		**Q_{anode} = 1.1 mL min^{-1}**	
$j_{applied}$	L_N	Condition	L_N	Condition
A m^{-2}	-		-	
0	0.00	Diffusion	0.00	Diffusion
10	1.20	Sufficient	0.22	Excess
20	2.54	Deficit	0.45	Excess
50	6.16	Deficit	1.33	Sufficient
20	2.72	Deficit (urine)	-	-
50	6.48	Deficit (urine)	1.18	Sufficient (urine)

3.2.5 Sampling and chemical analysis

Before starting each experiment, samples were taken from the influent container and recirculation vessel of both anode and cathode. At the completion of one hydraulic retention time (HRT), a sample was taken from the anolyte recirculation vessel and from the acid. Two samples were taken from the recirculation vessel of both anode and cathode at steady state (determined by a constant anode and cathode pH, as well as anode and cathode potentials) within a period of 15 to 20 minutes. Steady state was reached within 20-40 hours, depending on the experiment. A final sample was taken from the acid and the anolyte effluent container, and the experiment was finished immediately afterwards.

The samples were filtered through 0.45 µm filters (PTFE syringe filters, VWR International B.V., Amsterdam, The Netherlands) prior to analysis. TAN and sodium concentrations for the synthetic wastewater experiments, as well as chloride, nitrite, nitrate, sulphate, potassium, magnesium and calcium concentrations from the urine experiments were measured by ion chromatography in duplicate. The ion chromatographs used were the Metrohm Compact IC Flex 930 with a cation column (Metrosep C 4- 150/4.0) and the Metrohm Compact IC 761 with an anion column (Metrosep A Supp 5- 150/4.0), both equipped with conductivity detectors. The acid samples from the TMCS were analysed by a cuvette test kit for ammonium (LCK 303, spectrophotometer XION 500, Dr. Lange Nederland B.V., The Netherlands).

3.2.6 Calculations

The equations for the calculations of removal efficiency of TAN (RE_{TAN}, how much was removed from the TAN that entered the system), recovery efficiency of TAN (how much of the TAN supplied via the anolyte inflow was recovered in the acid), flux of TAN over the CEM (J_{TAN}), flux of NH_3 over the TMCS membrane ($J_{NH3,TMCS}$), transport efficiency of NH_4^+ (tE_{NH4+}) and transport energy input can be found in the Supporting information.

3.2.7 Model development

A simple removal efficiency model was derived (Equation 3.2; derivation shown in Supporting information) based on the anode and cathode mass balance equations, the transport equations for the NH_3 and NH_4^+ fluxes, and initial assumptions of: i) steady state and ii) completely mixed anode and cathode chambers. Assumption i) implies 100% transport efficiency for NH_4^+, since it is the only ion effectively removed from the catholyte, by the TMCS unit, at steady state.

$$RE_{TAN,model} = ((1 - \beta) * L_N + \beta * \gamma) * 100 \qquad \text{Equation 3.2}$$

Where $RE_{TAN, model}$ (%) is the predicted removal efficiency of TAN, L_N (-) is the load ratio (Equation 3.1), and β (-) and γ (-) are parameters described by Equation 3.3 and Equation 3.4, respectively.

$$\beta = \frac{k_m}{k_m + K_g}$$ Equation 3.3

Where k_m (m s^{-1}) is the mass transfer coefficient of ammonia through the CEM and K_g (m s^{-1}) is a term which includes the gas transfer coefficient of ammonia through the TMCS (Equation S3.15).

$$\gamma = \frac{K_g * A_m}{Q_{anode}} * f_{NH3,anode}$$ Equation 3.4

Where A_m (0.01 m^2) is the surface area of the CEM, Q_{anode} (m^3 s^{-1}) the anolyte inflow rate and $f_{NH3,anode}$ (-) the fraction of NH_3 in the anolyte.

The experimental data of synthetic wastewater were used to estimate the model parameters ß and ɣ (Equations 3.3 and 3.4, respectively). K_g was determined by plotting the TMCS flux ($J_{NH3,TMCS}$, in mol N m^{-2} s^{-1}) against the NH_3 concentration in the catholyte (mol m^{-3}). K_g is the slope of the linear regression curve.

After obtaining K_g, γ was calculated for each experimental point. Only the current-induced experiments were included in the model. Then, an optimum β was obtained by minimizing the sum of the squares of the differences between the experimental removal efficiencies and Equation 3.2. Once the optimal β was obtained, we calculated k_m. Equation 3.2 was then used to predict the removal efficiency of the system depending on the load ratio.

3.3 Results and discussion

3.3.1 TAN flux over the CEM equals TAN flux over the TMCS

There are two fluxes of nitrogen in the system: TAN over the cation exchange membrane (J_{TAN}) and NH_3 over the TMCS membrane ($J_{NH3, TMCS}$). When both fluxes are the same, steady state is reached. Figure 3.2 shows that there is a direct linear relationship with a slope of 1.06 and a R^2 of 0.98 for the synthetic wastewater data points. The slope shows that the flux over the cation exchange membrane was around 6% higher than the one over the TMCS, which indicates near steady state. The system thus effectively transported ammonia from the influent to the acid. This was also the case for urine as influent, as both fluxes across CEM and TMCS membrane were similar, too.

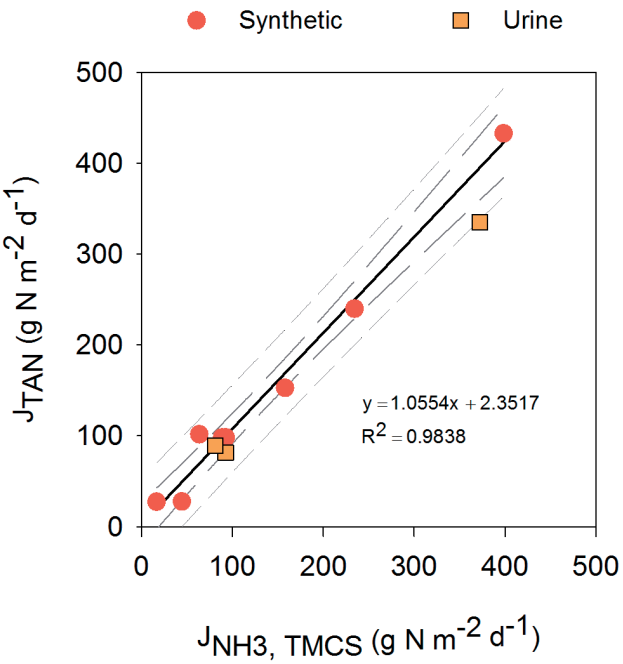

Figure 3.2. TAN flux over the cation exchange membrane (J_{TAN}) against NH_3 flux over the TMCS membrane ($J_{NH3, TMCS}$). The regression line was fitted only for the synthetic wastewater points for modelling purposes. Long-dashed and short-dashed curves represent the 95% confidence interval and 95% prediction interval for the linear regression, respectively. This figure shows that the system was near steady state.

3.3.2 Load ratio is an essential parameter to assess TAN removal efficiency and transport energy input

To study TAN removal efficiency and energy input under different experimental conditions, we defined the load ratio, which is the ratio between the applied current (in A m^{-2}) and the TAN loading rate (in A m^{-2}) (Equation 3.1). The main trends and figures are shown in this section, while all results are summarized in Table S3.2.

Figure 3.3 shows the experimental data for TAN removal efficiency (RE_{TAN}) as a function of the load ratio. At L_N much higher than 1, there is limited TAN compared to the applied current, and for synthetic wastewater this resulted in TAN removal efficiencies between 99% and 100%. For L_N lower than 1, there is excess TAN compared to the applied current, and therefore, TAN removal efficiencies were much lower. In a situation where current is applied, TAN is transported through the membrane by a combination of migration (current-induced) and diffusion (concentration gradient-induced). At L_N 0, no current is

applied, so RE_{TAN} is determined by diffusion alone. The model, as seen in Figure 3.3, is well suited to describe the relation between load ratio and TAN removal efficiency.

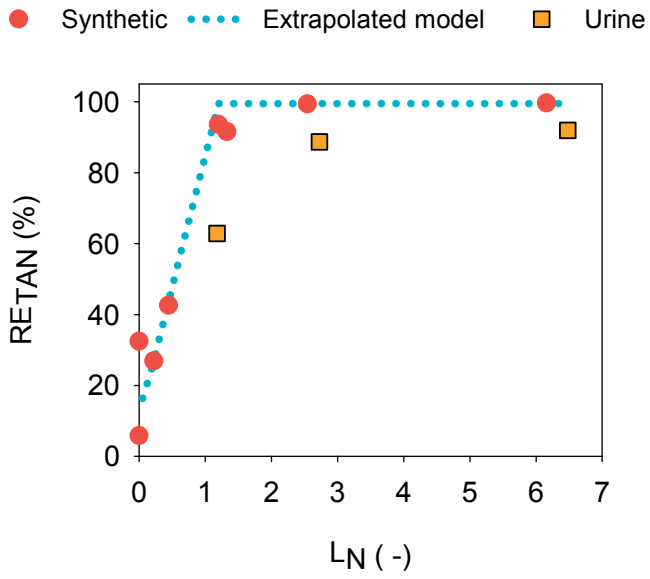

Figure 3.3. TAN removal efficiency (RE_{TAN}) with respect to load ratio (L_N). L_N is the ratio between the applied current and the TAN loading rate, both in units of A m^{-2}. The synthetic wastewater data set was used for modelling purposes. The dotted line depicts the model results. Data points at 0 load ratio belong to the open circuit experiments and are not fitted in the model. The model based on the load ratio can accurately describe the system performance in terms of removal efficiency.

A RE_{TAN} of 100% would be expected at a L_N of 1 in steady state, since at this load ratio the applied current equals the TAN supplied. Our experiments show, however, that the system needs to be operated at a load ratio higher than 1 to achieve complete TAN removal, because ammonia diffusion from cathode to anode also contributes to TAN transport. When NH_3 diffuses through the CEM from cathode to anode, it is protonated to NH_4^+ when close to the anode [146], so energy is spent in transporting NH_4^+ back to the cathode.

In addition to TAN removal, the load ratio is also a useful parameter to assess energy efficiency. The transport energy input is defined here as the electrical energy input to the EC that was used for transport processes, independent of the reactions occurring at the electrodes. Therefore, it only takes into account the potential loss due to the transport of ions through the membrane ($E_{transport}$, measured as the potential difference between the reference electrodes) and the potential loss due to the pH gradient over the membrane ($E_{\Delta pH}$) [72]. Values for $E_{transport}$, E_{pH} (along with final anolyte and catholyte pH) and the total

electrical energy input can be found on Table S3.3. Figure 3.4 shows the relation between the load ratio (L_N) and transport energy input for the recovery of TAN.

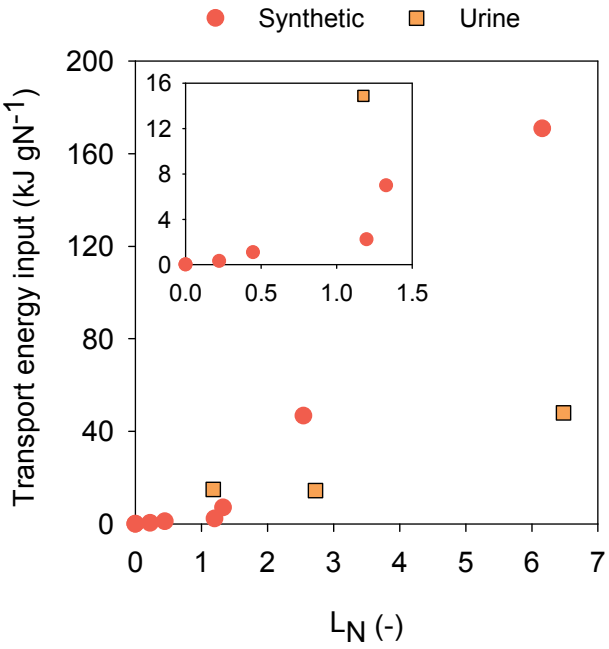

Figure 3.4. Energy input used to transport TAN (in kJ per g N removed) with respect to load ratio (L_N). L_N is the ratio between the applied current and the TAN loading rate, both in units of A m^{-2}. The transport energy input takes into account only the potential losses due to transport and pH gradient over the membrane. This figure shows that working at load ratios much higher than the 'limiting' one (1.2) costs considerably more energy, even though no considerable increase in removal efficiency can be achieved.

In our experiments with synthetic wastewater, at L_N <1.2, the energy input for transport of TAN was minimal (see insert in Figure 3.4), but the TAN removal efficiency was low (Figure 3.3). At L_N > 1.2, the applied current was higher than the current that can be carried by NH_4^+. This resulted in depletion of NH_4^+ at the membrane surface (anode side), and therefore higher energy input for TAN transport. In these experiments, where energy input for transport increases steeply, the RE_{TAN} reached values close to 100%. At L_N around 1, however, 92- 94% TAN removal efficiencies were already achieved, even though the energy input for transport was considerably lower than that for L_N > 1.2. Thus, working at higher load ratios than the 'limiting' one does not provide an advantage anymore: it costs more energy, and no considerable increase in removal efficiency can be achieved.

3.3.3 System performance using urine

For the experiments with urine, a similar trend in transport energy input was observed (Figure 3.4), although at L_N > 1.2 it was considerably lower than for synthetic wastewater. In the two urine cases with L_N > 1.2, the potential loss due to transport was 10 to 30 times lower than the corresponding synthetic wastewater cases (Table S3.3). The reason for a lower $E_{transport}$ in the urine experiments may be related to the difference in composition between synthetic wastewater and urine. Urine contains a more complex mixture of ions than the synthetic wastewater (K^+, Mg_2^+, Ca_2^+, Cl^-, SO_4^{2-}, etc.), so its conductivity is higher, which affects transport losses. In the urine case at L_N 1.18, the transport energy input was higher than its synthetic counterpart because the TAN removal efficiency was relatively low (63% vs. 92% for synthetic), resulting in higher transport energy input per kg TAN removed.

The experiments with urine and synthetic wastewater also showed a similar trend regarding TAN removal efficiency (Figure 3.3). Higher load ratios resulted in higher RE_{TAN}, even though removal efficiencies with urine were lower than those with synthetic wastewater. The reason for this lower removal efficiency could be explained by the presence of chloride (Cl^-). Urine contains Cl^-, which can potentially be oxidized electrochemically to produce chlorine (Cl_2). Chloride oxidation can result in hypochlorite production, which can react with the ammonium in the anolyte to form chloramines [68, 81, 147–149]. The chloramine formation decreases the amount of NH_4^+ available for transport, which would result in lower TAN removal efficiency. Hypochlorite can also oxidise the ammonium to nitrogen [148, 150, 151], in which case the TAN would be removed as N_2 gas, but not recovered in the acid. Chloride concentration was measured in the three urine experiments, and only in the case of the highest L_N (6.48) a decrease in chloride concentration was found (see Table S3.4). The experiment at L_N 6.48 is also the one in which the difference between TAN removal and recovery efficiencies was the highest from the data set (Table S3.2), and where the highest anode potential (1.874 V vs. Ag/AgCl) was measured. The above suggests that chloride oxidation might have occurred and, since the TAN was removed but not found back in the acid, it was probably removed as N_2 gas. The presence of Cl^- in urine might therefore have affected the performance of the system, resulting in lower removal efficiencies and also deviations from the model based on chloride-free synthetic wastewater.

3.3.4 TAN flux and transport efficiency performance

The TAN flux (J_{TAN}) is the total flux of ammonium and ammonia that was transported from the anode to the cathode chamber through the CEM. Figure 3.5A shows J_{TAN} for all experiments, plotted as function of the load ratio. When no current is applied (L_N 0), only diffusion determines the overall membrane transport process. For this reason, J_{TAN} for both diffusion experiments was the same (27 gN m^{-2} d^{-1}). The effect of applied current on J_{TAN} was

clearly seen at the high inflow rate experiments (1.1 mL min^{-1}) with synthetic wastewater. At this inflow rate there was sufficient (or excess) TAN in the system, so the flux increased with increasing applied current, as expected. On the other hand, for the low inflow rate experiments (0.2 mL min^{-1}), the effect of applied current density was not apparent due to the TAN limitation in the system, meaning that already at the lowest current, TAN flux was highest. The highest flux obtained was 433 gN m^{-2} d^{-1}, corresponding with the experiment at the highest inflow rate and applied current (L_N = 1.33).

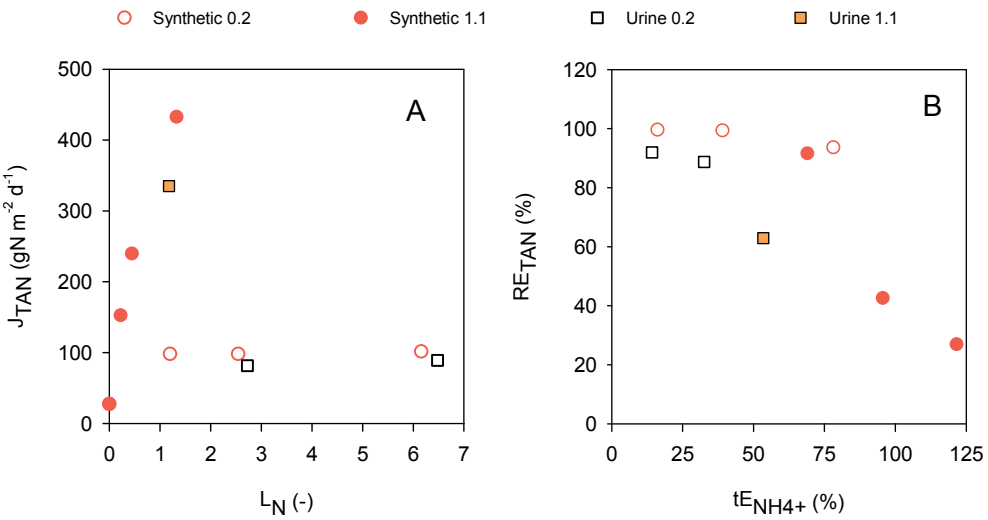

Figure 3.5 (**A**) TAN flux over the cation exchange membrane (J_{TAN}) against load ratio (L_N). (**B**) TAN removal efficiency (RE_{TAN}) in relation to NH_4^+ transport efficiency (tE_{NH4+}). L_N is the ratio between the applied current and the TAN loading rate, both in A m^{-2}. In the legend, 0.2 and 1.1 represent the anolyte inflow rate (mL min^{-1}). The effect of applied current density is not apparent in A) for the low inflow rate due to TAN limitation in the system. In B), it can be seen that high removal efficiencies can be obtained at both high and low transport efficiencies.

The transport efficiency refers to the contribution of an ion to the total charge transport across the CEM. In one experiment with TAN in excess (synthetic wastewater, 1.1 mL min^{-1} and 10 A m^{-2}, L_N 0.22) the transport efficiency of NH_4^+ was higher than 100%; likely due to the effect of diffusion. This study shows that the highest TAN removal efficiencies were obtained at the lowest NH_4^+ transport efficiencies (tE_{NH4+}) (Figure 3.5B), which is in agreement with other studies [40, 88]. High TAN removal efficiencies, however, were also obtained at high NH_4^+ transport efficiencies (Figure 3.5B). This fact indicates that transport efficiency alone is not well suited to predict how much TAN the system can remove.

The three experiments at L_N around 1 showed very different TAN fluxes (Figure 3.5A). On one hand, the experiment with synthetic wastewater at 0.2 mL min^{-1} (L_N 1.20) had a lower

TAN flux compared to the two experiments at 1.1 mL min^{-1} (L_N 1.33 and 1.18 for synthetic wastewater and urine, respectively), which is explained by the fact that there was less TAN entering the system (low inflow rate). On the other hand, J_{TAN} for the urine experiment at 1.1 mL min^{-1} (L_N 1.18) was lower than the corresponding synthetic (L_N 1.33). The TAN flux for the urine experiment at L_N 1.18 might be lower than its synthetic one because its NH_4^+ transport efficiency was lower (Figure 3.5B). In the case of the lowest inflow rate the transport efficiency of NH_4^+ for urine and synthetic are similar, which relates to their similar TAN fluxes.

Transport efficiency is dependent on both current density and TAN loading rate. In TAN limited systems, the current carries more charge than can be supplied via TAN, and the result is that other ions are transported across the CEM. This can be seen in Figure 3.5B, where the lowest transport efficiencies coincide with the cases in which TAN was limiting: all TAN was removed, so other ions contributed to the charge transport. Transport efficiency calculations show that 53-100% of the total charge (in the cases of load ratios lower than 1.3) was carried by NH_4^+. The transport efficiency of other ions (i.e. K^+, Na^+ and H^+/OH^-) is shown in Figure S.3.1. Thus, the combination between TAN loading rate and current, as reflected in the load ratio, is essential to draw conclusions on the system's performance.

3.3.5 High removal and recovery efficiencies are achieved in the EC-TMCS system

Overall, high removal and recovery efficiencies were achieved except for the situations with TAN in excess. Even though from Figure 3.5B it is clear that in these situations most of the current was used to transport ammonium (highest tE_{NH4+}), the applied current was not enough to remove all TAN.

As seen in the open circuit experiments, the system was able to remove part of the TAN without applying any current (Figure 3.3). Diffusion showed to account for a substantial part of the TAN removal in the system, especially in the case of the low inflow rate. A RE_{TAN} of 32% was obtained in the 0.2 mL min^{-1} open circuit experiment, while for the 1.1 mL min^{-1} it resulted in 6%. This difference might be due to the longer hydraulic retention time of the lower inflow rate (16.7 vs. 3 h). Previous studies using MECs or ECs using recovery methods other than the TMCS obtained similar removal efficiencies even under influence of combined diffusion and migration [40, 87].

Most of the TAN removed from the system (84% or more) was recovered in the acid in all cases, with the urine experiment at 0.2 mL min^{-1} and 50 A m^{-2} showing the lowest recovery. This was probably due to chloride oxidation, as mentioned in Section 3.3.3. In two cases, recoveries were slightly higher than removals (Table S3.2). Whereas the removal efficiency is calculated based on steady state measurements, the recovery efficiency is determined

from the increase in TAN concentration in the sulphuric acid solution over the whole experimental period, which may result in small imbalances.

3.3.6 Load ratio as a parameter of comparison to other studies

Usually, it is difficult to find a good measure of comparison between different (bio) electrochemical systems for TAN removal and recovery, since different hydraulic retention times, current densities and inflow TAN concentrations are used. We propose here the use of the load ratio as a fair parameter of comparison. It is important to take into account, however, that steady-state situations are essential for these comparisons to be valid.

Figure 3.6 compares the model developed here to the results obtained in four recent studies for the recovery of ammonia: one of an EC attached to a stripping-absorption unit in which synthetic urine and real urine were used [88], another one in which an MEC was coupled to a TMCS unit (such as the one used in this study) [143], one in which an MEC and an EC attached to a stripping-absorption unit treated synthetic wastewater [145] and one in which an EC coupled to the same stripping-absorption units used in the other two studies treated digestate [40]. These studies were chosen because they are similar to this work in terms of the use of an integrated system in the cathode for the recovery of NH_3. The data points are calculated based on the inflow TAN concentrations, inflow rates, current densities and removal efficiencies provided by the different studies. As in the case of urine shown in Figure 3.3, the data points do not match completely, because the model is fitted to our synthetic wastewater data. It is expected then, that with varying systems and wastewater composition, the optimum load ratio will change. The RE_{TAN} determined in the first two studies [88, 143], however, is similar to what would be expected by using the model. The other two studies differ significantly from the model, due to, among other reasons, some complications during the experiments (such as a low stripping-absorption efficiency) and varying wastewater composition [40, 145]. The simple model presented here is therefore also suited to predict the performance of other optimally functional and similar systems for TAN recovery.

This model based on the load ratio provides a reasonable description of the expected outcomes in terms of removal efficiency and the threshold in which the system can be optimally operated. Since the focus of this study was to design a simple steady-state model to describe a complex system, the model may be further optimized by taking into account other processes occurring in the system, such as ionic speciation.

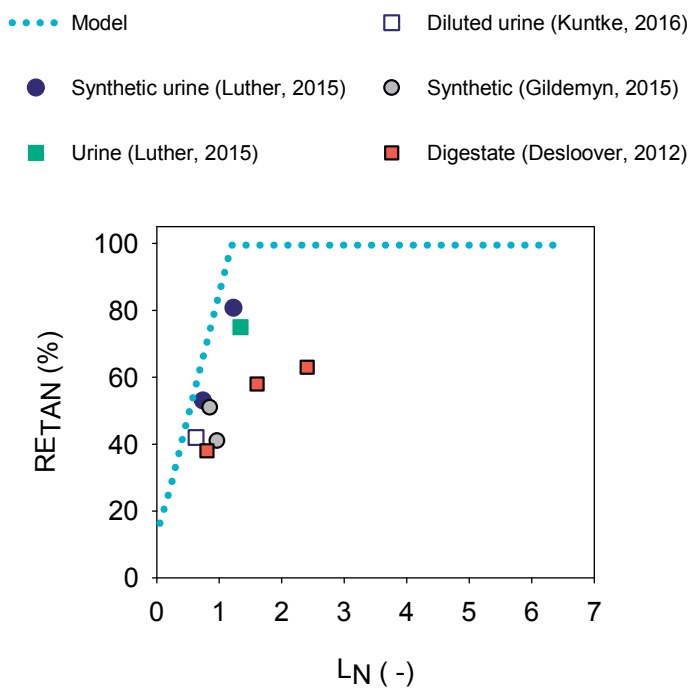

Figure 3.6. TAN removal efficiency (RE_{TAN}) with respect to load ratio (L_N). L_N is the ratio between the applied current and the TAN loading rate, both in units of A m^{-2}. The dotted line is the model developed in this study, while the other data points are based on four other studies.

3.4. Conclusions

- The load ratio (ratio between applied current and TAN loading rate) is an essential parameter to assess TAN removal efficiency and energy input of current-driven processes.
- Working at higher load ratios than the 'limiting' one does not provide an advantage anymore: it costs more energy, and no considerable increase in removal efficiency can be achieved.
- A RE_{TAN} of 100% would be expected at a L_N of 1 in steady state, since at this load ratio the applied current equals the TAN supplied. Our experiments show, however, that the system needs to be operated at a load ratio higher than 1 to achieve complete TAN removal, because ammonia diffusion from cathode to anode also contributes to TAN transport.
- A similar trend in system performance was observed for both synthetic wastewater (with TAN and sodium concentrations similar to urine) and urine.
- The model based on the load ratio described well the experimental data, is also suited to predict the performance of similar systems for TAN recovery, and can be used to optimize their operation.

Acknowledgements

This work was performed in the cooperation framework of Wetsus, European Centre of Excellence for Sustainable Water Technology (www.wetsus.eu). Wetsus is co-funded by the Dutch Ministry of Economic Affairs and Ministry of Infrastructure and Environment, the European Union Regional Development Fund, the province of Fryslân, and the Northern Netherlands Provinces. This research has received Funding from the European Union's Seventh Programme for research, technological development and demonstration under grant agreement No 308535. The authors like to thank the participants of the research theme "Resource Recovery" for the fruitful discussions and their financial support.

3.5 Supporting information

Table S3.1. Concentration of anions and cations measured in urine used in experiments (after struvite precipitation)

Ion	Concentration (g L^{-1})
Cl^-	3.59 ± 0.22
NO_2^-	<0.01
NO_3^-	<0.02
PO_4^{3-}	<0.01
SO_4^{2-}	0.54 ± 0.04
Na^+	1.73 ± 0.10
NH_4^+	4.25 ± 0.12
K^+	1.61 ± 0.06
Mg^{2+}	<0.02
Ca^{2+}	<0.02

Table S3.2. TAN removal efficiency (RE_{TAN}), recovery efficiency, flux (J_{TAN}), transport efficiency (tE_{NH4+}), and energy input due to transport obtained in the set of experiments at different load ratios (L_N). Synthetic wastewater and urine were used as anolyte

Q_{anode}	$j_{applied}$	Experiment	L_N	RE_{TAN}	Recovery efficiency TAN	J_{TAN}	tE_{NH4+}	Transport energy input
mL min^{-1}	A m^{-2}		-	%	%	gN m^{-2} d^{-1}	%	kJ g N^{-1}
0.2	0	Open circuit	0.0	32	32	27	0	0.0
	10	Sufficient	1.2	94	83	98	78	2.3
	20	Deficit	2.5	99	93	98	39	49.2
	50	Deficit	6.2	100	101	101	16	164.7
1.1	0	Open circuit	0.0	6	10	27	0	0.0
	10	Excess	0.2	27	27	152	122	0.3
	20	Excess	0.4	43	37	240	96	1.1
	50	Sufficient	1.3	92	84	433	69	7.1
0.2	20	Deficit (urine)	2.7	89	83	82	33	14.5
1.1	50	Sufficient (urine)	1.2	63	56	335	53	14.2
0.2	50	Deficit (urine)	6.5	92	77	89	14	47.6

Table S3.3. Potential loss due to transport ($E_{transport}$), final anolyte and catholyte pH, potential loss due to the pH gradient over the membrane (E_{pH}) and total electrical energy input. Urine experiments are marked as (*)

Q_{anode}	$j_{applied}$	$E_{transport}$	Final anolyte pH	Final catholyte pH	E_{pH}	Total electrical energy input
mL min^{-1}	A m^{-2}	V	-	-	V	kJ g N^{-1}
0.2	0	-	8.8	8.1	-	0.0
	10	0.08	6.9	9.9	0.18	21.5
	20	2.33	5.0	12.8	0.46	81.2
	50	3.30	3.2	13.0	0.57	249.6
1.1	0	-	9.0	8.5	-	0.0
	10	0.01	8.9	9.6	0.04	13.2
	20	0.06	8.4	10.0	0.10	18.2
	50	0.36	6.5	12.4	0.35	30.6
0.2*	20	0.09	2.1	12.3	0.60	64.8
1.1*	50	0.69	5.9	13.0	0.42	48.9
0.2*	50	0.33	1.6	12.7	0.65	166.7

Table S3.4. Chloride concentration in the beginning and end of urine experiments

		Cl$^-$ concentration (g L^{-1})			
Q_{anode}	$j_{applied}$	*Anode*		*Cathode*	
mL min^{-1}	A m^{-2}	*Initial*	*Final*	*Initial*	*Final*
0.2	20	3.40	3.43	0.00	0.10
1.1	50	3.55	3.60	0.00	0.07
0.2	50	3.83	2.70	0.00	0.12

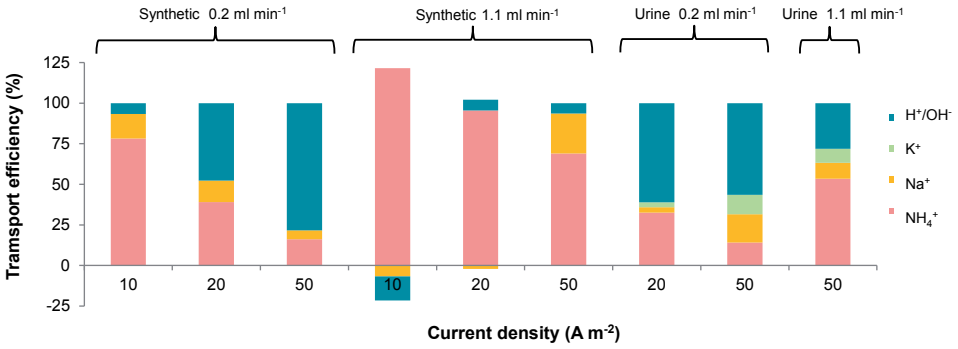

Figure S3.1. Transport efficiency of NH_4^+, Na^+, K^+ and H^+/OH^- over the membrane. Negative numbers mean transport from cathode to anode, and efficiencies higher than 100% indicate diffusion. Mg^{2+} and Ca^{2+} were not detected and therefore did not contribute the charge transport.

Calculations

- *Removal efficiency of TAN (%)*

The removal efficiency is a measure of how much was removed from the TAN that entered the system.

$$RE_{TAN} = \left(1 - \frac{C_{\text{anolyte end,TAN}}}{C_{\text{anolyte inflow,TAN}}} \right) * 100 \qquad \text{Equation S3.1}$$

Where $C_{\text{anolyte end, TAN}}$ (g m^{-3}) and $C_{\text{anolyte inflow, TAN}}$ (g m^{-3}) represent the TAN concentration in the anolyte at steady state and in the inflow, respectively.

- *Recovery efficiency of TAN (%)*

Part (or all) of the TAN supplied via the inflow is recovered in the acid in the TMCS unit; this number is called recovery efficiency.

$$Recovery\ efficiency_{TAN} = \left(\frac{C_{\text{acid end,NH4+}} * V_{\text{acid}}}{Q_{\text{anode}} * t * C_{\text{anolyte inflow,TAN}})} \right) * 100 \qquad \text{Equation S3.2}$$

Where $C_{\text{acid end,NH4+}}$ (g m^{-3}) is the NH_4^+ concentration measured in the acid at the end of the experiment, V_{acid} (m^3) the volume of acid, Q_{anode} (m^3 s^{-1}) is the anolyte flow rate, while t (s) is the duration of the experiment.

- *Flux of TAN over the cation exchange membrane (mol N m^{-2} s^{-1})*

$$J_{TAN} = \frac{\frac{C_{anolyte\ inflow,TAN} - C_{anolyte\ end,TAN}}{M_{NH4+}} * Q_{anode}}{A_m} \qquad \text{Equation S3.3}$$

Where A_m (0.01 m^2) is the surface area of the cation exchange membrane and M_{NH4+} (18 g mol^{-1}) the molar mass of ammonium.

- *Flux of NH_3 over the TMCS membrane (mol N m^{-2} s^{-1})*

$$J_{NH3,TMCS} = \frac{\frac{C_{acid\ end,NH4+} - C_{acid\ HRT1,NH4+}}{M_{NH4+}}}{t_{stable} * A_m} \qquad \text{Equation S3.4}$$

Where $C_{\text{acid HRT1,NH4+}}$ (g m^{-3}) is the NH_4^+ concentration measured in the acid at the first HRT, while t_{stable} (s) is the time between the first HRT and the end of the experiment, which is the time considered as steady state.

- *Transport efficiency of NH_4^+ (%)*

The transport efficiency is the contribution of an ion to the total charge transport over the cation exchange membrane.

$$tE_{NH4+} = \left(\frac{J_{TAN} * z_{NH4+} * F}{j_{applied}} \right) * 100 \qquad \text{Equation S3.5}$$

Where z_{NH4+} (-) represents the charge of NH_4^+, F (96485 C mol^{-1}) the Faraday constant and $j_{applied}$ (A m^{-2}) the applied current density.

- *Transport energy input (kJ g N $removed^{-1}$)*

The transport energy input reflects only the electrical input to the EC that was used for transport. This term takes into account only the potential losses due to transport and pH gradient over the membrane, independent of the reactions occurring at the electrodes.

$$Transport\ energy\ input = \frac{X_{TAN} * (E_{transport} + E_{\Delta pH}) * F}{1000 J/kJ * 14\ gN/mol} \qquad \text{Equation S3.6}$$

Where X_{TAN} (-) is the charge input (Equation S3.7), $E_{transport}$ (V) is the potential loss due to transport (Equation S3.8) and $E_{\Delta pH}$ (V) is the potential loss due to the pH gradient over the membrane (Equation S3.9).

- *Charge input (-)*

$$X_{TAN} = \frac{j_{applied}}{J_{TAN} * F} \qquad \text{Equation S3.7}$$

- *Transport potential loss (V)*

The potential loss due to the transport of ions across the membrane was defined as the potential difference between the cathode and anode reference electrodes.

$$E_{transport} = (E_{cathode,measured} - E_{anode,measured}) - E_{cell,measured} \qquad \text{Equation S3.8}$$

- *pH gradient potential loss (V)*

$$E_{\Delta pH} = \frac{RT}{F} * ln(10^{(pH_{cathode} - pH_{anode})}) \qquad \text{Equation S3.9}$$

- Total electrical energy input (kJ g N removed^{-1})

In **Table S3.3**, the total electrical energy input was calculated similar to the transport energy input (Equation S3.6), by substituting the sum of $E_{transport}$ and E_{pH} for the cell voltage (E_{cell}).

Model derivation (Equation 3.2)

For the model derivation, concentrations are expressed in mol m^{-3}.

- Balance equations for anode and cathode

$$Q_{anode} * C_{anode\ media,TAN} - (J_{NH4+} + J_{NH3}) * A_m - Q_{anode} * C_{anode\ end,TAN} = 0 \quad \text{Equation S3.10}$$

$$(J_{NH4+} + J_{NH3}) * A_m - k_g * A_{TMCS} * C_{cathode,NH3} = 0 \quad \text{Equation S3.11}$$

Where J_{NH4+} (mol m^{-2} s^{-1}) is the ammonium flux, J_{NH3} (mol m^{-2} s^{-1}) the ammonia flux, k_g (m s^{-1}) is the gas transfer coefficient of ammonia through the TMCS, A_{TMCS} (0.04 m^2) is the surface area of the TMCS membrane, and $C_{cathode,NH3}$ (mol m^{-3}) the concentration of ammonia in the catholyte.

- Transport equations

$$J_{NH4+} = \alpha * I \quad \text{Equation S3.12}$$

$$J_{NH3} = k_m * (C_{anode,NH3} - C_{cathode,NH3}) \quad \text{Equation S3.13}$$

Where α (-) is the fraction of current transported by ammonium, I (mol m^{-2} s^{-1}) is the applied current, k_m (m s^{-1}) is the mass transfer coefficient of ammonia through the CEM, and $C_{anode,NH3}$ (mol m^{-3}) the concentration of ammonia in the anolyte.

We derived the model shown in Materials and Methods (Equation 3.2) by rewriting Equation S3.10 in terms of both Equation S3.14 and Equation S.3.1, Equation S3.11 in terms of S3.15, taking into account the assumptions mentioned (thus α= 1), substituting and rearranging.

$$N_{load} = \frac{Q_{anode} * C_{anode\ media,TAN}}{A_m} \quad \text{Equation S3.14}$$

The N load is the TAN loading rate expressed in mol m^{-2} s^{-1} (instead of A m^{-2}).

$$K_g = k_g * \frac{A_{TMCS}}{A_m}$$ Equation S3.15

K_g is a term which includes the gas transfer coefficient of ammonia through the TMCS (k_g).

CHAPTER 4

Hydrogen gas recycling for energy efficient ammonia recovery in electrochemical systems

ABSTRACT

Recycling of hydrogen gas (H_2) produced at the cathode to the anode in an electrochemical system allows for energy efficient TAN (Total Ammonia Nitrogen) recovery. Using a H_2 recycling electrochemical system (HRES) we achieved high TAN transport rates at low energy input. At a current density of 20 A m^{-2}, TAN removal rate from the influent was 151 g_N m^{-2} d^{-1} at an energy demand of 26.1 kJ g_N^{-1}. The maximum TAN transport rate of 335 g_N m^{-2} d^{-1} was achieved at a current density of 50 A m^{-2} and an energy demand of 56.3 kJ g_N^{-1}. High TAN removal efficiency (73-82%) and recovery (60-73%) were reached in all experiments. Therefore, our HRES is a promising alternative for electrochemical and bioelectrochemical TAN recovery. Advantages are the lower energy input and lower risk of chloride oxidation compared to electrochemical technologies, and high rates and independence of organic matter compared to bioelectrochemical systems.

This chapter has been published as: Kuntke P, Rodríguez Arredondo M, Widyakristi L, Ter Heijne A, Sleutels THJA, Hamelers HVM, Buisman CJN. Hydrogen gas recycling for energy efficient ammonia recovery in electrochemical systems. *Environ. Sci. Technol.* 2017, *51* (5), 3110-3116.

4.1 Introduction

Our modern society relies on fertilizers to ensure sufficient crop yield for food production. The Food and Agriculture Organization of the United Nations (FAO) estimated that in 2016 approximately 117 million tonnes of nitrogen (N) and 45 million tonnes phosphorus (P) fertilizer will be applied in agriculture [152]. Whereas P is a scarce and non-replaceable resource [153, 154], N is vastly available as nitrogen gas (N_2) in our atmosphere. However converting inert N_2 into reactive nitrogen (i.e., NH_3/NH_4^+, NO_3^-, NO_2^-) is energy demanding [58]. About 1 to 2% of the worldwide energy demand is allocated to the production of ammonia (i.e. for fertilizer usage) [8, 155]. Ammonia production is responsible for approximately 20% of the energy consumption in the chemical industry in the US [156].

After food consumption, a large amount of this reactive nitrogen ends up in domestic wastewater. This reactive nitrogen in wastewater needs to be removed to protect sensitive water bodies and comply with current discharge regulations. Nowadays, common practise for the removal of nitrogen from wastewater is the nitrification/denitrification process, which requires aeration and organic matter to convert reactive nitrogen to inert N_2, thereby destroying a potential resource. Newer technologies, like Anammox, which are more energy efficient, also lead to the destruction of reactive nitrogen [58, 103]. Collecting nutrient rich streams separately is a strategy to improve the energy efficiency of wastewater treatment system and allow for nutrient recovery. Source separated urine as a suitable nutrient rich stream for nutrient recovery was already recognized in the 1990's, as urine contains about 80% of the nitrogen found in wastewater in a small volume fraction (approximately 1 vol%) [83, 157].

In recent years, current driven TAN (Total Ammonia Nitrogen) recovery using electrochemical or bioelectrochemical systems have been proposed as an alternative to conventional TAN removal/recovery strategies [89, 99]. Both types of systems use the electric current derived from redox reactions at electrodes to transport TAN through a cation exchange membrane (CEM) and thereby separate it from the wastewater and concentrate it in the catholyte prior to extraction. TAN recovery from the cathode compartment is possible due to the high pH of the catholyte which deprotonates the ammonium into volatile ammonia. The pH of the catholyte increases as a result of the reduction of water or oxygen and transport of cations other than protons through the CEM. The volatile ammonia is then extracted from the catholyte by gas permeable hydrophobic membranes or by conventional ammonia stripping process [40, 48, 69, 143, 145]. Bioelectrochemical systems (i.e. Microbial Electrolysis Cells (MECs) and Microbial Fuel Cells (MFCs)) for TAN recovery rely on bacteria to catalyze the oxidation reaction of organic matter, whereas in electrochemical systems (ESs) the electrochemical oxidation reaction is water splitting, which produces oxygen and protons [89].

Bioelectrochemical TAN recovery from wastewater has been shown to be more energy efficient compared to electrochemical recovery, as bacteria at the anode can convert chemical energy stored in organic matter into electrical energy [89, 99]. In this context, urine seems to be an interesting wastewater, as it is rich in TAN and COD which can be utilized in BES [81, 158, 159]. The conversion of organic matter, at the same time, is a challenge, as BESs rely on readily available organic matter. Competition with other bacteria for the substrate can reduce the maximum current available for the TAN transport, which can limit the recovery of TAN [89, 160, 161]. Additional challenges are related to other parameters in the anode chamber (i.e., pH, conductivity, temperature), that can limit the performance of the anodic biofilm and thus TAN recovery.

Electrochemical TAN recovery has been demonstrated at higher current densities than bioelectrochemical TAN recovery, but requires a higher energy input for TAN recovery due to the oxidation of water instead of organic substrate oxidation [40, 88]. An additional challenge is that chloride oxidation can occur, due to high overpotentials at the anode for oxygen evolution reaction. Chloride oxidation can lead to the production of chlorine gas, chlorinated by-products and adsorbable organohalogens (AOX) [76, 162]. Chlorine gas, chlorinated compounds and AOX are toxic and therefore pose a serious concern for widespread application of electrochemical TAN recovery. Here we propose a hydrogen recycling electrochemical system (HRES) to overcome these two challenges of high energy input and chloride oxidation. Our aim was to recycle the hydrogen gas (H_2) produced at the cathode, thereby changing the oxidation reaction from water oxidation to H_2 oxidation. Recycling H_2 from the cathode to be oxidized at the anode will reduce the energy input for TAN transport, as the anode potential for H_2 oxidation is -0.414 V vs normal hydrogen electrode (NHE) which is identical to the cathode potential for water reduction to H_2, while the anode potential for oxygen evolution is 0.815 V vs NHE (all evaluated at pH=7 using equations S4.1-S4.4, Supporting Information). An additional advantage of this low anode potential is a low risk of chloride oxidation, which occurs at much higher anode potentials (1.3 V vs NHE). Therefore, the HRES is an attractive alternative method for electrochemical TAN recovery that has previously not been explored.

In this work, we investigated the performance of a HRES to generate electric current and drive TAN transport over the CEM. The HRES was operated at different current densities and was supported by an extra electrochemical system in case insufficient H_2 could be recycled. We analyzed TAN transport rates, removal efficiencies, recovery efficiencies, and the energy input required for the HRES, and show that the HRES is an attractive alternative method for TAN recovery.

4.2 Materials and methods

4.2.1 Hydrogen Recycling Electrochemical System for TAN recovery

The HRES for TAN recovery consisted of a three compartment electrochemical system (Figure 4.1), in which water is reduced to H_2 at the cathode and the produced $H_2$was recycled to and oxidized at the anode.

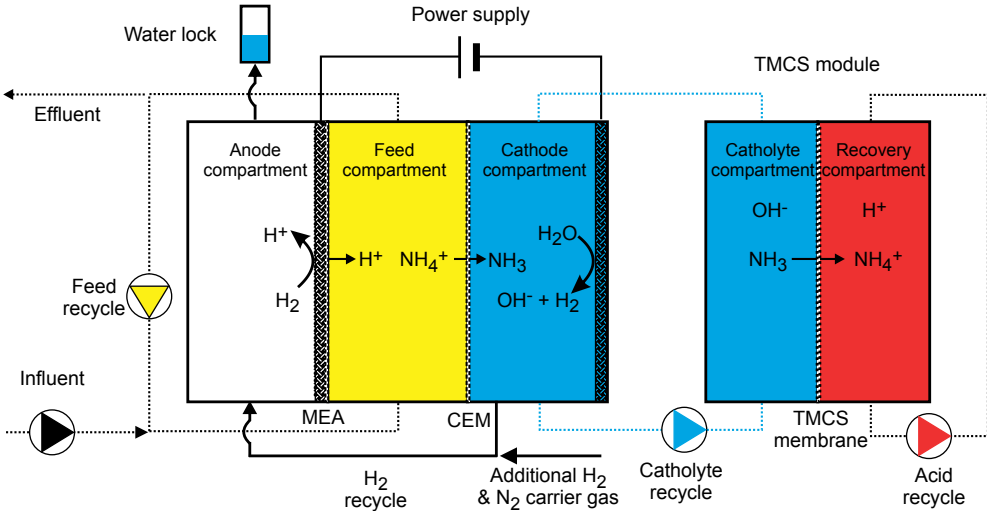

Figure 4.1. Schematic of the HRES for TAN recovery. H_2 produced at the cathode is transported to the anode, where it is oxidized, using N_2 as carrier gas enriched with additional H_2 from the electrolyser. The electric current produced by the HRES is used to transport ammonium (NH_4^+) and other cation over the CEM to the cathode. Ionic ammonium is deprotonated by the alkaline conditions in the catholyte forming volatile ammonia (NH_3). Ammonia is extracted from the catholyte using a gas-permeable hydrophobic membrane module (TMCS module).

The three compartments were (i) anode chamber in which the H_2 is fed, (ii) feed compartment for the wastewater, and (iii) cathode chamber in which H_2 is produced. The anode was a membrane electrode assembly (MEA) consisting of a 15 cm x 15 cm Nafion N117 cation exchange membrane (CEM) coated with a 10 cm x 10 cm of Platinum - Vulcan (carbon) catalyst (0.5 mg Pt cm^{-2}) with an integrated gas diffusion layer (GDL) purchased from Fuelcellsetc (Texas, USA). The reactive side of the MEA (catalyst with GDL) was facing the anode chamber, while the side without catalyst coating and without GDL was facing the feed compartment. The urine feed compartment, which was situated in between the anode and cathode chamber, consisted of a custom made polypropylene (PP) plate (21 cm x 21 cm x 1.2 cm) and included a serpentine shaped flow field (10 cm x 10 cm x 1.2 cm, 60% open). The feed compartment was separated from the anode by the MEA and from the cathode compartment by a Nafion N117 CEM (15 cm x 15 cm Fuelcellsetc, Texas, USA). The cathode was a platinum (Pt) coated titanium mesh electrode (9.8 cm x 9.8 cm, 5 mg Pt

cm^{-2} Magneto Special Anodes BV, The Netherlands). An identical Pt coated titanium mesh electrode was used as a current collector in the anode chamber (Figure S4.1). The housing of the anode and cathode was made from poly (methyl methacrylate) (PMMA (21 cm x 21 cm x 2.5 cm)), which housed a machined flow field (10 cm x 10 cm x 0.2 cm) with the feed channel situated at the bottom and an exhaust/effluent channel situated at the top of the flow field. The carrier gas (N_2) enriched with H_2 was not dried and injected in close proximity to the MEA. Custom made silicone rubber gaskets were used to create a water/gas-tight seal in the electrochemical system. Nitril spacers (50% open) were used between the CEM and the cathode as well as the serpentine flow field and the adjunct CEMs. All ion exchange membranes and electrodes had a projected surface area of 100 cm^2, identical to flow field dimensions of the different compartments.

A custom made electrolyser (operated at constant current with 10 mM H_2SO_4 as electrolyte) was used to supply H_2 during start-up of the ammonia recovery system and supplied approximately 10% additional H_2 during ammonia recovery experiments, to compensate for H_2 losses. Nitrogen was used as a carrier gas to transport the H_2 produced at the cathode to the anode. Anode and recovery compartment had a water lock (approximately 5 mbar pressure) to ensure oxygen free conditions.

A transmembrane chemisorption (TMCS) module was used to recover the TAN from the catholyte solution in an acid solution as previously described [143]. The TMCS unit was a custom made membrane module housing a tubular gas permeable hydrophobic membrane (pore size 200 nm, type Accurel PP V8/HF, CUT Membrane technology GmbH, Germany) [143]. Volatile ammonia in the catholyte is transported over this gas permeable hydrophobic membrane from the catholyte side to the acid side, due to the concentration gradient across the membrane and is protonated in the acid. Oxygen was removed from the acid compartment using nitrogen gas (0.2 mL min^{-1}).

Four Masterflex peristaltic pumps (Masterflex L/S, Metrohm Applikon BV, Schiedam, The Netherlands) were used to supply new influent (0.2, 0.4 and 1 mL min^{-1}), and to recycle feed media, catholyte and 1M sulphuric acid for the TMCS (80 mL min^{-1}). The total liquid volume of the feed compartment was 0.83 L including the recirculation vessel (500 mL), tubing (258 mL) and feed chamber (72 mL) inside the HRES. The cathode compartment had a total liquid volume of 1 L including the recirculation vessel (500 mL), tubing (430 mL), cathode chamber (20 mL) inside the HRES and the volume inside the TMCS module (50 mL).

Ag/AgCl reference electrodes (+0.2 V vs NHE, QM711X, QiS-Prosence BV, Oosterhout, The Netherlands) were placed in the catholyte and feed compartment to measure anode (MEA) potential, cathode potential and membrane potential. The reference electrodes

were connected to a high impedance preamplifier (Ext-Ins Technologies, Leeuwarden, The Netherlands). Temperature and pH were measured in the feed stream and catholyte using Orbisint CPS11D sensors connected to a Liquiline CM444 transmitter (Endress+Hauser BV, Naarden, The Netherlands). The conductivity of the feed stream and catholyte were measured using QC205X EC electrodes and P915-85 – Controller (QiS-Prosence BV, Oosterhout, The Netherlands). Constant current (CC) or constant voltage (CV) was supplied to the ES by a Delta power supply (ES 030-5, Delta Elektronika BV, Zierikzee, The Netherlands). A Memograph M RSG40 datalogger (Endress+Hauser BV) was used to record pH, temperature, conductivity, current density, cell voltage, anode potential, and cathode potential.

4.2.2 Experimental strategy

Two sets of experiments were performed using synthetic urine and male urine collected in the Wetsus building (The Netherlands). Synthetic urine was used for a proof-of-concept of the HRES for TAN recovery. Urine was used to investigate the performance of the HRES on real wastewater. Synthetic urine contained 13.7 g L^{-1} $(NH_4)_2CO_3$ and 4.6 g L^{-1} Na_2CO_3. The HRES was fed with synthetic urine at a rate of 0.4 mL min^{-1} corresponding to a hydraulic retention time (HRT) of 34.6 h and operated at a constant voltage of 1.6 V to achieve a high current density. The system was operated for a period of 7 days.

The collected urine was pre-treated by a combination of struvite precipitation and softening to recover P and remove excess Mg^{2+} and Ca^{2+} to prevent scaling inside the system as described by Zamora et al., 2017 [163] The composition of the pre-treated urine was 3.4 g L^{-1} TAN, 3.5 g L^{-1} chloride, 0.02 g L^{-1} phosphate, 1.4 g L^{-1} potassium, 1.6 g L^{-1} sodium, 0.5 g L^{-1} sulphate, 3.6 g L^{-1} COD and 1.2 g L^{-1} total organic carbon, at pH 9 and conductivity of 16 mS cm^{-1}. No calcium, magnesium, nitrate and nitrite were detected in the pre-treated urine. The pre-treated urine was supplied continuously to study TAN recovery from urine. Experiments were performed at three different current densities (i.e. 10, 20 and 50 A m^{-2}). The inflow rate for a current density of 10 A m^{-2} was 0.2 mL min^{-1} corresponding to an HRT of 69.2 hours. The inflow rate for a current density of 20 A m^{-2} was 0.4 mL min^{-1} corresponding to an HRT of 34.6 hours. The inflow rate for a current density of 50 A m^{-2} was 1 mL min^{-1} corresponding to an HRT of 13.8 hours. These chosen flowrates and current densities correspond to a load ratio (electrical current to TAN loading) of approximately 1.3, which should lead to high recoveries. The load ratio describes the ratio between applied current density (A m^{-2}) and TAN load expressed as current density (A m^{-2}) according to equation S8. TAN recovery from urine was investigated over a period of 7 days for each applied current density.

In all experiments, the cathode compartment and recovery compartment were operated as batch systems. The acid for TAN recovery was replaced once the concentration exceeded

20 g/L of ammonium-nitrogen, while the catholyte was never replaced. In the beginning, 800 mL of a 0.1 M NaOH solution was used as the catholyte. The system was operated at room temperature (24.5±1°C).

4.2.3 Chemical analysis

Samples from the influent, effluent, catholyte and acid were analysed for relevant parameters. All samples were filtered through a 0.45µm filter (PTFE syringe filter, VWR international BV, The Netherlands) prior to analysis, and were analyzed in duplicate. Cations (Ca^{2+}, Mg^{2+}, Na^{+}, K^{+}, NH_4^{+}) and anions (PO_4^{3-}, SO_4^{2-}, Cl^{-}, NO_3^{-}, NO_2^{-}) were analyzed with a Metrohm Compact IC Flex 930 with a cation column (Metrosep C 4-150/4.0) and a Metrohm Compact IC 761 with an anion column (Metrosep A Supp 5- 150/4.0) each equipped with an conductivity detector (Metrohm Nederland BV, Schiedam, The Netherlands). Ammonium-nitrogen in the acid was determined by cuvette test kit LCK303 and a spectrophotometer DR3900 (HACH NEDERLAND, Tiel, The Netherlands). Organic carbon, inorganic carbon and total carbon were analysed using a TOC analyser (TOC-L CPH, Shimadzu BENELUX, 's-Hertogenbosch, The Netherlands). Adsorbable organohalogens (AOX) were analysed in a specialized laboratory (WLN, Glimmen, The Netherlands).

4.2.4 Calculations

All calculations are explained in the Supporting information (Equations S4.1-S4.23).

4.3 Results and discussion

4.3.1 TAN recovery from synthetic urine – a proof-of-concept.

Synthetic urine was fed to the system as a first proof-of-principle of the HRES. The supporting electrochemical cell was used to supply additional H_2 and was operating at a current density which was 12% of the current density of the HRES. Over a course of 7 days the current density and electrode potential were recorded and TAN removal was measured, while the system was operated at a constant applied cell voltage of 1.6 V. The current density was stable at 16.7 ± 0.48 A m^{-2} throughout the experimental period of 7 days. An average anode potential of +0.017 ± 0.029 V vs Ag/AgCl and average cathode potential of -1.229 ± 0.061 V vs Ag/AgCl were measured during this period. These results show that H_2 produced at the cathode can be recycled to the anode and used as electron donor, as the anode potential of +0.017 V vs Ag/AgCl is suited for hydrogen oxidation, but not sufficiently positive for the oxygen evolution reaction (OER). TAN removal and recovery efficiency over the 7 days measurement period was 90% at a TAN transport rate of 190 g_N m^{-2} d^{-1}. This TAN transport was achieved at a load ratio of 1, meaning that the current exactly matched the TAN loading. Overall, these results show that TAN can be recovered using the H_2 recycling system with minor H_2 supply from the electrolyser.

4.3.2 Successful TAN recovery from real urine

After determining that TAN can be recovered using H_2 recycling, HRES performance was investigated with real urine. The system was operated at controlled current of 10, 20 and 50 A m^{-2} , and the TAN inflow was chosen at such a rate that the load ratio was 1.2 to 1.3. Table 4.1 shows a summary of the results for these conditions. The average anode potential was between 0.27 and 0.73 V vs Ag/AgCl, well below the anode potential for OER in acidic conditions (>0.97 V vs. Ag/AgCl at pH 1, calculated using the Nernst equation). The cathode potential remained relatively stable throughout the experiment between -0.93 to -1.07 V vs. Ag/AgCl, a value typical for hydrogen evolution. The lowest cell voltage (2.11 ± 0.16V) was measured during experiments at 20 A m^{-2}, while the highest cell voltage (4.35 ± 0.28V) was measured at 50 A m^{-2}. With increasing current density, the removal rate increased. This is in agreement with earlier studies, where similar TAN transport rates over the CEM between feed and cathode compartment were reached [88]. TAN removal efficiency was higher than 73% in all experiments. The highest TAN removal efficiency (82%) was reached at the lowest current density (10 A m^{-2}). The TAN recovery efficiency was in general slightly lower than the TAN removal efficiency, indicating that not all the removed ammonia was recovered in the acid, except for the experiment at 20 A m^{-2}. Overall these results show high TAN removal and recovery efficiency, outperforming other studies at similar conditions (i.e. current density and TAN loading) [40, 88].

Table 4.1. HRES performance during experiments with urine

i	L_N	E_{anode}	$E_{cathode}$	E_{Cell}	Transport $rate_{TAN}$	$Removal_{TAN}$	$Recovery_{TAN}$
(A m^{-2})	(-)	(V vs Ag/AgCl)	(V vs Ag/AgCl)	(V)	(g_N m^{-2} d^{-1})	(%)	(%)
10	1.3	0.36 ± 0.18	-0.93 ± 0.01	2.51 ± 0.22	78.3	82	64
20	1.2	0.27 ± 0.15	-1.07 ± 0.04	2.11 ± 0.16	151.0	73	73
50	1.3	0.73 ± 0.21	-1.03 ± 0.02	4.35 ± 0.28	342.1	73	60

4.3.3 H_2 recycling prevents the risk of Cl_2 and AOX formation

The application of an electrochemical system (ES) in combination with wastewater containing chloride ions poses the risks of chlorine gas formation and production of AOX at a certain anode overpotential (E_{anode}> 1.1 V vs Ag/AgCl) [76]. Table 4.2 shows the concentration of AOX, chloride ions, and total organic carbon (TOC) in samples taken from influent and effluent of the feed compartment of the HRES. While the chloride analysis showed stable Cl^- concentrations in influent and effluent, the AOX analysis showed only small quantities of AOX (< 1.5 mg L^{-1}) that were produced during the experiments. These findings are further supported by the observation that the measured anode potentials were below the standard electrode potential for chloride oxidation (+1.1 V vs Ag/AgCl). In

comparison, a recent study on electrochemical urine treatment by Zöllig et al. (2015) [76] showed a production of more than 6 mg L^{-1} of AOX at comparable transferred charge (6 Ah) at anode potential higher than +3.25 V vs mercury-mercurous sulfate electrode (MSE) (about +2.8 V vs Ag/AgCl). Therefore, AOX production seems limited in the HRES, but future research should investigate the risk of AOX formation in the HRES in more detail.

Only marginal changes in the total organic carbon concentration between influent and effluent of the HRES were detected (< 10%). As the effluent of our HRES is to a large extent depleted of the TAN (>73%), and the effluent still contains considerable concentrations of organic carbon, the effluent could be an interesting feed stream for anaerobic biological systems such as BES to recover energy.

Table 4.2. Results of the AOX, chloride ions and total organic carbon (TOC)

i	AOX analyses		Cl^- analyses		TOC analyses	
	Influent	Effluent	Influent	Effluent	Influent	Effluent
(A m^{-2})	(mg L^{-1})	(mg L^{-1})	(g L^{-1})	(g L^{-1})	(g L^{-1})	(g L^{-1})
10	0.25	1.77	3.3 ± 0.02	3.6 ± 0.02	1.2 ±0.01	1.1 ± 0.02
20	0.28	0.35	3.6 ± 0.08	3.6 ± 0.03	1.2 ± 0.03	1.1 ± 0.02
50	0.32	0.71	3.6 ± 0.01	3.6 ± 0.0	1.1 ± 0.04	1.1 ± 0.00

4.3.4 The energy demand is lower than competing processes and losses originate from anode overpotential and membrane transport

Important for the success of the HRES is the specific energy demand required for TAN recovery (in kJ g_N^{-1}). This energy demand allows us to compare the HRES with other technologies used to remove and recover TAN from wastewater. The energy demand for any current driven TAN recovery is determined by three main factors; (i) the required cell voltage needed as driving force for the redox reactions, (ii) the ion transport number and (iii) the recovered TAN (Equations S4.5-S4.7, Supporting information). The cell voltage of any (B)ES is determined by the equilibrium voltage (E_{eq}) and the internal potential losses. In general, all electrochemical systems (including BES) suffer from similar potential losses (i.e. anode and cathode overpotentials, ionic losses, and ion transport losses over the CEM). Table 4.3 evaluates the E_{eq} for the three different current driven TAN recovery systems with HER at the cathode, (i) a BES with acetate oxidation reaction (AOR) at the anode, (ii) an ES with the OER at the anode and (iii) the HRES with hydrogen oxidation reaction (HOR).

Table 4.3. Overview of standard potential (E^0), conditional potential (E_{pH7}), the equilibrium voltage (E_{eq}) of selected (bio)electrochemical systems and their theoretical energy demand for TAN recovery (P_{theory}). Conditional potentials were determined using the Nernst equation and assumes a temperature of 25°C, a partial pressure of 1 atm of the respective gasses in the headspace, a pH of 7 at the anode and cathode, and an acetate (Ac^-) and bicarbonate (HCO_3^-) concentration of 5 mM. All potentials are reported versus normal hydrogen electrode (NHE). The energy demand was calculated assuming a TAN load of 1 kg m^{-2} d^{-1}, a CEM surface area of 1 m^2, an internal resistance of 0.025 Ω m^{-2} and a recovery efficiency of 100%. For further details see Supporting Information.

Type of ES	Electrode	Reaction	E^0 (V)	E_{pH7} (V)	E_{eq} (V)	P_{theory}
			vs NHE	vs NHE		(MJ kg_N^{-1})
all	Cathode	HER: $2H_2O + 2e^- \rightarrow H_2 + 2OH^-$	0.828	-0.414	-	-
BES	Anode	AOR: $2HCO_3^- + 9H^+ + 8e^- \rightarrow CH_3COO^- + 4H_2O$	0.187	-0.296	-	-
		$E_{eq} = E_{HER} - E_{AOR}$			**-0.118**	**14.5**
ES	Anode	OER: $4H^+ + 4e^- + O_2 \rightarrow 2H_2O$	1.229	0.815	-	-
		$E_{eq} = E_{HER} - E_{OER}$			**-1.229**	**22.2**
HRES	Anode	HOR: $2H^+ + 2e^- \rightarrow H_2$	0	-0.414	-	-
		$E_{eq} = E_{HER} - E_{HOR}$			**0**	**13.7**

The energy demand (Equation S4.12) for TAN recovery in the HRES was 30.5 kJ g_N^{-1} at 10 A m^{-2}, 26.1 kJ g_N^{-1} at 20 A m^{-2} and 56.3 kJ g_N^{-1} at 50 A m^{-2}. This indicates that the most energy efficient performance of the HRES occurred at 20 A m^{-2} under the specific conditions of the experiments (see Table S4.1 in the Supporting Information). Although this energy demand is higher than the theoretical energy demand reported in Table 4.3, our system outperforms the best performing ES systems reported by Luther et al., 2015 (31 kJ g_N^{-1}), which includes theoretical savings from the recovery of H_2, at current densities of 20 A m^{-2} [88]. Furthermore, the energy demand of other infrastructure (i.e. pumping, possible measurement and control) will contribute to the energy demand of the technology and should be assessed in future research. In comparison, energy demand of other competing technologies is also higher: the combination of Anammox with the Haber-Bosch (HB) process requires 37 kJ g_N^{-1}, conventional nitrification/denitrification with HB process requires 51 kJ g_N^{-1}, and ammonia stripping requires 32 kJ g_N^{-1} [58].

To investigate the causes for the difference between the theoretical and practical energy demand, we analyzed the voltage losses and the ion transport numbers in the HRES at different current densities. As the equilibrium voltage for our system is 0 V at pH 7, the cell voltage should be determined by the internal voltage losses. An in-depth analysis of the internal potential losses (i.e., ionic, membrane transport, anode and cathode overpotentials) and the E_{eq} allows us to investigate bottlenecks of the HRES

during operational conditions. Figure 4.2 shows the voltage losses and the energy input distributed over the different parts of the HRES.

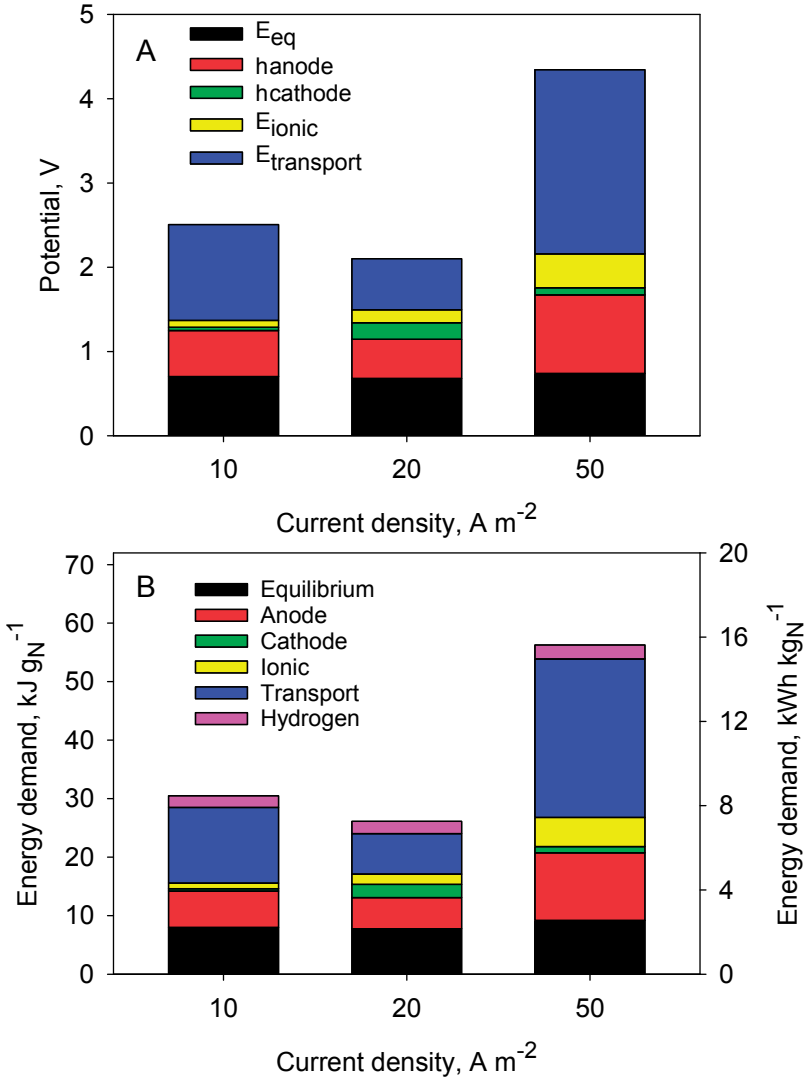

Figure 4.2. (A) Analysis of the internal voltage losses and **(B)** energy demand determined during the experiments at different current densities. Equilibrium voltage (E_{eq}), anode overpotential and transport losses over the CEM (between feed and cathode compartments) are the main source of potential in all experiments. The additional H_2 (about 10%) supplied by the electrolyser account for only 4 to 9 % of the energy demand.

The equilibrium voltage (E_{eq}), anode overpotential (η_{anode}) and transport potential losses ($E_{transport}$) over the CEM between feed and cathode compartment were the main contributors to the overall potential losses, while the ionic potential losses and cathode overpotential were considerably lower. The transport potential losses originated from the concentration gradient across the membrane that develops when multiple cations are transported [164]. The anode overpotentials are usually dominated by activation losses and diffusion losses at the catalyst. Additionally, the low H_2 partial pressure (see Table S4.1, Supporting Information) can further increase the overpotential of the anode. The CEM of the MEA (at the anode) further affected the anode overpotential, as the potential loss at this membrane is measured as part of overpotential. The equilibrium voltage originated from the pH difference between anode and cathode. Therefore, further reductions in energy demand can be achieved by optimizing the operation conditions, especially related to the decrease of concentration gradients and lower pH at the cathode. Furthermore, catalyst deactivation by for instance chloride ions can also play an important role on the overpotentials and future research should focus on this [165]. Energy wise, it has to be noted that the additional hydrogen (10%) supplied by the supporting electrolyser only accounts for approximately 7% of the overall energy demand at 10 A m^{-2}, 9% at 20 A m^{-2} and 4% at 50 A m^{-2}.

The ion transport number shows the contribution of the specific ion to the ionic current (equations S4.22 and S4.23). The ammonium transport number is an important parameter for current driven TAN recovery systems, as it is one of the factors that determine the current required for TAN recovery and therefore the energy demand. Figure 4.3 shows the ion transport numbers for NH_4^+, Na^+, K^+ and H^+/OH^- during the experiments on urine. At all current densities, $NH_4^+$was the main charge carrier (0.56), while remaining charge was transported by protons (hydronium)/hydroxyl ions (0.26), sodium (0.11) and potassium (0.06). The transport numbers for these ions were similar at the different current densities. Therefore, on average only 56% of the current invested in the HRES is used for the recovery, which also leads to a higher energy demand for TAN recovery. Other studies showed similar ion transport numbers ranging from 0.3 to 0.7 under comparable conditions [40, 87, 88].

4.4 Implication

The results obtained with the HRES for TAN recovery are very promising. The HRES can compete with current ES and BES technology for TAN recovery, while outcompeting either in critical points such as achieving high rates (BES) and requiring a low energy input (ES). Furthermore, hydrogen recycling in a BES could be an interesting option for TAN recovery from wastewater streams, which have insufficient biodegradable organic matter for

current production. Additionally, lowering the risk of chloride oxidation and not being dependent on available organic matter as substrate are of an advantage to other (B)ESs based TAN recovery technologies. Future research should focus on further lowering the energy demand (i.e. optimization of H_2 flow through better cell design, optimization of the HOR/HER catalyst, optimization of the pH profile), use of less expensive materials (i.e. Pt-free catalysts, membranes) and upscaling of this technology.

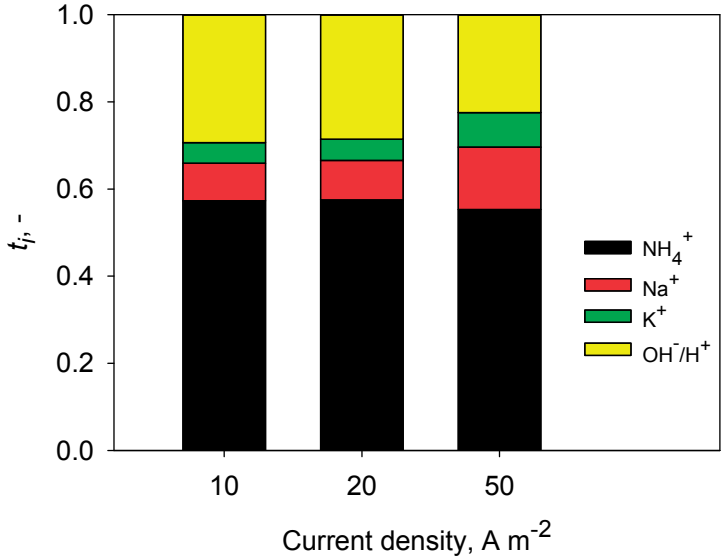

Figure 4.3. Contribution of ionic species to the total charge transport through the CEM. Ammonium ions were the main charge carrier in all experiments independent of the current density.

Acknowledgements

This work was performed in the cooperation framework of Wetsus, European Centre of Excellence for Sustainable Water Technology (www.wetsus.eu). Wetsus is co-funded by the Dutch Ministry of Economic Affairs and Ministry of Infrastructure and Environment, the European Union Regional Development Fund, the Province of Fryslân, and the Northern Netherlands Provinces. This research has received funding from the European Union's Seventh Programme for research, technological development and demonstration under grant agreement No 308535. The authors would like to thank the participants of the research theme "Resource Recovery" for the fruitful discussions and their financial support. The authors would also like to thank Martin Ulbricht from 3M for the support on the TMCS membranes.

4.5 Supporting information

4.5.1 HRES in detail

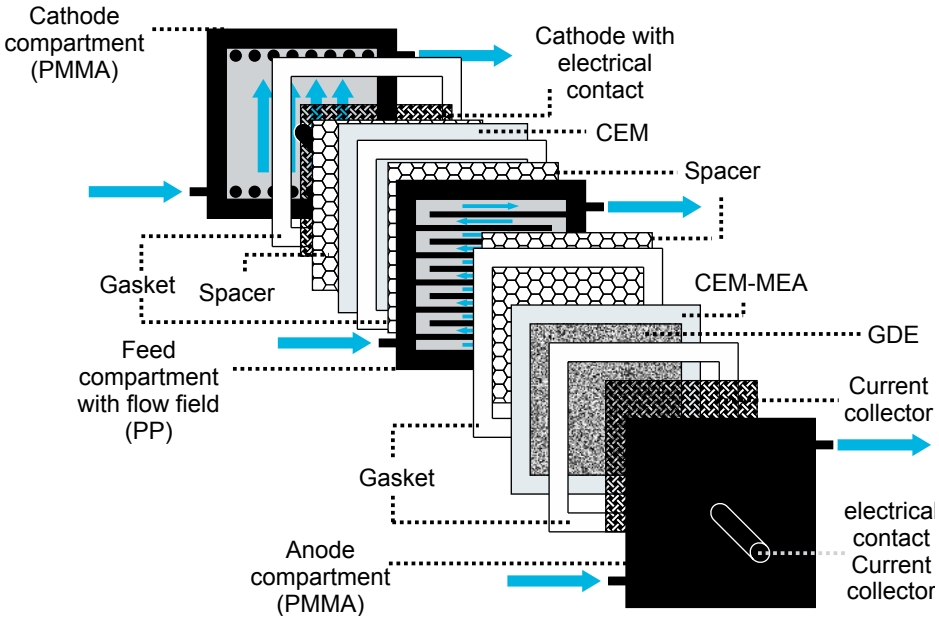

Figure S4.1. Schematic representation of the HRES cell design and its components.

4.5.2 Calculations

All potentials in the theoretical calculation are expressed in Volts versus normal hydrogen electrode (NHE), all other potentials are expressed in Volts versus Ag/AgCl (0.2V vs NHE).

(M)EC Cathode

The cathode potential for an MEC and EC was determined using:

$$E_{pH7,HER} = E^{0}_{cathode,HER} - \frac{R \times T}{2 \times F} \times ln\,(pH_2 \times [OH^-]^2) \qquad \text{Equation S4.1}$$

Where $E_{pH7,HER}$ is the calculated cathode potential (V), $E^0_{cathode,HER}$ is the standard cathode potential for water reduction in neutral/alkaline conditions (-0.828 V vs NHE), R is the ideal gas constant (8.3144 J mol^{-1} K^{-1}), T is the absolute temperature (298.15 K), 2 is the amount of electrons transferred, F is the Faraday constant (96485 C mol^{-1}), pH_2 is hydrogen partial pressure (1 atm), and $[OH^-]$ is the hydroxyl ion concentration at the cathode (calculated according from the $pOH=pK_W - pH = 14-7 = 7$).

MEC Anode

The anode potential of an MEC for acetate oxidation was determined using:

$$E_{pH7,AOR} = E^{0}_{anode,AOR} - \frac{R \times T}{8 \times F} \times ln \frac{[CH_3COO^-]}{[HCO_3^-]^2\,[H^+]^2} \quad \text{Equation S4.2}$$

Where $E_{pH7,AOR}$ is the calculated anode potential for the AOR (V), $E^0_{anode,AOR}$ is the standard anode potential for acetate oxidation (0.187 V vs NHE), R is the ideal gas constant, T is the absolute temperature in Kelvin (298.15 K), 8 is the amount of electrons transferred, F is the Faraday constant (96485 C mol^{-1}), $[CH_3COO^-]$ is the concentration of acetate (5mM), $[HCO_3^-]$ is the concentration of bicarbonate (5mM) and $[H^+]$ is the proton (hydronium) concentration at the anode (calculated from a pH of 7).

EC Anode

The anode potential of an EC for Oxygen Evolution Reaction (OER) was determined as:

$$E_{pH7,OER} = E^{0}_{anode,OER} - \frac{R \times T}{4 \times F} \times ln \left(\frac{pO_2}{[H^+]^2} \right) \quad \text{Equation S4.3}$$

Where $E_{pH7,OER}$ is the calculated anode potential for the OER (V), $E^0_{anode,OER}$ is the standard anode potential for OER (1.229 V vs NHE), R is the ideal gas constant, T is the absolute temperature in Kelvin (298.15 K), 4 is the amount of electrons transferred, F is the Faraday constant (96485 C mol^{-1}), pO_2 is the oxygen partial pressure (0.2 atm) , and $[H^+]$ is the proton (hydronium) concentration at the anode (calculated from a pH of 7).

HRES Anode

The anode potential of an HRES for hydrogen oxidation reaction (HOR) was determined by:

$$E_{pH7,HOR} = E^{0}_{anode,HOR} - \frac{R \times T}{2 \times F} \times ln \left(\frac{pH_2}{[H^+]^2} \right) \quad \text{Equation S4.4}$$

Where $E_{pH7,HOR}$ is the calculated anode potential for the HOR (V), $E^0_{anode,HOR}$ is the standard anode potential for hydrogen oxidation (0 V vs NHE), R is the ideal gas constant (8.3144 J mol^{-1} K^{-1}), T is the absolute temperature (298.15 K), 2 is the amount of electrons transferred, F is the Faraday constant (96485 C mol^{-1}), pH_2 is hydrogen partial pressure (1 atm), and $[H^+]$ is the proton (hydronium) concentration at the anode (calculated from a pH of 7).

P_{theory}

The required current density (i_{theory}) for TAN recovery was determined by using a TAN loading (Nload) of 1 kg_N m^2 d^{-1} (expressed in g_N m^{-2} s^{-1}) and the molar mass of nitrogen (M_N = 0.014 Kg mol^{-1}) according to:

$$i_{theory}\,(Am^{-2}) = \frac{Nload\,(g_N\ m^{-2}\ s^{-1})\ *F\,(C\ mol^{-1})}{M_N\,(g\ mol^{-1})}$$ Equation S4.5

The theoretical cell voltage (E_{theory}) of the different systems was determined using the equilibrium voltage (E_{eq}), an internal resistance (R_{int}) of 0.025 Ω m^2 and the required current density (i_{theory}) according to:

$$E_{theory}\,(V) = E_{eq}\,(V) + R_{int}\,(\Omega\,m^2)\times i(A\,m^{-2})$$ Equation S4.6

The theoretical energy demand (P_{theory}) for the TAN recovery was then calculated based on the theoretical cell voltage (E_{theory}), the required current density (i_{theory}), the amount of seconds per day(t = 86,400 s) and the Nload according to:

$$P_{theory}\,(MJ\,kg_N) = \frac{E_{theory}\,(V)\ \times i_{theory}\ (A\,m^{-2})\times t\,(s\,d^{-1})}{Nload\,(kg_N\ m^{-2}\ d^{-1})*10^6\,(MJ\,J^{-1})}$$ Equation S4.7

Additionally, the dependence of the theoretical energy demand (P_{theory}) on the internal resistance (R_{int}) is evaluated in the Figure S4.2.

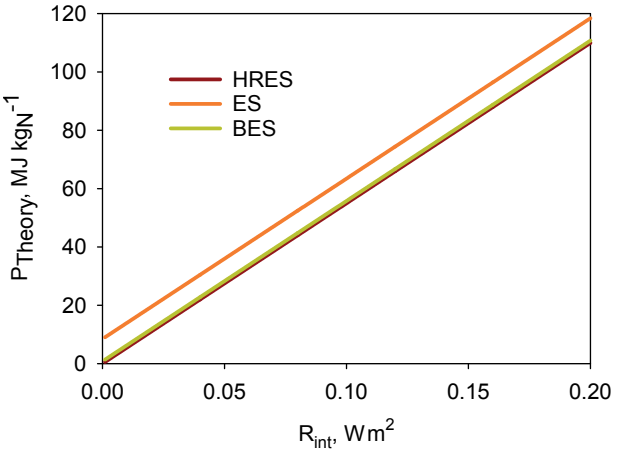

Figure S4.2. Theoretical power demand evaluated as a function of the internal resistances.

Load ratio

The load ratio, which describes the relation between the current density and the TAN loading of the system, was calculated according to:

$$L_N = \frac{i}{C_{TAN}/M_N \times Q_{influent} \times F \times 1/A_M}$$ Equation S4.8

Where L_N is the load ratio (-), i is the current density (A m^{-2}), C_{TAN} is the TAN concentration in the influent (kg$_N$ m^{-3}), M_N is the molar mass of nitrogen (0.014 kg mol^{-1}), $Q_{influent}$ is the

influent flowrate ($m^3\ s^{-1}$), F is the Faraday constant ($C\ mol^{-1}$) and A_M is the CEM surface area (0.01 m^2).

TAN transport rate, removal efficiency and recovery efficiency

Total Ammonia Nitrogen (TAN) transport rate, removal efficiency and recovery efficiency were determined according to equations S4.9, S4.10 and S4.11, respectively.

$$Transport\ rate_{TAN}\ (g_N\ m^{-2}\ d^{-1}) = \frac{(C_{TAN,influent} - C_{TAN,effluent}) \times Q_{influent} \times t}{A_M} \qquad \text{Equation S4.9}$$

Where $C_{TAN,influent}$ is the measured TAN concentration in the influent ($g\ L^{-1}$), $C_{TAN,effluent}$ is the measured TAN concentration in the effluent ($g\ L^{-1}$), $Q_{influent}$ is the influent flow speed ($L\ s^{-1}$), t is the amount of seconds per day (86,400 $s\ d^{-1}$), and A_M is the CEM surface area (0.01 m^2).

$$Removal_{TAN}(\%) = \left(1 - \frac{C_{TAN,effluent}}{C_{TAN,influent}}\right) x100 \qquad \text{Equation S4.10}$$

Where $C_{TAN,influent}$ is the measured TAN concentration in the influent ($g\ L^{-1}$) and $C_{TAN,effluent}$ is the measured TAN concentration in the effluent ($g\ L^{-1}$).

$$Recovery_{TAN}(\%) = \left(\frac{\Delta C_{TAN,acid} \times V_{acid}}{Q_{influent} \times HRT \times C_{TAN,influent}}\right) x100 \qquad \text{Equation S4.11}$$

Where $\Delta C_{TAN,acid}$ is the change of TAN concentration during one HRT ($g\ L^{-1}$), V_{acid} is the volume of the acid (L), $Q_{influent}$ is the influent flow speed ($L\ s^{-1}$), HRT is the hydraulic retention time expressed in seconds (s), and $C_{TAN,influent}$ is the measured TAN concentration in the influent ($g\ L^{-1}$).

Energy input TAN recovery

The energy requirement for the ammonia recovery was determined from the TAN transport rate and the electrical energy input of the HRES and electrical energy input of the electrolyser according to:

$$Energy\ input\ (kJ\ g_N^{-1}) = \frac{i \times E_{Cell} \times t + i_2 \times E_{Cell2} \times t}{transport\ rate_{TAN} \times 1000} \qquad \text{Equation S4.12}$$

Where i is the current density ($A\ m^{-2}$) of the HRES, E_{cell} is the average cell voltage (V) of the HRES, t is the amount of seconds per day (86,400 $s\ d^{-1}$), i_2 is the applied current density ($A\ m^{-2}$) of the electrolyser, E_{Cell2} is the average cell voltage (V) of the electrolyser, transport $rate_{TAN}$ is the TAN transport rate ($g_N\ m^{-2}\ d^{-1}$), and 1000 is the amount of J per kJ .

Determination of the potential losses in the HRES

As explained earlier, the applied voltage (E_{Cell}) of the HRES is required as the driving force for the redox reaction at the electrodes and can be calculated using equilibrium potential (E_{eq}) and the internal potential losses (E_{int})

$$E_{Cell} = E_{eq} + E_{int}$$ Equation S4.13

The internal potential losses are composed of anode overpotential (η_{anode}), cathode overpotential ($\eta_{cathode}$), ionic losses (E_{ionic}), and the transport losses ($E_{transport}$) across the CEM separating feed and cathode compartment as shown in equation S4.14.

$$E_{Cell} = E_{eq} + E_{int} = E_{eq} + \eta_{anode} + \eta_{cathode} + E_{ionic} + E_{transport}$$ Equation S4.14

The equilibrium voltage was calculated from the pH difference between anode and cathode according to equation S4.15 using a potential loss of 59.2 mV per pH unit difference of the cathode and anode.

$$E_{eq} = 0.0592V \times (pH_{cathode} - pH_{anode})$$ Equation S4.15

Where E_{eq} is the equilibrium voltage, $pH_{cathode}$ is the measured catholyte pH, and pH_{anode} is the pH at anode assuming a pH of 0.26, corresponding to a proton concentration of 0.54M in a fully saturated Nafion membrane [166].

The anode overpotential (η_{anode}) was determined from the measured anode potential and the calculated anode potential based on actual conditions using the Nernst equation as shown in equation S4.16 and S4.17.

$$\eta_{anode} = E_{anode} - E_{anode,measured}$$ Equation S4.16

$$E_{anode} = E^{0}_{anode} - \frac{R \times T}{z \times F} \times ln\left(\frac{pH_2}{[H^+]^2}\right)$$ Equation S4.17

Where E_{anode} is the calculated anode potential (V), $E_{anode,measured}$ is the measured anode potential (V), E^0_{anode} is the standard anode potential (-0.2 V vs Ag/AgCl), pH_2 is the calculated hydrogen partial pressure (atm), and $[H^+]$ is the calculated proton (hydronium) concentration assuming a pH of 0.26, corresponding to a proton concentration of 0.54M in a fully saturated Nafion membrane [166].

The cathode overpotential ($\eta_{cathode}$) was determined from the measured cathode potential and the calculated cathode potential based on actual conditions using the Nernst equation as shown in equation S4.18 and S4.19.

$$\eta_{cathode} = E_{cathode,measured} - E_{cathode}$$ Equation S4.18

$$E_{cathode} = E^{0}_{cathode} - \frac{R \times T}{z \times F} \times ln\,(pH_2 \times [OH^-]^2)$$ Equation S4.19

Where $E_{cathode}$ is the calculated cathode potential (V), $E_{cathode,measured}$ is the measured cathode potential (V), $E^0_{cathode}$ is the standard cathode potential (-1.028V vs Ag/AgCl), pH_2 is the calculated hydrogen partial pressure (atm), and $[OH^-]$ is the concentration of the hydroxyls ions in the catholyte based on the measured pH ($pOH=pK_W - pH$).

The ionic potential losses were calculated based on the measured conductivity in feed and cathode compartment according to:

$$E_{ionic} = i \times A_M \times \left(\frac{d_{feed}}{A_M \times \sigma_{feed}} + \frac{d_{cathode}}{A_M \times \sigma_{cathode}} \right)$$ Equation S4.20

Where d_{feed} is the thickness of the feed compartment (1.2 cm), σ_{feed} is the conductivity of feed media (mS cm^{-1}), $d_{cathode}$ is the distance of the cathode to the membrane (0.05cm), $\sigma_{cathode}$ is the conductivity of feed media (mS cm^{-1}).

The transport potential losses across the CEM between feed and cathode compartment were calculated based on the applied cell voltage (E_{Cell}), the measured electrode potentials (i.e. E_{anode}, $E_{cathode}$), the ionic potential losses (E_{ionic}) and the equilibrium voltage (E_{eq}) according equation S4.21.

$$E_{transport} = E_{Cell} + (E_{cathode} - E_{anode} - E_{ion} - E_{eq})$$ Equation S4.21

Determination of ion transport number

The ion transport numbers (t_i) over the CEM, which separates feed from cathode compartment, were determined based on the change in the ion concentration between influent and effluent of the feed compartment over one HRT in dependence of the current according to:

$$t_i\ (-) = \frac{\Delta C_i \times z_i \times F \times Q_{influent} \times HRT}{M_i \times \left(\frac{i \times HRT}{A_M}\right)}$$ Equation S4.22

Where ΔC_i is the change in concentration of the ion (i.e., Na^+, K^+, NH_4^+, Mg^{2+}, Ca^{2+}) during one HRT (g L^{-1}), z_i is the net charge of the ion (-), F is the Faraday constant (96,485 C mol^{-1}), $Q_{influent}$ is the influent flow speed (L s^{-1}), HRT is the hydraulic retention time (s), M_i is the molar mass of the ion (g mol^{-1}), i is the applied current density (A m^{-2}), and A_M is the CEM surface area (0.01 m^2). The transport number for the sum of the hydroxyl and hydronium ions was calculated as the difference between the total charge transport over the membrane

(equal to the total current during the same time period) and the sum of the transport numbers of the cations based on equation S4.22 according to

$$t_{H^+/OH^-}\ (-) = 1-\sum t_i \qquad \text{Equation S4.23}$$

Additional data from the TAN recovery experiment using urine

Table S4.1. Measured pH and conductivity in the feed and cathode compartments, as well as the calculated H_2 partial pressure

Current density	**Feed compartment**		**Cathode compartment**		**pH_2***
i	pH	Conductivity	pH	Conductivity	
A m^{-2}	(-)	(mS cm^{-1})	(-)	(mS cm^{-1})	
10	2.57 ± 0.36	15.4 ± 0.2	12.17 ± 0.14	72.5 ± 2.1	0.05
20	4.87 ± 0.38	16.4 ± 0.7	11.77 ± 0.53	67.7 ± 5.3	0.09
50	2.52 ± 0.06	15.2 ± 0.5	12.79 ± 0.08	136.0 ± 25.2	0.20

* calculated for the applied current densities and the supplied N_2 carrier gas

CHAPTER 5

The concept of load ratio applied to bioelectrochemical systems for ammonia recovery

ABSTRACT

Background: The load ratio is a crucial parameter to optimize the current driven recovery of total ammonia nitrogen (TAN) from urine. The load ratio is the ratio between the current density and the TAN loading rate. It is currently not known if the load ratio concept applies to a bioelectrochemical system (BES) because the current density and TAN loading rate cannot be controlled independently.

Results: We found a clear increasing trend in TAN removal efficiency with respect to load ratio in the BES for both human and synthetic urine. The maximum TAN removal efficiency was 60.9% at a load ratio of 0.7, corresponding to a TAN transport rate of 119 gN m^{-2} d^{-1} at an electrical energy input of 1.9 kWh kgN^{-1} (synthetic urine). Low load ratios (<1) were obtained, indicating that the current was not enough to transport all the TAN across the membrane.

Conclusions: BES and ES show the same general relation between TAN removal efficiency and load ratio. Therefore, given a stable current density, the concept of load ratio can also predict the TAN removal efficiency in BES. Higher current densities, and insights in the factors limiting current, are needed to increase the load ratio and therefore the TAN removal efficiency.

This chapter has been published as: Rodríguez Arredondo M, Kuntke P, ter Heijne A, Buisman CJN. The concept of load ratio applied to bioelectrochemical systems for ammonia recovery. *J. Chem. Technol. Biotechnol.* 2019, *94 (*6), 2055-2061.

5.1 Introduction

Around 1- 2% of the total world energy consumption is used to produce ammonia (NH_3) from atmospheric nitrogen gas (N_2) [23]. A large part of this produced reactive nitrogen ends up in the environment, mainly in agricultural waste streams and domestic wastewater [77, 94]. At the same time, removing nitrogen compounds from wastewater is one of the most energy-intensive processes for conventional wastewater treatment plants [58]. The widely used nitrogen-removal processes (i.e. nitrification/denitrification and Anammox) in conventional wastewater treatment plants convert usable reactive nitrogen compounds back to inert N_2. In order to reduce the cost and environmental impact of these processes, the focus of technological development has shifted from the removal of nitrogen to the recovery of nitrogen [27]. Direct recovery of nitrogen (i.e. NH_3 stripping, struvite precipitation or ion exchange [39]) from waste streams avoids its conversion first to N_2 and then back to a reactive form [89].

Two of the newest technologies aiming for the recovery of total ammonia nitrogen (TAN; the sum of NH_3 and NH_4^+ nitrogen) from wastewaters are electrochemical systems (ES) and bioelectrochemical systems (BES) [62, 77, 89, 99]. In order to recover a cleaner, purer product, these systems are usually coupled to stripping-absorption units [40, 48, 88, 145, 167] or gas-permeable hydrophobic membrane units (TransMembrane ChemiSorption or TMCS) [75, 143, 168–170]. The main advantage of these integrated systems is their sustainability: there is no need for the addition of chemicals such as caustics, and useful by-products are obtained (such as electricity or hydrogen).

In general, (bio) electrochemical systems ((B)ESs) consist of an anode connected over an external circuit to a cathode. At the anode, an oxidation reaction occurs, whereas at the cathode a reduction reaction occurs. These reactions are catalysed by different materials, and in the case of bio-electrochemical systems, by electrochemically-active microorganisms. The anode pH decreases due to the oxidation reaction leading to proton production, while the cathode pH increases due to the hydrogen evolution reaction that leads to hydroxide production [89]. An ion exchange membrane is usually placed between anode and cathode chambers. An insufficient transport of protons and/or hydroxyl ions over these membranes results in pH differences between anode and cathode [124]. In (B)ESs for the recovery of TAN, a cation-exchange membrane (CEM) is used to allow for the transport of NH_4^+ from the feed to the cathode chamber, where it is converted to NH_3 due to the high catholyte pH. The catholyte is then hydraulically connected to a stripping-absorption or TMCS unit for the recovery of NH_3 in an acid. TAN in (B)ESs can be transported over the CEM via diffusion (concentration-gradient induced) and electromigration (current-induced) [146].

The complexity of reactions occurring in (B)ESs and the interdependence of the parameters involved make the complete, large-scale recovery of TAN a challenge [168, 170]. The load ratio was recently identified as a crucial parameter to optimize the recovery of TAN in an ES treating urine [170]. The load ratio is the ratio between the current density and the TAN loading rate of the system. In theory, one mole of electrons is needed to remove one mole of TAN, given that under acidic conditions (commonly found in the anode) all TAN is present as ammonium. Accordingly, three conditions can be defined: a load ratio <1 describes a situation in which the current density is not enough to transport all the TAN in the system; a load ratio of 1 describes a situation in which the current density and the TAN loading rate are equal; and a load ratio >1 describes a situation in which the current density is higher than the TAN loading rate, so that ideally all TAN could be transported. The higher the load ratio, the higher the removal efficiency of the system, but also the higher the energy input. Therefore, working at an optimum load ratio allows maximum TAN removal efficiency at minimal energy input [170].

The load ratio can be manipulated either by changing the current density (such as in an electrochemical system) or the TAN loading rate. In an electrochemical system, the load ratio can be easily manipulated, since both the applied current density and the TAN loading rate can be controlled independently. In a bioelectrochemical system, however, the current density and the TAN loading rate cannot be controlled independently. We recently investigated the influence of the load ratio in a ES [170], but the application of the load ratio concept in a BES has not been studied. In a BES, the current density depends on the oxidation of organic matter (COD) by microorganisms. The oxidation of organic matter by microorganisms, in turn, depends on the amount and nature of organic compounds, anode potential, and other factors also affecting the microorganisms, such as pH [161, 171, 172]. At the same time, the COD/TAN ratio of a certain wastewater is fixed, so manipulating the TAN loading rate would also affect the COD loading and therefore the current density. The load ratio, thus, might be a difficult parameter to control in a BES.

The goal of this study was to investigate the validity and applicability of the concept of load ratio in a BES treating urine. BES with integrated TMCS units were run on human urine and synthetic urine at different dilutions, flowrates, and modifications (such as reduced TAN concentration, lower pH, feeding the effluent of the cell, etc.) in order to obtain a variety of load ratios.

5.2 Materials and methods

5.2.1 Experimental setup

The experiments were performed in microbial electrolysis cells (MECs) coupled to hydrophobic, gas-permeable membrane modules, also called TransMembrane ChemiSorption (TMCS) units. The cathode chamber of each cell was hydraulically connected to an individual TMCS unit as described previously [170]. The catholyte (cathode electrolyte) was recirculated over the TMCS unit for the recovery of NH_3 in sulphuric acid [143, 170]. The setup scheme and reactions occurring at the anode and the cathode can be found on the Supporting Information (Figure S5.1).

Three MECs were used in total, one for each experimental run. Each cell consisted of two titanium plates (16 cm x 16 cm) which a machined flow field (10 cm x 10 cm x 0.2 cm) coated with a thin Pt layer (50 g m^{-2}) (Magneto Special Anodes, Schiedam, The Netherlands). The platinized flow field served as an anodic current collector or as a cathode (acting as a catalyst for a hydrogen evolution reaction). Graphite felt (FMI Composites Ltd., Galashiels, Scotland) was used as the anode, whereas the cathode was either the platinized flow field itself or a 100 µm titanium mesh (10 x 10 cm) with a ruthenium mixed metal oxide (RuMMO) coating (Magneto Special Anodes B.V., Schiedam, The Netherlands). Both cathode materials are known as excellent catalysts for hydrogen evolution [173]. The hydraulic volume of the anode chamber, including the recirculation vessel, was 200 mL. The hydraulic volume of the cathode chamber, including the recirculation vessel and the volume encased in the TMCS unit, was 300 mL. Anode and cathode chambers were separated by a cation exchange membrane (Nafion®117, Ion Power GmbH, Germany) with a projected surface area of 0.01 m^2 (same as anode and cathode). Spacer material (PETEX 07-4000/64, Sefar BV, Goor, The Netherlands) was placed on both anode and cathode sides of the membrane.

Each TMCS unit consisted of a tubular polyproplylene membrane (pore size 200 nm, type Accurel PP V8/HF, CUT Membrane Technology GmbH, Germany) encased in a custom made membrane module. The TMCS membrane has an outer surface area of 0.04 m^2. It was operated in crossflow mode, with the catholyte on the inner and the acid on the outer side of the TMCS membrane. The acid recirculation vessel was placed on top of a magnetic stirring plate in order to provide better mixing.

Anode and cathode potentials were measured versus reference electrodes (Ag/AgCl 3M KCl, +0.2 V vs. NHE, QM711X, ProSense BV, Oosterhout, The Netherlands), which were placed in the respective electrolytes near the inlet of anode and cathode chambers. The anode potential was controlled by a potentiostat (KP 07, Bank 116 Elektronik - Intelligent Controls GmbH, Pohlheim, Germany). Temperature and pH of both anolyte (anode

electrolyte) and catholyte were measured by pH meters (Orbisint CPS11D sensor with Liquisys M COM 253 transmitter, Endress + Hauser BV, Naarden, The Netherlands) placed in each recirculation vessel. A data logger (Memograph M RSG40, Endress + Hauser BV, Naarden, The Netherlands) recorded each minute the anode and cathode potentials, anode and cathode pH and temperature, cell voltage and current density.

Two peristaltic pumps (Masterflex L/S, Metrohm Applikon BV, Schiedam, The Netherlands) were used in each system: one to provide fresh anolyte continuously and the other to recirculate anolyte, catholyte and acid through the TMCS unit.

Both anode and cathode recirculation vessels had a gas vent connected to a water lock to let CO_2, CH_4 and H_2 to escape and to prevent oxygen from coming into the system.

5.2.2 Media composition and inoculation

Media composition

Pre-treated human urine and synthetic urine were used as stock solutions to prepare varied anolyte inflows. Human urine was collected from the water-free urinals (Urimat®, Biocompact, Rotterdam, The Netherlands) installed in the male bathrooms of the Wetsus building (Leeuwarden, The Netherlands). The collected urine was stored in a tank for approximately 7 days, and later pre-treated by struvite precipitation and filtration to remove phosphate as described previously [170]. The composition of the pre-treated human urine can be found in Table S5.1 (Supporting Information). The synthetic urine stock was adapted from Ledezma et al. (2017) [174] by reducing the amounts of acetate and TAN. This was done to match the chemical oxygen demand (COD) and TAN concentration of the pre-treated human urine used in this study. The carbon source was ammonium acetate, while the TAN came from three sources: the ammonium acetate, ammonium hydroxide and ammonium bicarbonate. The complete recipe can be found in Table S5.2 (Supporting Information).

Modifications were made to the stocks of human urine and synthetic urine before feeding them to the BES (Table 5.1). Depending on the experiment, these modifications included dilution, pH adjustment, and reduction of the TAN concentration. The reduction of the TAN concentration was achieved, in the case of human urine, by performing a pre-treatment with the TMCS. In the case of synthetic urine, the TAN concentration in one experiment was reduced by 33% by adding half of the ammonium bicarbonate. For some human urine experiments, the effluent from the BES was collected and later fed back to the cell. The catholyte consisted of a 0.01M NaCl solution. One liter of 1M H_2SO_4 was used as the acid for absorption in the TMCS unit.

Inoculation and start-up

The cell from the first run was inoculated with effluent from an active, acetate oxidizing bioanode. The two other cells (second and third run) were inoculated with a mixture of two effluents: 20 ml from an active, acetate oxidizing bioanode and 10 ml effluent from a bioanode previously running on urine (cell from first run). For the start-up period, synthetic wastewater (composition in Table S5.3 (Supporting Information)) with 10 mM sodium acetate as the carbon source was used. All cells were started up with cell potential control at -0.5V. After stable current densities were established, the configuration was changed to anode potential control. The bioanode from the first run was constantly poised at a potential of -0.35 V vs Ag/AgCl and later changed to -0.3 V vs Ag/AgCl. For the second and third runs, the bioanodes were initially poised at a potential of -0.4 V vs Ag/AgCl and gradually increased to -0.3 V vs Ag/AgCl. After a start-up period of around 1 month in all cases, pre-treated urine was introduced.

5.2.3 System operation

Each experimental run lasted 5 months. The second and third runs were performed at the same time. After the start-up phase of each run, the anode potential was constantly controlled at -0.3 V vs Ag/AgCl. There was an exception in which, due to deterioration in performance, the bioanode of cell 3 was controlled at -0.4V vs Ag/AgCl for 34 days.

The temperature of the cells was controlled (30.3 ± 0.3°C). The anode chambers had a continuous inflow of anolyte (inflow rate), while both the cathode chamber and TMCS unit were operated in batch mode. All three liquids (anolyte, catholyte and acid) were recirculated over their respective chambers at either 70 mL min^{-1} (first run, and first 67 days of the second and third runs) or 140 mL min^{-1} (after 67 days of the second and third runs). The anolyte inflow rates were varied throughout the experiments (ranging from 0.2 to 6.3 ml min^{-1}), which resulted in varied current densities and load ratios as shown in Table 5.1. In most of the experiments, water transport over the TMCS membrane was observed. Catholyte was added once the volume was lower than 100 ml, and the acid volume was lowered if it was more than 1.1L or renewed if it contained more than 14 gTAN L^{-1}. Both the catholyte and acid solutions were continuously sparged with a very low amount of N_2 gas (≤ 2 ml/min) to maintain anaerobic conditions.

After the start-up phase of the first run, the synthetic wastewater was switched to 5x diluted urine and gradually changed to undiluted urine, while trying to maintain TAN loading rates constant, as shown in Table 5.1.

After the start-up phase of the second and third runs, the synthetic wastewater was first switched to 5x diluted urine containing 70% less TAN, followed by other experiments with 5x diluted urine containing 34% less TAN, and later urine in different dilutions and other

amendments, as explained in the "Media composition" section. Part of the TAN in urine was removed to manipulate the TAN loading rate in order to test different load ratios. Afterwards, experiments with synthetic urine at different dilutions were performed (Table 5.1). All experiments performed with pre-treated human urine, with the exception of the one with 70% less TAN, are referred to as 'urine' experiments. The experiments performed without TMCS or in which the TMCS was not working are not taken into account in Table 5.1 or the results.

The three BESs were operated on a large variety of operational condition (i.e. synthetic urine, pre-treated urine, different dilutions, adjustments in pH, TAN and COD concentration). Those conditions were categorized as seen in Table 5.1.

Table 5.1. Overview of experiments performed in each run. The experiments were separated in three categories: urine, urine 70% less TAN, and synthetic urine. In each category, different dilutions, flowrates, and modifications (such as different pH or using collected effluent, etc.) were tested. The urine from which 34% of the TAN was removed is included in the category "urine". The range of TAN loading rate tested, as well as the range of current density (J) and load ratio (L_N) obtained are shown.

Run	Influent	Dilution or conditions tested	Duration	TAN loading rate	J	L_N
			(days)	(g m^{-2} d^{-1})	(A m^{-2})	(-)
1	**Urine**	5x	16	61- 78	3.3-4.5	0.6- 0.8
		2.5x	21	76-82	2.6- 3.5	0.4- 0.6
		2.5x, lower flowrate	14	59-63	2.3- 2.7	0.5
		-	13	73-81	0.5-0.8	0.1
		Lower pH (7.6)	42	74-83	0.5-0.6	0.1
		+60 mM acetate	15	75-80	0.4- 0.5	0.1
2	**Urine 70% less TAN**	5x	7	49-80	5.9- 9.2	1.5
	Urine	34% TAN removed (5x), 6x, 7.5x, effluents, different flowrates	51	109-565	0.9-5.0	0.0- 0.6
	Synthetic urine	33% TAN removed (9x), 9x, 4x, 2x	21	139-226	5.1 -10.6	0.4- 0.7
3	**Urine 70% less TAN**	5x	7	49- 80	5.9- 9.5	1.5
	Urine*	34% TAN removed (5x), 6x, 7.5x, effluents, different flowrates	62	109- 449	1.1- 6.3	0.0- 0.7
	Synthetic urine	33% TAN removed (9x), 9x, 4x, 2x	30	137-226	1.4- 3.1	0.1- 0.3

* Anode potential was -0.4 V during 34 days, instead of -0.3 V as for the rest of the experiments

5.2.4 Sampling and chemical analysis

Samples were taken after a minimum of 4 hydraulic retention times (HRTs) after a parameter was changed. For each condition, two to seven samples were taken from the inflow and each recirculation vessel (anolyte, catholyte and acid), with a sampling interval of at least 24 h.

The samples were filtered through 0.45 µm filters (PTFE syringe filters, VWR International B.V., Amsterdam, The Netherlands) prior to analysis. COD concentration (inflow, anolyte and catholyte), as well as TAN concentration from the acid samples were measured using photometric test kits (LCK 514 and LCK 303, spectrophotometer XION 500, Dr. Lange Nederland B.V., The Netherlands). TAN concentration from the inflow, anolyte and catholyte samples in the first run were also measured as described previously. In the second run, TAN, cations and anions were measured by ion chromatography as described earlier [170].

5.2.5 Calculations

The load ratio was calculated as described previously by Rodriguez Arredondo et al. (2017) [170]. The load ratio is the relation between the current density and the TAN loading rate, both expressed in A m^{-2} (Equation 5.1).

$$L_N = \frac{j_{applied}}{C_{anolyte\ inflow,TAN} * Q_{anode} * \frac{F}{A_m}} \qquad \text{Equation 5.1}$$

where $j_{applied}$ is the applied current (A m^{-2}), $C_{anolyte\ inflow,\ TAN}$ is the molar concentration of TAN in the anolyte inflow (mol m^{-3}), Q_{anode} the anolyte inflow rate ($m^3\ s^{-1}$), F the Faraday constant (96,485 C mol^{-1}) and A_m the surface area of the cation exchange membrane (0.01 m^2).

The equations for TAN removal efficiency (RE_{TAN}), TAN transport rate over the CEM (J_{TAN}), TAN transport efficiency (tE_{TAN}) and total energy input can be found in the Supporting Information.

5.3 Results and discussion

5.3.1 There was a clear increasing trend in TAN removal efficiency with load ratio

The current density from the BESs ranged, in average, from 0.4 to 10.6 A m^{-2}, and resulted in varying load ratios (Table 5.1). The load ratio is the ratio between the current and the TAN loading rate, both expressed in A m^{-2}. As seen in Figure 5.1, there is a clear increasing trend in TAN removal efficiency with respect to load ratio for both human and synthetic

urine. The maximum removal efficiency was 60.9% for a load ratio of 0.68. In some cases, TAN removal efficiency was lower than expected. This occurred in two specific situations: (1) when ammonia was not effectively removed from the catholyte by the TMCS, and (2) for urine with the lowest TAN concentration (urine 70% less TAN).

Negative TAN removals were observed for the situation without a TMCS, or when the TMCS was not operational (data not shown). This was caused by diffusion of TAN from the cathode chamber back into the anode chamber when TAN was not effectively removed from the catholyte [87, 139, 146].

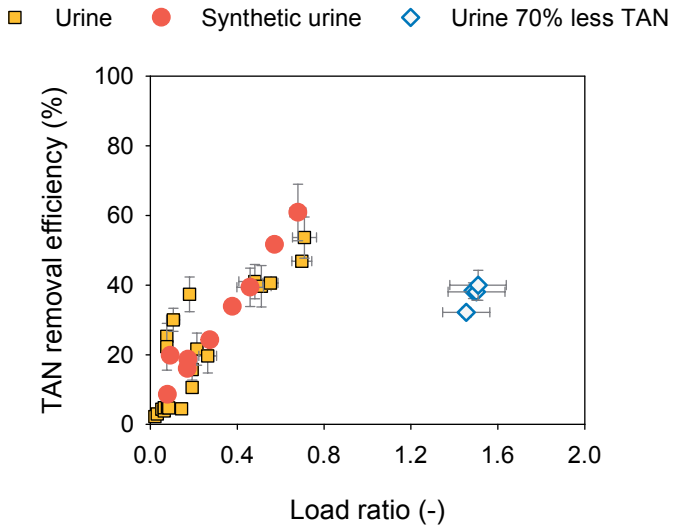

Figure 5.1. TAN removal efficiency with respect to load ratio from a bioelectrochemical system treating real and synthetic urine at different dilutions, and urine with 70% less TAN (pre-treated with a TMCS).

The experiments with urine with 70% less TAN in Figure 5.1 show the highest load ratio. The general expected trend is for the TAN removal efficiency to increase with the load ratio, reaching a maximum and then stabilizing. For that reason, these experiments were expected to result in the highest TAN removal efficiencies, yet this was not the case. In these experiments, the initial TAN concentration was the lowest: 199.6± 7.3 mg/L. This low TAN concentration was the result of a pre-treatment step, in which around 70% of the TAN in urine was removed with a TMCS, the pH was adjusted with NaOH and then the urine was diluted 5 times. For this reason, the proportion of NH_4^+ compared to other ions was much lower than in other experiments, which lead to the relatively high transport of other ions. Therefore, even though the current density was sufficient to transport all the TAN (load ratio higher than 1), the lower TAN transport efficiency resulted in an overall lower TAN removal efficiency.

5.3.2 Effect of TAN transport efficiency on TAN removal efficiency

The transport efficiency shows the contribution of an ion to the total charge transport across the membrane. According to our previous study [170], the load ratio is better suited as a single parameter to predict TAN removal efficiency than the TAN transport efficiency. Our current results on BESs (Figure 5.2) support this finding. In Figure 5.2, no defined relationship can be observed between the transport efficiency and TAN removal efficiency. Even though most of the charge was transported by ammonium in the majority of the experiments (TAN transport efficiencies between 50 and 100%), the TAN removal efficiencies varied widely.

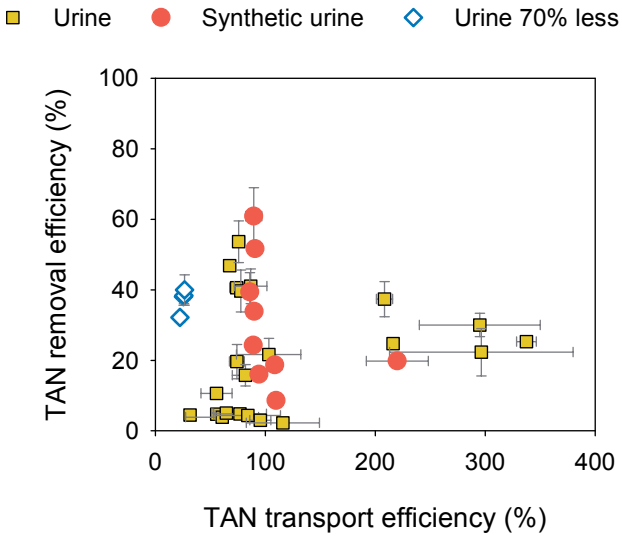

Figure 5.2. TAN removal efficiency with respect to transport efficiency from a bioelectrochemical system treating real and synthetic urine at different dilutions and urine with 70% less TAN (pre-treated with a TMCS).

Transport efficiencies higher than 100%: Diffusion and charge exchange

The data points in Figure 5.2 with TAN transport efficiencies >200% correspond to the data points in Figure 5.1 with load ratios <0.2 and higher TAN removal efficiencies than others. One of the reasons for transport efficiencies >100% is diffusion. The contribution of diffusion compared to migration increases at low current densities [69, 146, 167]. Some of the data points in Figure 5.2 with transport efficiencies >200% were the ones with the lowest current densities overall: 0.5- 0.7 A m^{-2}. Therefore, even though the load ratio was very low because of the low current, the TAN removal efficiency was high because of the contribution of diffusion.

Another reason for transport efficiencies >100% is the charge exchange process [61, 125]. When cations other than NH_4^+ (such as Na^+ and K^+) diffuse from cathode to anode, an equivalent amount of NH_4^+ is transferred from anode to cathode to maintain electroneutrality. This was the case of another experiment: the concentration of competing cations (Na^+ and K^+) in the catholyte was much higher than in the anolyte, promoting their diffusion from cathode to anode (Figure S5.2B (Supporting Information) experiment 4). To maintain electroneutrality, an equivalent amount of NH_4^+ can diffuse from anode to cathode, which resulted in transport efficiencies higher than 100%.

Transport efficiencies lower than 30%: Ionic composition

The transport efficiency is influenced, among other factors, by the ionic composition (in this case, the proportion of NH_4^+ compared to other competing ions, such as Na^+ and K^+). The experiments in which the urine was pre-treated to remove 70% of the TAN resulted in the lowest transport efficiencies. As mentioned previously, even though the current density was sufficient to transport all the TAN (load ratio higher than 1), mostly other cations were transported across the CEM, resulting in an overall lower TAN removal efficiency.

This can be explained by the ionic composition of the feed. The mole fraction of TAN to the total cations ($n_{TAN}/n_{total\ cations}$) in the experiments with 70% less TAN was around three times lower than for the rest of the experiments (mole fractions were 0.23 and 0.69, respectively). Other studies have shown that high TAN removal efficiencies (> 60%) can be achieved at low transport efficiencies (15- 30%), but in those cases the mole fraction of TAN was higher (from 0.38 to 0.70) [40, 88, 170]. Therefore, a much higher load ratio (higher current density) is required to reach high TAN removal efficiencies in this situation (low TAN mole fractions), which will increase the energy demand. These results show that even though the load ratio is a crucial parameter to optimize the operation of the nitrogen-recovery system, there are limitations to this simple model. As shown in this and earlier studies [170], the wastewater composition (i.e. TAN concentration relative to other cations) does affect the current density required to reach high recoveries. Therefore, the model needs to be adapted to the specifics of the wastewater.

5.3.3 The relationship between the load ratio and the total energy input

There is a linear increase in TAN transport rate (or flux) with current density, as expected (Figure 5.3A). Again, the urine experiments with the lowest TAN concentration (urine 70% less TAN) were the exception to this trend. These experiments showed lower TAN fluxes than other urine experiments, even at higher current densities. Therefore, a higher current density is needed to remove the same amount of TAN from a stream with a low TAN concentration compared to a stream with a high TAN concentration. As a result, the energy input for TAN recovery is higher (Figure 5.3B). For some experiments the urine was

pre-treated with the TMCS to remove about 34% of the initial TAN, resulting in a TAN mole fraction of 0.46 (1.5 times lower than the other urine experiments). However, this did not seem to have an effect as radical on the overall performance as the experiments with 70% less TAN (mole fraction of 0.23).

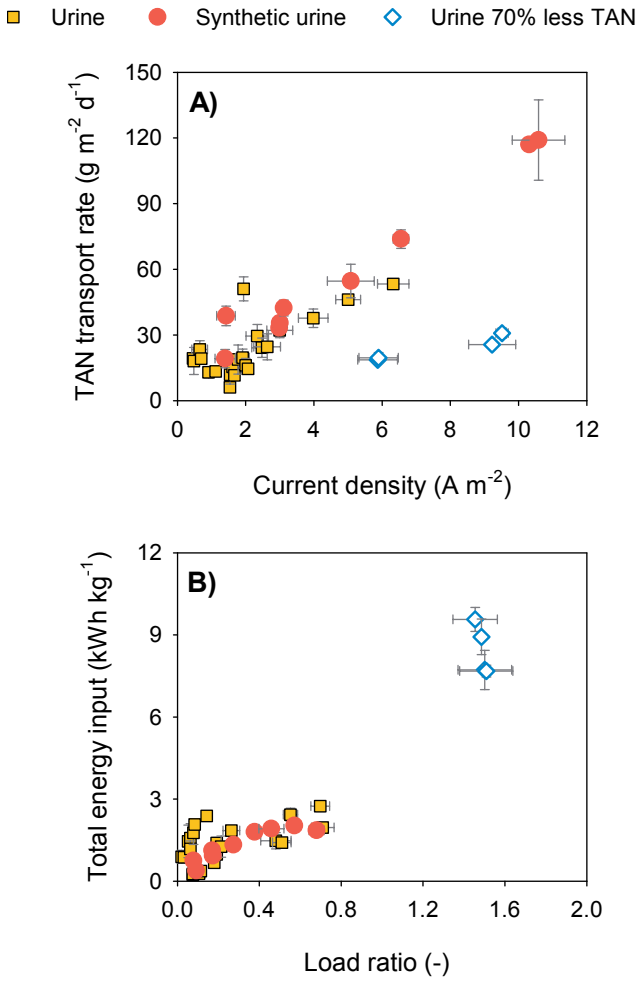

Figure 5.3 A) TAN transport rate with respect to current density and **B)** total energy input with respect to load ratio from a bioelectrochemical system treating real and synthetic urine at different dilutions and urine with 70% less TAN (urine was pre-treated with a TMCS).

In our previous study with an electrochemical system [170], a "limiting" load ratio (1.2) was found. This meant that working at a load ratio higher than the limiting one costed more energy without providing a considerable increase in removal efficiency. In this study, except for the urine with 70% less TAN, there was no steep increase of energy input with

load ratio at any point (Figure 5.3B). Since we did not obtain load ratios higher than 0.8, an optimal or "limiting" load ratio was never reached.

5.3.4 TAN removal efficiency was limited in a BES: high load ratios cannot be achieved

Figure 5.4 compares the results from this study with similar BES studies for TAN recovery and with the results in our previous ES study. The selected studies also use an integrated system in the cathode for the effective recovery of NH_3 (such as stripping-absorption or a TMCS unit). The load ratio was calculated with the data provided by these studies. The results from these studies were similar to ours (except from the 70% less TAN cases), and follow the general trend of increasing TAN recovery with increasing load ratio. This trend is the same for both BES and ES. Higher TAN removal efficiencies were achieved with an ES compared to the BESs, due to the higher load ratios obtained.

As observed in Figure 5.4A, a load ratio below 1.5 was obtained in all our bioelectrochemical experiments. Except for the experiments at the lowest TAN concentration, the load ratio in all experiments was below 0.8. This was also the case in other studies of BESs for TAN recovery [143, 145, 168]. At these load ratios, the current was not high enough to transport all the TAN across the membrane.

Figure 5.4B shows the correlation between the predicted TAN removal efficiencies (using the load ratio model based on ES experiments [170]) and the measured TAN removal efficiencies in this study. Overall, a good correlation (R^2= 0.81) was found. The slope of the linear regression was lower than one (0.96), which means that, in general, the prediction slightly overestimates the actual TAN removal efficiency. Therefore, the concept of load ratio is a useful tool to predict the TAN removal efficiency in BESs too; however, it was not possible in this study to achieve high TAN recovery efficiencies (maximum of 47% for human diluted urine and 60% for synthetic urine). The reason for this is the lack of control of the current density due to microbial processes involved in a BES, compared to an electrochemical system.

For the load ratio (and therefore the TAN removal efficiency) to increase, higher current densities are needed. In electrochemical systems, higher load ratios can be achieved by applying higher current densities without the dependence on COD removal. As mentioned earlier, the current density in a BESs depends on the oxidation of organic matter by microorganisms, which in turn depends on the amount and nature of organic compounds, anode potential, and other factors also affecting the microorganisms, such as pH (Table S5.4). Compared to an ES, a BES offers a lower energy input [143] and an effluent with a lower COD load. In these BES experiments, the COD removal efficiencies were usually lower than 40% (data not shown). High coulombic efficiencies (>60%, data

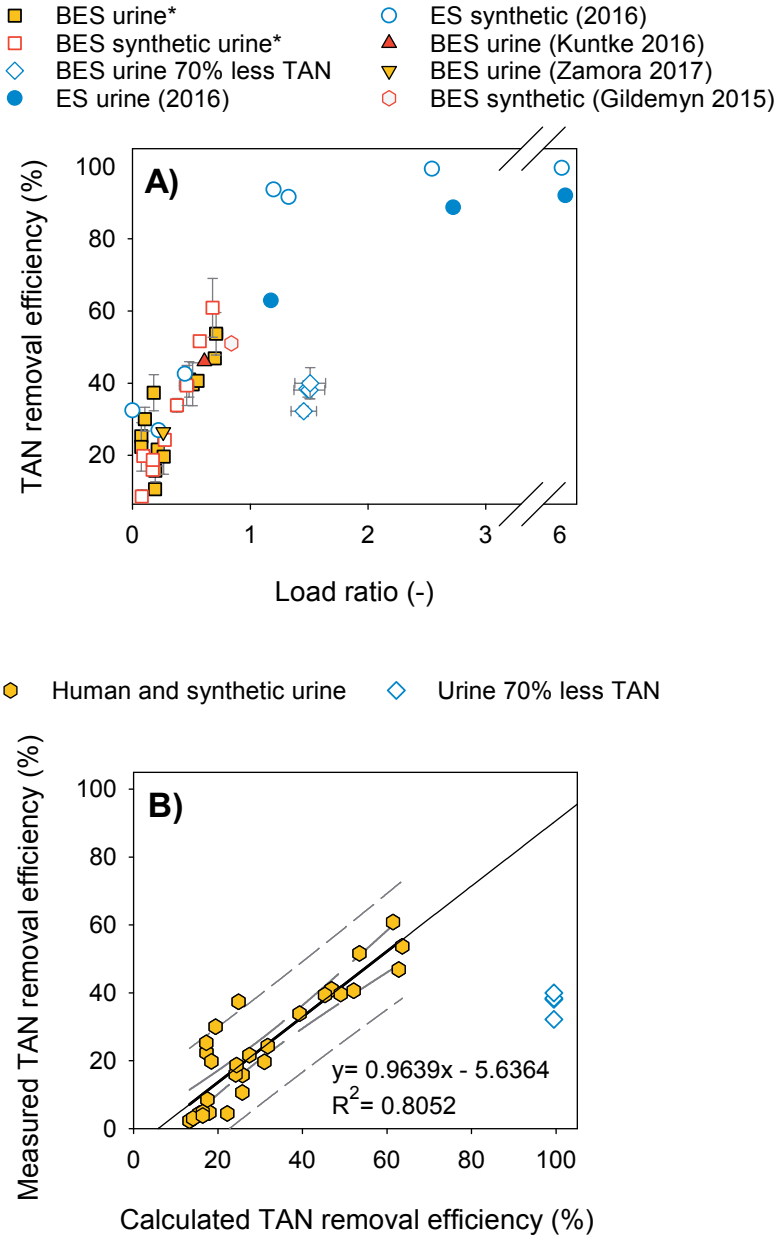

Figure 5.4 A) TAN removal efficiency with respect to load ratio in bioelectrochemical systems (BES) and electrochemical systems (ES) based on this study and four other different studies. This study (*) used a BES to treat real and synthetic urine at different dilutions, and urine with 70% less TAN (pre-treated). **B)** Correlation between the predicted and the measured TAN removal efficiency in this BES study. The predicted TAN removal efficiency was calculated using the load ratio model based on ES experiments [170]). Long-dashed and short-dashed curves represent the 95% confidence interval and 95% prediction interval for the linear regression, respectively.

not shown) were obtained in most cases, meaning that most of the COD consumed was converted to electric current. For this reason, more insights are needed into what is limiting the removal of COD and its relation with TAN removal.

Acknowledgements

This work was performed in the cooperation framework of Wetsus, European Centre of Excellence for Sustainable Water Technology (www.wetsus.eu). Wetsus is co-funded by the Dutch Ministry of Economic Affairs and Ministry of Infrastructure and Environment, the European Union Regional Development Fund, the province of Fryslân, and the Northern Netherlands Provinces. Part of this research has received Funding from the European Union's Seventh Programme for research, technological development and demonstration under grant agreement No 308535. The authors like to thank the participants of the research theme "Resource Recovery" for the fruitful discussions and their financial support.

5.4 Supporting information

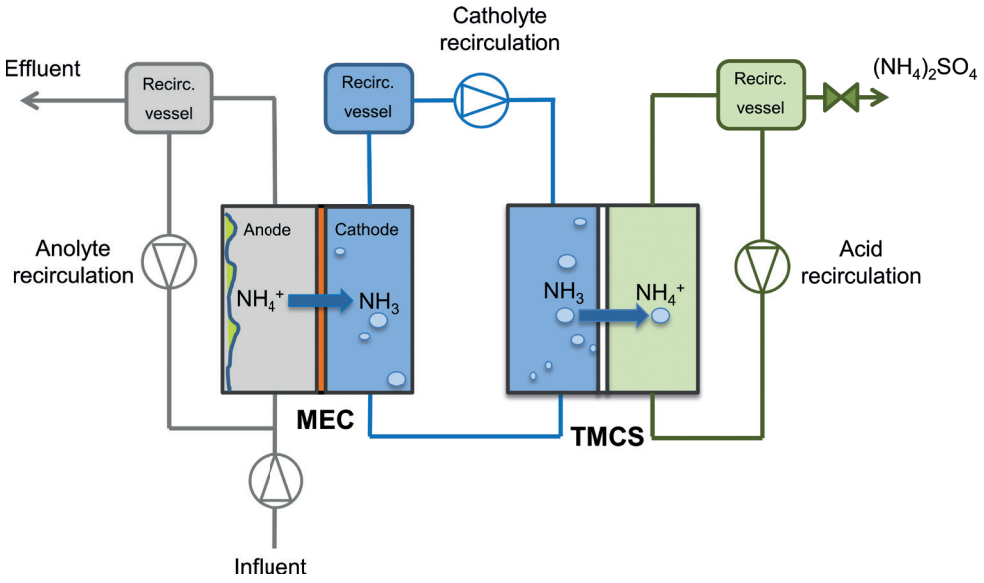

Figure S5.1. Schematic representation of experimental setup. MEC= Microbial Electrolysis Cell; TMCS=TransMembrane ChemiSorption. There were two membranes in the system: a cation exchange membrane in the MEC and a gas-permeable hydrophobic membrane in the TMCS unit.

At the anode of the MEC, anaerobic microorganisms can oxidize biodegradable organic matter to bicarbonate, protons and electrons, which is often represented by the oxidation of acetate:

$$CH_3COO^- + 4H_2O \rightarrow 2HCO_3^- + 8e^- + 9H^+$$

At the cathode of the MEC protons are reduced to hydrogen gas (hydrogen evolution reaction (HER)):

$$2H_2O + 2e^- \rightarrow H_2 + 2OH^-$$

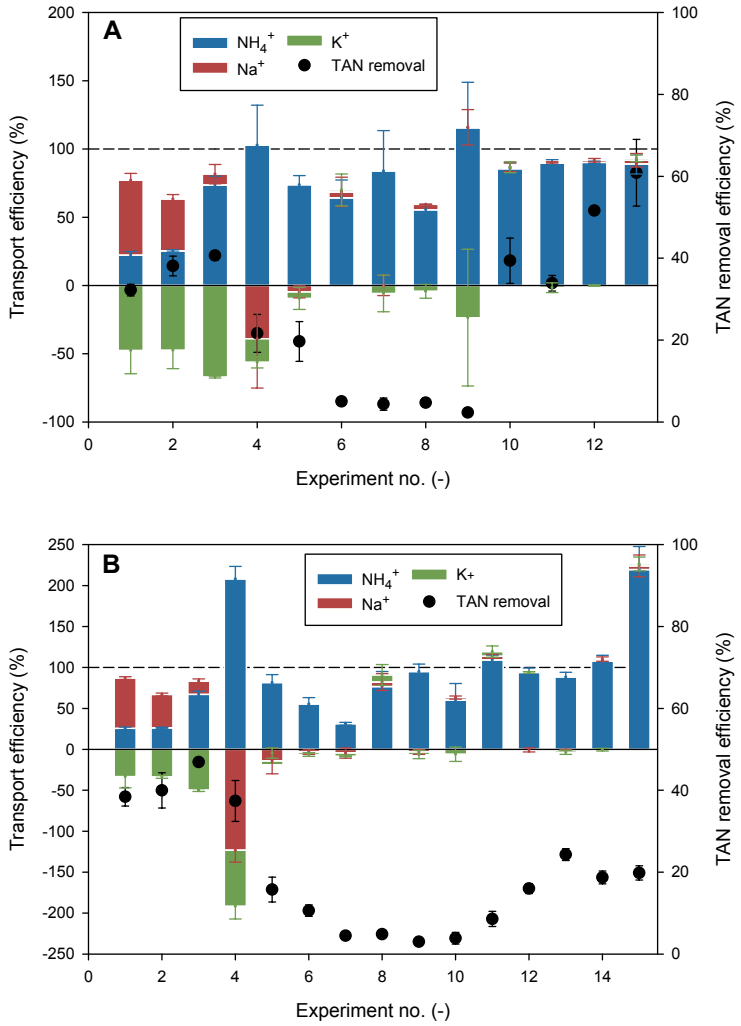

Figure S5.2. Membrane transport efficiency of the main cations and TAN removal efficiency for each experiment performed in **A)** Run 2, and **B)** Run 3

Pre-treated human urine stock composition

Table S5.1. Pre-treated human urine stock composition

Parameter	Value	Unit
pH	9.27 ± 0.5	
Conductivity	30.6 ± 1.9	mS cm^{-1}
COD	3.09 ± 0.41	g L^{-1}
TAN	4.02 ± 0.51	g L^{-1}
Na^{+}	1.54 ± 0.08	g L^{-1}
K^{+}	1.36 ± 0.09	g L^{-1}
Mg^{2+}	0.06 ± 0.01	g L^{-1}
Ca^{2+}	0.01 ± 0.00	g L^{-1}
Cl^{-}	3.31 ± 0.14	g L^{-1}
PO_4^{3-}	0.03 ± 0.03	g L^{-1}

This pre-treated human urine stock was later modified depending on the experiment carried out, as explained in the "Media composition" section of the study.

There were 2 experiments performed with 70% less TAN and 2 experiments performed with 34% less TAN. For these experiments, the stock was pre-treated with the TMCS until 70 or 34% of the TAN was removed. This treatment would result in urine with a lower pH, so in 3 of those experiments (2 with 70% less and 1 with 34% less TAN), the pH was increased with 1M NaOH. Afterwards, all of them were diluted 5x with ultrapure water.

Synthetic urine stock recipe

The synthetic urine stock recipe was adapted from Ledezma et al. (2017) [174]. The amounts of acetate, TAN and sulphate were significantly reduced to match the concentration found in the pre-treated human urine used in this study.

The stock had a chemical oxygen demand (COD) concentration of 3.94 ± 0.30 g L^{-1} and a TAN concentration of 4.9 ± 0.3 g L^{-1}, a pH of 9.12 ± 0.03 and a conductivity of 40.5 ± 1.0.

The stock was filtered and diluted 9, 4 and 2 times with ultrapure water. During one experiment with 9x diluted synthetic urine, the TAN concentration was reduced by 33% by adding half of the ammonium bicarbonate (11.07 instead of 22.1 g L^{-1}). Furthermore, during the last experiment with synthetic urine (2x diluted), ammonium carbonate (13.4 g L^{-1}) was used instead of ammonium bicarbonate, which resulted in a slightly higher pH (9.62 ± 0.05) and lower conductivity 29.0 ± 0.3.

Table S5.2. Synthetic urine stock recipe (adapted from Ledezma et al. (2017) [174]).

Compound	Concentration	Unit
NH_4CH_3COOH	5.4	g L^{-1}
NH_4OH	1.4	g L^{-1}
NH_4HCO_3	22.1	g L^{-1}
Na_2SO_4	1.2	g L^{-1}
NaOH	3.4	g L^{-1}
KCl	0.3	g L^{-1}
K_2HPO_4	4.2	g L^{-1}
$MgCl_2.6H_2O$	0.8	g L^{-1}
$Ca_2Cl.2H_2O$	0.4	g L^{-1}
Trace elements solution (Zehnder et al. (1980) [175])	1	mL/L

Synthetic wastewater composition (used during the start-up period)

Table S5.3. Synthetic wastewater composition used during start-up

Compound	Concentration	Unit
$NH_4CH_3COO.3H_2O$	1.36	g L^{-1}
NH_4Cl	0.28	g L^{-1}
NaCl	0.58	g L^{-1}
NaOH	3.4	g L^{-1}
KCl	0.74	g L^{-1}
KH_2PO_4	0.87	g L^{-1}
K_2HPO_4	0.68	g L^{-1}
$MgSO_4.7H_2O$	0.01	g L^{-1}
$Ca_2Cl.2H_2O$	0.1	g L^{-1}
Trace elements solution (Zehnder et al. (1980) [175])	0.1	mL/L

Table S5.4. Overview of experiments performed in each run. The experiments were separated in three categories: urine, urine 70% less TAN, and synthetic urine. In each category, different dilutions, flowrates, and modifications (such as different pH or using collected effluent, etc.) were tested. The urine from which 34% of the TAN was removed is included in the category "urine". The anode pH, cathode pH and TAN removal (%) are shown.

Run	Influent	Dilution or conditions tested	pH anode	pH cathode	TAN removal (%)
1	**Urine**	5x	7-8	9-13	47-63
		2.5x	8	9	35-45
		2.5x, lower flowrate	8	8-9	36-44
		-	9	8	28-32
		Lower pH (7.6)	8	8	18-27
		+60 mM acetate	9	8-9	24-27
2	**Urine 70% less TAN**	5x	8	14	32-38
	Urine	34% TAN removed (5x), 6x, 7.5x, effluents, different flowrates	7-9	8-14	2-41
	Synthetic urine	33% TAN removed (9x), 9x, 4x, 2x	7-8	9	34-61
3	**Urine 70% less TAN**	5x	8	14	38-40
	Urine*	34% TAN removed (5x), 6x, 7.5x, effluents, different flowrates	7-9	8-14	3-47
	Synthetic urine	33% TAN removed (9x), 9x, 4x, 2x	9	8-9	9-24

Calculations

Removal efficiency of TAN (%)

The removal efficiency is a measure of how much was removed from the TAN that entered the system.

$$RE_{TAN} = \frac{C_{anolyte\ inflow,TAN} - C_{anolyte\ effluent,TAN}}{C_{anolyte\ inflow,TAN}} * 100 \quad \text{Equation S5.1}$$

TAN transport rate (over the cation exchange membrane, gN m^{-2} d^{-1})

$$J_{TAN} = \frac{(C_{anolyte\ inflow,TAN} - C_{anolyte\ effluent,TAN}) * Q_{anode}}{A_m} \quad \text{Equation S5.2}$$

Where Q_{anode} (L d^{-1}) is the anolyte inflow rate and A_m (0.01 m^2) is the surface area of the cation exchange membrane.

TAN transport efficiency (%)

The transport efficiency is the contribution of an ion to the total charge transport over the cation exchange membrane.

$$tE_{TAN} = \frac{\frac{J_{TAN}}{M_{TAN}} * z_{NH4+} * F}{j_{applied} * 100} * 100 \quad \text{Equation S5.3}$$

Where M_{TAN} (14 g mol^{-1}) is the molar mass of nitrogen, z_{NH4+} (-) represents the charge of NH_4^+, F the Faraday constant (96485 C mol^{-1}) and $j_{applied}$ (A m^{-2}) the current density.

Total electrical energy input per kg N removed (kWh kgN^{-1})

$$Total\ energy\ input = \frac{j_{applied} * E_{cell} * \frac{1\ kJ}{1000\ J} \frac{1\ kWh}{3600\ kJ}}{J_{TAN} * \frac{1\ kg}{1000\ g} * \frac{1\ d}{24\ h} * \frac{1\ h}{60\ min} * \frac{1\ min}{60\ s}} \quad \text{Equation S5.4}$$

Where E_{cell} (V) is the cell voltage.

General discussion and future perspectives

In this thesis, we evaluated the use of (bio)electrochemical systems for the recovery of total ammonia nitrogen (TAN) from urine. Our focus was on improving the understanding and performance of the system in terms of TAN recovery. This is crucial to get the technology closer to application as, at the start of this research, the proof-of-principle had just been demonstrated, and the highest TAN recoveries were around 30% [87].

During the course of this research, understanding of TAN recovery in (B)ESs and their performance was improved, while further research questions emerged. We demonstrated that an ES coupled to a gas-permeable hydrophobic membrane can effectively remove and recover TAN from urine (*Chapter 3*). Furthermore, we studied the effect of the relationship between current density and TAN loading rate (here defined as the load ratio) on TAN removal efficiency and energy input (*Chapters 3 and 5*). The load ratio is useful to find the conditions in which a (B)ES for the recovery of TAN can be operated optimally, but it does not take into account other parameters essential to assess the performance of (B)ESs. Moreover, a hydrogen-recycling electrochemical system (HRES) was developed, which allows for ammonia recovery at high rates and relatively low energy input compared to conventional electrochemical systems (*Chapter 4*). Lower energy demand can be achieved by reducing the anode overpotentials and transport losses, so the system design needs to be further optimized. Finally, we studied the concept of load ratio in a BES. Load ratios higher than 0.8 were not achieved because the current was not enough to transport all the TAN, which resulted in low TAN removal efficiencies. We concluded that further insight is needed into what is limiting the removal of COD.

In this chapter, we will focus on *why (bio)electrochemical systems for TAN recovery from urine have not been applied on a larger scale yet*, based on the work performed in this thesis and on literature. First, we give an overview of the status of this technology, including the most recent studies in the field. Later, we address the main limitations of TAN recovery by (B)ESs. Finally, we discuss the future perspectives and propose recommendations to bring this technology closer to application.

6.1 TAN recovery in (B)ES: State-of-the-art and limitations of the load ratio concept

At the early stages of development of (B)ESs for the recovery of TAN from nitrogen-rich wastewaters, around the time the proof-of-principle was reported [61], TAN removal rates from nitrogen-rich wastewaters ranged from 3-162 g m^{-2} d^{-1} (Table 2.1, *Chapter 2*) and TAN removal efficiencies were low, up to 30%. Most importantly, a proper concept to recover TAN from the catholyte was not developed, so TAN was only removed and not recovered. Since then, many researchers have aimed to increase TAN recovery, resulting

in TAN removal rates up to 3 to 6 times higher (with BESs and ESs, respectively) and TAN removal efficiencies up to around 90% (Tables 6.1 and 6.2). These advances were mainly due to improvements on the system design and the development of new configurations for the recovery of TAN from the catholyte.

The TAN recovery configurations are based on a combination of the (B)ES and more conventional technologies to recover NH_3 from the catholyte, such as stripping, membrane stripping (or transmembrane chemisorption, TMCS) and forward osmosis (FO). Most studies shown in Tables 6.1 and 6.2 can be classified as (B)ES-Stripping, (B)ES-TMCS and BES-FO. Within the BES-FO category there is also an "OsMFC", which is an MFC using a forward osmosis membrane to separate anode and cathode, instead of a cation exchange membrane [176]. Similarly, within the BES-Stripping category there are "submersible microbial desalination cells", which can be submerged into anaerobic reactors to recover TAN in situ. In this concept, the anode and cathode compartments are not separated by a membrane from each other, but rather separated by a membrane from the exterior, where the wastewater is (the anode compartment by an anion exchange membrane and the cathode compartment by a cation exchange membrane) [177, 178]. In this category there is also a "bipolar bioelectrodialysis" cell, which has two additional compartments and contains a bipolar membrane, a cation exchange membrane and an anion exchange membrane for the recovery of both ammonia and sulphate [179].

Other configurations include a TMCS unit within the same cell (an additional compartment separated from the cathode compartment by a flat-sheet gas-permeable membrane) [180]; an additional (third) compartment between the anode and cathode compartments for the improved concentration of NH_3 [174, 181]; TMCS integrated with the cathode as a membrane-electrode assembly (MEA) [182] and urine fed to the cathode compartment [167, 183]. The final product range has also extended from liquid solutions of ammonium salts to NH_4HCO_3 crystals [174] and NH_3 in growth medium for the production of microbial protein [167, 183].

The great variety of configurations complicates both the assessment of these technologies' performance and the objective comparison among them. In *Chapter 3*, we proposed the load ratio as a parameter of comparison between different (B)ESs for TAN removal and recovery. In the following section, we focus on the limitations of the load ratio concept as a parameter of comparison based on the studies reported in Tables 6.1 and 6.2.

Table 6.1. Performance of bioelectrochemical systems (BES) for the recovery of TAN reported in literature. Parameters included are current density (j), load ratio (L_N), TAN removal efficiency, TAN recovery efficiency, TAN transport rate, TAN transport efficiency, electrical energy input and the molar ratio of TAN compared to the total cations ($C_{TAN}/C_{cations}$). Blue values were calculated with data provided in the studies, green values were re-calculated to different units (modified and updated from [62])

Wastewater	System	Recovery method	j	L_N	TAN removal	TAN recovery	TAN transport rate	TAN transport efficiency	Electrical energy input	$C_{TAN}/C_{cations}$	Reference
			A m^{-2}	-	%	%	g_{TAN} m^{-2} d^{-1}	%	kWh kg_{TAN}^{-1}	-	
Urine	MFC	Stripping	2.6	0.06	1.6	-	10	29	-1.7	0.7	[54]
Synthetic (anode) and reject water (cathode)	(M)EC[d]	Stripping[f]	28	-	-	79	n.a.	n.a.	20.5	-	[43]
Urine	MEC	Stripping[g]	14.6 ± 1.7	0.36	33.9 ± 0.6	-	162 ± 10	-	1.8	-	[87]
Synthetic piggery wastewater	MEC[d]	Stripping-FO	1.5 ± 0.1	-	79.7 ± 2.0	-	8	-	2.7	-	[184]
Synthetic	MEC	Stripping	27	0.87	51 ± 0.5	-	226 ± 1	67.1 ± 0.3	6.04 ± 1.78	0.7	[145]
Pig slurry	MFC	Stripping	0.15	0.01	-	6.4	7 ± 0	-	-	-	[48]
Pig slurry	MEC	Stripping	-	-	-	94.3	25 ± 0	-	-	-	[48]
Synthetic	MFC[d]	Stripping	7.6 ± 0.3	0.74	88	-	80	119	-0.1	0.9	[177]
Synthetic	MFC	Stripping	4.3	0.31	55.3	40.8	86	-	0.0	0.9	[178]
Synthetic	MEC[d]	Stripping	2.7	-	91.7	71.2	12	-	2.8	1.0	[179]
Urine[b]	MEC	TMCS	1.7 ± 0.2	0.33	42 ± 6	39.9	27	70 ± 17	2.49 ± 0.67	-	[143]
Landfill leachate	MEC[d]	Stripping-FO	0.8	-	63.7 ± 6.6	53.8 ± 5.5	-	-	5.5	-	[50]
Synthetic urine	MEC[c]	Electro-concentration	29.3 ± 2.3	0.42	59.7 ± 2.47	49.5 ± 1.8	520	-	2.0[i]	0.7	[174]
Synthetic reject water	OsMFC[e]	FO	1.8 ± 0.1	1.32	85.3 ± 3.5	-	15	69.3 ± 1.9	-	0.6	[176]
Urine[a]	MEC	TMCS	1.7 ± 0.2	0.32	31 ± 13	31 ± 59	-	92 ± 25	1.4	-	[168]

Synthetic centrate	MEC[d]	Stripping-FO-MAP	0.8	1.49	81.3	99.7	5	-	1.10 ± 0.05	-	[185]
Synthetic centrate	MEC[d]	MEA[h]	3.0	-	-	-	36 ± 1	36.9 ± 0.7	1.61 ± 0.03	0.6	[182]
Synthetic urine	MEC	TMCS	10.6	0.68	60.9	-	119	89	1.85	0.7	[186]
Urine[b]	MEC	TMCS	4.0	0.71	53.7	-	38	76	1.96	0.7	[186]

(-) Not reported or not possible to determine with the data provided. n.a. Not applicable. [a] After struvite precipitation and softening. [b] After struvite precipitation. [c] 3 compartments. [d] Batch. [e] Osmotic MFC, forward osmosis (FO) membrane is used instead of a cation exchange membrane. [f] In batch, 20 hours. [g] Passive, with H_2 produced in the cathode compartment. [h] Membrane electrode assembly, TMCS integrated with the cathode. [i] This value is reported as 2.4 kWh per kg_N recovered, but it was recalculated to reflect per kg_N removed (as most studies)

Table 6.2. Performance of electrochemical systems (ES) for the recovery of TAN reported in literature. Parameters included are current density (j), load ratio (L_N), TAN removal efficiency, TAN recovery efficiency, TAN transport rate, TAN transport efficiency, electrical energy input and the molar ratio of TAN compared to the total cations ($C_{TAN}/C_{cations}$). Blue values were calculated with data provided in the studies, green values were re-calculated to different units (modified and updated from [62]).

Wastewater	System	Recovery method	j	L_N	TAN removal	TAN recovery	TAN transport rate	TAN transport efficiency	Electrical energy input	$C_{TAN}/C_{cations}$	Reference
			$A\ m^{-2}$	-	%	%	$g_{TAN}\ m^{-2}\ d^{-1}$	%	$kWh\ kg_{TAN}^{-1}$	-	
Digestate	EC	Stripping	30	2.41	63 ± 1	-	94	25	26.0 ± 0.7	0.4	[40]
Synthetic digestate	EC	Stripping	30	0.96	41 ± 2	-	142	38	16.8 ± 1.4	1.0	[40]
Digestate	EC	Stripping	10	0.80	38 ± 2	-	51	41	13.1 ± 0.9	0.4	[40]
Synthetic	EC	Stripping	30	0.94	41 ± 2	-	143 ± 7	38 ± 0.6	16.8 ± 1.4	1.0	[145]
Urine	EC	Stripping	40	1.34	75 ± 0.5	57 ± 0.5	275 ± 5	55 ± 0.9	12.7 ± 0.37	0.7	[88]
Urine	EC	Stripping[d]	40	3.78	65	77	83	16	41	0.7	[88]
Urine	EC	Stripping[e]	20	0.54	87.1 ± 6.0	25 ± 12.1	160	n.a.	2.9	0.7	[167]
Urine	EC	Stripping[e,f]	20	0.54	68.4 ± 14.6	13.3 ± 3.3	129	n.a.	3.6	0.7	[167]
Urine[a]	HRES	TMCS	10	1.30	82	64	78	57	8.5	0.7	[169]
Urine[a]	HRES	TMCS	20	1.20	73	73	151	58	7.3	0.7	[169]
Urine[a]	HRES	TMCS	50	1.30	73	60	342	55	15.6	0.7	[169]
Urine[b]	EC	TMCS	50	1.20	63	56	335	53	14.2	0.7	[170]
Urine[b]	EC	TMCS	50	6.50	92	77	89	14	47.6	0.7	[170]
Synthetic urine	HRES[c]	TMCS	20	1.30	74 ± 2	-	141 ± 8	56	4.2	0.7	[181]
Synthetic urine	HRES[c]	TMCS	100	1.30	58 ± 2	-	598 ± 24	48	6.5 ± 0.3	0.7	[181]
Urine	EC	TMCS[g]	100	0.86	61	49.6	891	>100	8.5	0.7	[180]
Urine	EC	Stripping[e]	20	0.44	45.1 ± 18.4	17.2 ± 8.1	100	n.a.	5.9 ± 3.1	0.7	[183]
Urine	EC	TMCS[e]	20	0.43	49.0 ± 9.3	38.7 ± 13.5	88	n.a.	4.6 ± 1.1	0.7	[183]

(-) Not reported or not possible to determine with the data provided, n.a. Not applicable, [a] After struvite precipitation and softening, [b] After struvite precipitation, [c] 3 compartments and up-scaled, [d] Stripping of the influent headspace included, [e] Urine was fed to the cathode, [f] Absorption in growth medium and not in an acid, as most studies, [g] TMCS integrated within the same cell

Limitations of the load ratio concept

The load ratio (L_N) is the ratio between the applied current density and the TAN loading rate in a (B)ES. As mentioned previously, the TAN removal efficiency is expected to follow an increasing trend with respect to L_N, up until a certain L_N. Assuming all current is used to transport TAN (TAN transport efficiency of 100%), complete TAN removal would be reached with a L_N of 1. As that is not the case in practical situations, this maximum L_N will be different depending on the wastewater composition, system design and operational conditions.

Figure 6.1A shows the TAN removal efficiency with respect to load ratio from the studies reported in Tables 6.1 and 6.2. Clearly, the simple model developed in *Chapter 3* fits our synthetic wastewater data, and does not accurately reflect the results from other systems. Therefore, the first limitation of the load ratio parameter is that the wastewater composition is not taken into account. Our synthetic wastewater was based on Na^+ as the only competing cation, which is far from what is found in real wastewaters. This effect can also be observed in the study with the lowest ratio of TAN to total cations ($C_{TAN}/C_{cations}$), where a removal efficiency around 60% was obtained even at a load ratio of 2.4 (Figure 6.1A).

The TAN removal efficiencies of different (B)ES were, in general, lower than 61% for load ratios lower than 1. The exceptions were 3 cases in which TAN removal efficiencies were between 68% and 88% [167, 177]. In these cases, the TAN removal was performed in batch [177] and the urine was first fed to the cathode compartment (for pH increase and NH_3 stripping) and then redirected to the anode compartment [167]. The performance of (B)ESs that rely on complimentary means to drive the TAN removal cannot be accurately assessed by the load ratio parameter. These systems can have TAN removals higher than what would be expected by the load ratio (such as [167]), which is based solely on current-driven removal. This can also be observed in Figure 6.1B, where the BES including stripping, forward osmosis and struvite precipitation (BES-Stripp-FO-MAP) shows very low energy input at a considerably high load ratio (1.5). Comparisons by means of the load ratio are thus also limited when system designs are not solely based on current-driven TAN removal or in non-steady state situations (batch systems).

On the other hand, for (B)ESs treating wastewaters with high $C_{TAN}/C_{cations}$ ratios, the load ratio can indicate how efficiently the (B)ESs are working. A load ratio much higher than 1 and low TAN removal efficiency indicates that either much higher currents than needed are being applied to the system (our study, load ratio 6.5) or that the system is not working optimally (Figure 6.1A, load ratio of 3.8 [88]). In the latter study, for example, vacuum pump failures and the decrease of TAN influent concentration due to the stripping of the influent headspace were reported [88]. This is also reflected on the relationship between the load

ratio and the electrical energy input of the systems, with the highest electrical energy inputs observed at the highest load ratios (Figure 6.1A). Therefore, the load ratio can be useful to assess under which conditions a system can be optimally operated in terms of TAN removal efficiency and energy input of a particular system, but it can only be useful to compare different (B)ES for the recovery of TAN to a limited extent.

The new configurations and improvements to the design of (B)ESs, including the ones in this thesis, have resulted in increased TAN removal efficiencies compared to earlier studies [61, 69, 87]. While these advances are promising, most (B)ESs are still at the lab-scale stage and operating with synthetic wastewaters. From Tables 6.1 and 6.2, only one ES has been tested on a relatively larger scale (0.04 m^2 membrane area) [181] and one BES on the pilot scale (0.5 m^2 membrane area) [168]. Furthermore, there is still a lack of systematic studies with real wastewaters in BES in particular: from 17 studies, only 7 dealt with real wastewaters (41%), compared to 8 out of 9 in ES (88%). The operation of the systems with real wastewaters and their successful operation at larger scale is essential to demonstrate the feasibility of (B)ESs as alternatives to conventional TAN recovery technologies.

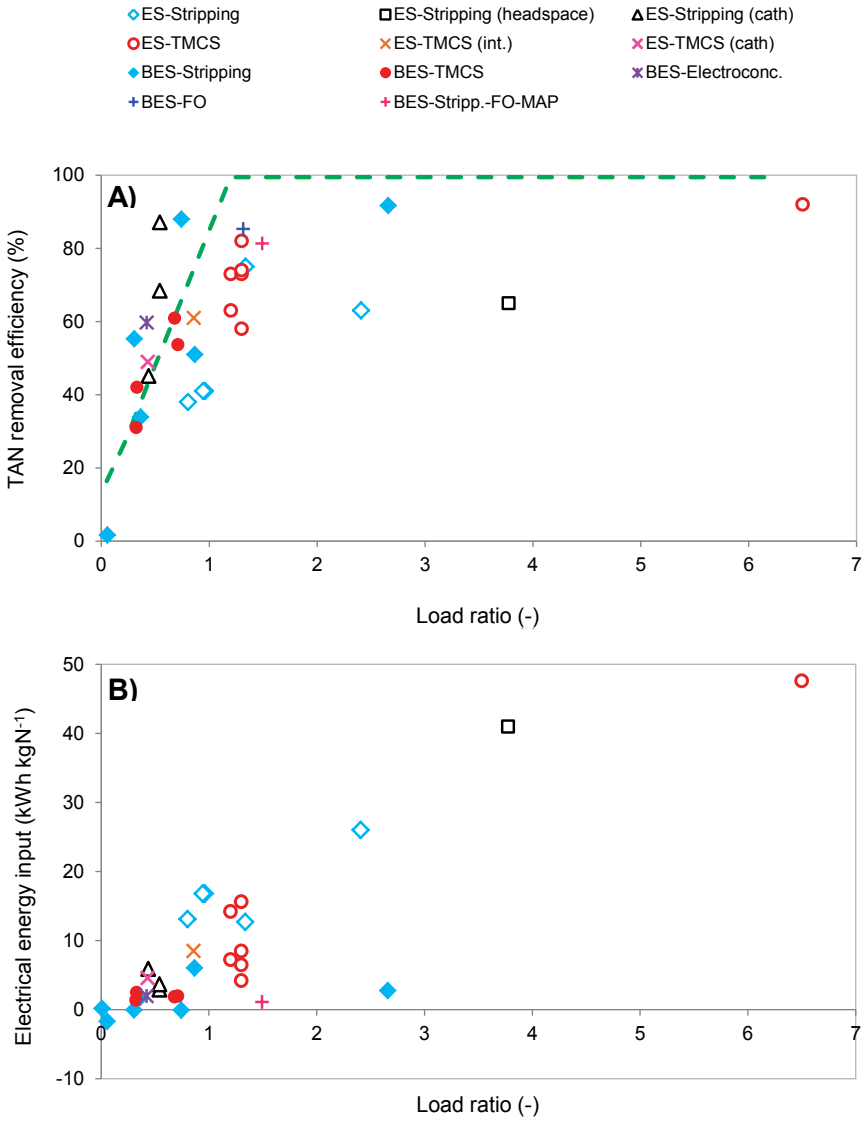

Figure 6.1. **(A)** TAN removal efficiency versus load ratio and **(B)** electrical energy input versus load ratio from different (bio)electrochemical studies for the recovery of TAN reported in Tables 6.1 and 6.2. Dashed line depicts the simple model fitted to our synthetic wastewater data in Chapter 3. The different abbreviations belong to different recovery systems such as stripping, forward osmosis (FO), gas-permeable hydrophobic membrane or TransMembrane ChemiSorption (TMCS), and struvite precipitation (MAP). Legends between brackets depict specific situations described in Tables 6.1 and 6.2.

6.2 Urine in (B)ES: opportunities and obstacles

In *Chapter 2* we showed, based on an energy and economic analysis, that BESs are a promising technology for the recovery of TAN from urine. In the analysis, we addressed the main challenges to overcome in order to scale up the technology. Some of those challenges, such as improving ammonia extraction from the catholyte, were tackled in this research. To date, however, there is no (B)ES applied in practice to recover nitrogen from urine or other wastewaters.

In the following section, we will discuss *why (bio)electrochemical systems for TAN recovery from urine have not been applied on larger scale* yet, based on literature and the work performed in this thesis. The discussion will focus in two critical aspects: first, the low TAN recovery efficiencies we obtained with a bioelectrochemical system, and second, the general upscaling challenges for (B)ESs for TAN recovery from urine.

6.2.1 Low TAN removal efficiencies in BES

The TAN removal efficiencies in our BES study (*Chapter 5*) were low even though the BES was coupled with an effective stripping concept (a gas-permeable hydrophobic membrane). The highest TAN removal efficiencies were around 40% with diluted urine at lower TAN concentration, 54% with diluted urine, 61% with diluted synthetic urine and 30% with (undiluted) urine. Apart from the system design and technical aspects such as the effective extraction of TAN from the catholyte, TAN recovery in (B)ES depends on the current density compared to the TAN loading (this ratio being the load ratio) (*Chapter 3*). All our experiments, except the ones with 70% lower TAN concentration, had load ratios lower than 1, meaning that the current was not enough to transport all the TAN. Therefore, the reasons for these low TAN removal efficiencies were a) low TAN transport efficiencies for diluted urine with 70% lower TAN concentration and b) low current densities compared to TAN loadings for urine and diluted urine.

The low TAN transport efficiencies for diluted urine with 70% lower TAN concentration were caused by the lower concentration of ammonium compared to other cations, as discussed in *Chapter 5*. This resulted in transport of other cations over ammonium, resulting in a lower TAN transport number. In this section, we discuss the probable reasons for low current densities in our BES study.

In BESs, the current density is directly related to the oxidation of organic matter by the electrochemically active microorganisms present in the system. Therefore, the TAN recovery efficiency in BES depends, among others, on three main aspects: the ratio of biodegradable organic matter to TAN (here referred to as the COD/TAN ratio), the removal efficiency of the biodegradable organic matter (here referred to as the COD removal

efficiency) and the Coulombic efficiency. As most studies report the chemical oxygen demand (COD) as an indication of the biodegradable organic matter in wastewaters, we will use this parameter for the calculations in this section.

The relevance of these aspects can be summarized as follows:

1.- **COD/TAN ratio**: How much organic matter (hence, potential for current generation) is available compared to the TAN in the wastewater? Is it enough to transport all the TAN?

2.- **COD removal efficiency:** How much of the organic matter is consumed? This aspect is also affected by the biodegradability of organic matter and potential toxicity of the wastewater to microorganisms.

   a) **Biodegradability of organic matter**: How much of the organic matter in the wastewater is readily biodegradable? Does the system need a high hydraulic retention time for the complete biodegradation of organic matter?

   b) **Toxicity**: Does the wastewater contain toxic compounds that might inhibit the microorganisms in the BES?

3.- **Coulombic efficiency (CE)**: How much of the organic matter consumed is actually used for current generation?

We will elaborate on these three aspects to determine how they can affect the TAN recovery from urine in BES.

1.- COD/TAN ratio

Theoretically, to remove TAN by means of current generation in BESs, 0.57 kg COD per kg TAN are needed (*Chapter 2*). Considering that the COD/TAN ratio of human urine after urea hydrolysis is 0.8-1 (Table 6.3), all TAN could be theoretically removed with the COD available. The theoretical requirement of COD, however, is higher in practice, because usually not all the COD available is consumed (COD removal efficiency <100%), not all the COD removed is used for current generation (Coulombic efficiency <100%), and not all the current is used for TAN transport (TAN transport efficiency <100%). Both COD removal and Coulombic efficiencies in BESs aiming to recover TAN from urine can be quite low (Table 6.3), which directly affects how much COD is needed to recover TAN. Assuming 100% TAN transport efficiency and the actual COD removal and Coulombic efficiencies, the COD/TAN ratio needed to remove all TAN is at least 2 times higher than what is found in human urine after urea hydrolysis (COD/TAN required, Table 6.3). This implies that the COD present in urine is not enough to remove all the TAN unless COD removal and Coulombic efficiencies are improved. Combined, these two efficiencies should be higher than 70% to remove all TAN present in urine, which is far from what has been accomplished so far. In our BES study (*Chapter 5*), we obtained both low coulombic efficiencies and low COD removal efficiencies with undiluted urine, and low COD removal efficiencies with diluted and synthetic urine (Table 6.3).

Table 6.3. COD/TAN ratio, COD removal efficiency (%), Coulombic efficiency (CE, %) and current density (j, A m^{-2}) from selected BES studies for the recovery of TAN from urine. "COD/TAN required" is the COD/TAN ratio that would be needed to remove all the TAN, based on the reported COD removal and Coulombic efficiencies.

System	Urine dilution	Operation	COD/TAN	COD loading	COD removal	CE	j	COD/TAN	Reference
				g m^{-2} d^{-1}	%	%	A m^{-2}	required	
MEC	5x[a]	C	0.9	432	30 ± 1	84 ± 1	14.6	2.3	[87]
MEC	5x[b]	C	n.d.	35	40 ± 5	78 ± 10	1.7 ± 0.2	1.8	[143]
MFC	-- [c]	B (40- 60 days)	1.5[e]	14-21	75	27	0.5 ± 0.0	2.8	[171]
MEC	Synthetic	C	1.2	1083	17 ± 3	94 ± 17	29.3 ± 2.3	3.6	[174]
MEC	2.5x[b]	C	1.0	46	37 ± 6	65 ± 10	1.7 ± 0.2	2.4	[168]
MEC	--[c]	C	1.5[e]	n.d.	39- 46	2-20	0.1 - 0.9	-	[187]
MEC	Raw[d]	B (≈ 42 days)	11.0*	17	65 ± 10	14 ± 2	0.1 ±0.0	6.3	[188]
MEC	Fermented[d]	B (≈ 42 days)	1.1	28	54 ± 3	17 ± 1	0.2 ±0.0	6.2	[188]
MEC	Synthetic 2-9x	C	0.8	159-188	7- 52	74- 117	1.4- 10.6	-	Chapter 5[f]
MEC	2.5-7.5x[b]	C	0.8	60-257	14- 34	49-125	1.5- 6.3	-	Chapter 5 [f]
MEC	--[b]	C	0.8	79-150	16- 27	15-22	0.5- 0.7	13.7	Chapter 5 [f]

C= continuous mode, B= batch mode, (--) is undiluted and n.d.= not determined due to lack of information

[a] Collected from water-free urinals and separation toilets

[b] Collected from water-free urinals and treated by struvite precipitation

[c] Collected from individuals and directly treated by struvite precipitation (no storage time)

[d] Collected from individuals, stored for 6 days and treated by struvite precipitation

[e] Assuming that TAN is 90% of the total Kjeldahl nitrogen reported

[f] These values come from new analysis based on experiments described in Chapter 5

* The COD/TAN ratio is higher compared to others because the TAN concentration is very low, due to the urea in urine not being hydrolyzed (pH 7.76)

2.- COD removal efficiency

Biodegradability of organic compounds in urine

The COD removal efficiency depends on several factors, from which the biodegradability of the organic compounds is key. The major carbon-containing compounds in urine are urea and creatinine [81], although urea is not used for current production because it is hydrolyzed to bicarbonate. It has been found that 67-85% of the organic compounds in urine are biodegradable [54], but this value is not an indication of their complexity. Complex organic compounds might need more time (longer HRTs) to be biologically degraded than simple compounds, such as acetate. This effect can be seen in Figure 6.2, which summarizes the coulombic efficiencies and COD removals from Table 6.3. In this Figure, it is clear that the highest COD removal efficiencies were obtained in batch experiments that lasted from 40 to 60 days. Observing these results, the question arises whether low COD removal efficiencies are the result of non-readily biodegradable organic matter.

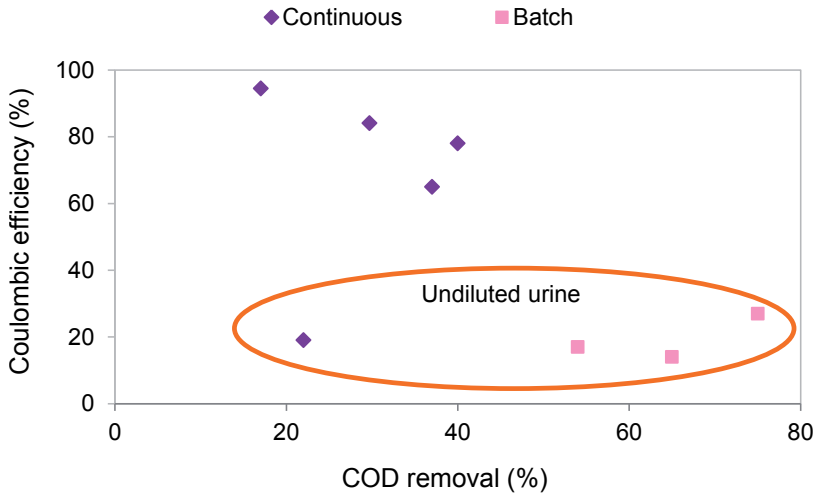

Figure 6.2. Coulombic efficiency versus COD removal from different BES studies for the recovery of TAN from urine (data from Table 6.3, taking the average of our data with undiluted urine)

Recent studies have shown that the concentration of easily degradable volatile fatty acids (VFAs) in urine can be increased after a pre-fermentation step, to a limited extent [188, 189]. Barbosa et al (2019) reported that after fermentation of raw urine, its composition changed from mainly urea and creatinine to mainly methylamine (a result of creatinine hydrolysis), acetate and propionate. Acetate concentration was higher in the fermented urine compared to the raw urine (4.7 and 2.8 g COD L^{-1}, respectively), demonstrating that

other complex organic compounds had been converted to acetate. When both raw urine and fermented urine were used in MECs, the peaks in current density observed when a new batch of urine was introduced (0.8 A m^{-2} for raw urine and 1.3 A m^{-2} for fermented urine) were related to the consumption of VFAs such as acetate. Both the COD removal rate and the average current density were significantly higher in the MEC treating fermented urine (0.14 g L^{-1} d^{-1} and 0.22 A m^{-2} compared to 0.08 g L^{-1} d^{-1} and 0.11 A m^{-2} with raw urine). The COD removal efficiency, however, was limited to 65% (raw urine) and 54% (fermented urine) even after 42 days of operation.

In another urine fermentation study, a maximum of 17 ± 9 % of the initial COD was converted to VFAs in anaerobic sequencing batch reactors (SBRs) at an HRT of 0.45 days. A higher conversion of up to 32 ± 2 % was accomplished in batch experiments, but it took 3.7 days in average [189].

This limited conversion of complex organic compounds into simpler compounds could be a result of the harsh physicochemical conditions of urine. Hydrolysis of the urea in urine [84] results in high pH, salinity and NH_3 concentrations, conditions known to inhibit anaerobic digestion [190, 191]. It has been demonstrated that anaerobic digestion in particular is inhibited at TAN concentrations ranging from 1.5- 2.5 g L^{-1} when the microbial consortia are not adapted to high TAN concentrations, whereas gradual adaptation to high TAN concentrations has resulted in tolerance levels exceeding 4 g L^{-1} [190]. Barbosa et al (2019) reported that methane production was inhibited during the fermentation of urine, and that this inhibition was more pronounced with increasing ammonium concentrations (the experiments were done with different urine dilutions). At a TAN concentration of 4.3 g L^{-1} and a pH of 8.45, methane production was completely inhibited. The question remains whether the conditions affecting anaerobic digestion also affect the microbial consortia found in bioelectrochemical systems, and if the COD removal efficiency is affected by the biodegradability of organic matter, inhibition to microorganisms, or both.

Probable toxicity of urine to microorganisms in BES

COD removal efficiencies in BES are limited even with fermented urine and synthetic urine based on acetate (Table 6.3), which implies that another factor other than biodegradability of organic compounds might be affecting the BES performance.

To date, it is unclear whether high concentrations of TAN or NH_3 inhibit COD biodegradation (and therefore, current production) in BES. Several studies have reported inhibition, or the lack thereof, of current generation, with no consensus. Inhibition in these studies is explained by one or more of these parameters: a) TAN concentration (independent of pH), b) NH_3 concentration (pH related), and c) ionic or osmotic stress.

Inhibition of electricity generation was reported at TAN concentrations as low as 0.5 g L^{-1} and neutral pH [190]. Other studies report different results, with current generation inhibited at TAN concentrations higher than 2.2 g L^{-1} at a pH of 7.35 [192], TAN concentrations higher than 4 g L^{-1} or at 4 g L^{-1} at pH higher than 8.5 [193]]. By contrast, other studies have found no negative effects on the bioanode performance at neutral anolyte pH and concentrations of up to 5 g L^{-1} [194], at anolyte pH around 8 with a TAN concentration of 3.9 g L^{-1} [195] and even at anolyte pH of 8.85 and a TAN concentration of 4 g L^{-1} [69]. Several studies report that the inhibition effects can be overcome by acclimatizing the system to increasingly high TAN concentrations, and it has been found that higher current densities are reached in acclimatized BES compared to controls without acclimatization [171, 196]. Other studies, however, report inhibition even after acclimatization periods [190, 192].

The decrease of acetate consumption or COD removal efficiencies with increasing TAN concentration, and its direct effect on current or power generation, was reported in three studies [190, 192, 197]. In one study, COD removal was higher than 90% up to TAN concentrations of 1 g L^{-1} at both high and low substrate concentrations (2 and 0.62 g L^{-1} sodium acetate, respectively). Afterwards, COD removal efficiency gradually decreased with increasing TAN concentration. At 4 gTAN L^{-1}, the COD removal decreased to 72% and 49% at high and low substrate concentrations, respectively [197]. Therefore, these studies suggest that both the COD consumption and the respiration rate to the anode might be affected by high concentrations of TAN. Ammonia toxicity due to high TAN or NH_3 concentrations, however, is not expected in a well operating BES for the recovery of TAN. In a well operating BES, TAN removal would result in low ammonia concentration and neutral pH in the anolyte.

Stress due to high conductivity of the medium has also been suggested as a cause of inhibition at high TAN concentrations. This effect was studied on *Corynebacterium glutamicum* (which has been found in the microbial community of urine MFCs [171]), *Escherichia coli,* and *Bacillus subtilis* [198]. All three bacteria were resistant to ammonium up until a concentration of around 1 M $(NH_4)_2SO_4$ (28 gTAN L^{-1}), where growth inhibition was observed. However, substituting ammonium sulphate with sodium sulphate at the same concentration generated the same inhibition response, which led to the conclusion that the cause of the inhibition was not ammonium, but the increased ionic strength of the medium. Other studies also reported inhibition due to osmotic stress, however they suggest that the type of ion does affect the inhibition response. Nam et al (2010) reported lower power densities when using NH_4^+ than when using K^+ at the same conductivity levels [190], whereas Kim et al (2011) indicated a stronger inhibitory effect by K^+ than by ammonium [196]. In the latter study, MFCs sustained the same power density up to a TAN concentration of 3.5 g L^{-1} and a conductivity of 35 mS cm^{-1}, whereas lower power densities

were obtained with KCl at the same conductivities. Thus, salinity in combination with TAN may be inhibiting current production.

Apart from TAN, NH_3 and salinity, urine might contain other compounds affecting the microorganisms in BES. Surfactants used to clean the urinals or separation toilets from where the urine is collected might inhibit electrochemically active bacteria [199], and the effect of antibiotics found in urine to the microorganisms in BES has also not been studied and is thus unclear. Due to the interactions between fermentative and electrochemically active bacteria in BES for TAN recovery from urine [171], the BES performance can be compromised even if one species is more sensitive than others to TAN concentration, NH_3, salinity or other factors. Therefore, further research to study which factors cause inhibition with urine is crucial to improve the performance of TAN recovery from urine by BES.

3.- Coulombic efficiencies

Current densities achieved by our BES were considerably lower with urine than with diluted or synthetic urine, even though we followed a step-wise approach to acclimatize it to urine (Table 6.3). These low current densities were related to both low COD removal efficiencies (described previously) and low coulombic efficiencies. In BESs, the coulombic efficiency is defined as the ratio of the electrons recovered at the anode (as current) to the total electrons obtained from the oxidation of substrate. In other words, the coulombic efficiency compares how much substrate was removed to how much current was generated. Coulombic efficiencies can be reduced when electrons from the substrate are lost to electron acceptors other than the anode (such as oxygen, sulphate or nitrate), to biomass growth or to other competitive processes, such as methanogenesis.

The low coulombic efficiencies for undiluted urine obtained in our study are in agreement with other studies treating urine by means of BES (Table 6.3). One reason for these low coulombic efficiencies can be the complexity of the organic compounds in urine mentioned earlier. The presence of complex, non-readily biodegradable compounds in real wastewaters increases the chances of fermentative processes to occur, which can lead to lower coulombic efficiencies compared to synthetic wastewaters based on simpler organic compounds [200]. Pre-fermentation of complex wastewaters, as mentioned previously, can be beneficial when the fermentation products are directly oxidized at the bioanode by electrochemically active bacteria [188]. In practice, however, the fermentation products can also be used by other microorganisms, which results in lower Coulombic efficiencies. For example, methylamine, which is found in fermented urine as a product of the hydrolysis of creatinine, can be used for methane production [201].

The coulombic efficiency also depends on other factors, such as the substrate concentration, anode potential, and pH. It has previously been proposed that low

substrate concentration in combination with sufficiently high anode overpotentials (>100 mV) favors high coulombic efficiencies in BES [161]. These conditions favor the growth of electrogens over methanogens, which are among the main competitors in bioanodes. All studies summarized in Table 6.3, with the exception of one, worked with anode potentials varying from -0.3 to -0.4 V vs Ag/AgCl. There was only one study which worked at an anode potential of -0.2 V vs Ag/AgCl, which coincided with the highest Coulombic efficiency for undiluted (synthetic) urine [174]. As all our experiments were conducted at the same anode potential (-0.3 V vs Ag/AgCl), the higher COD concentration in undiluted urine might have been the cause for the lower Coulombic efficiencies compared to the diluted urine experiments. This is also observed in the other studies in Table 6.3, in which experiments with diluted urine show higher Coulombic efficiencies compared to undiluted.

Concluding remarks of urine in BESs

The low current densities in our BES in relation to the TAN supplied were the main cause of low TAN removal efficiencies. So far, high current densities with undiluted urine in BES have not been achieved. The nature of urine after urea hydrolysis, with complex organic compounds and harsh physicochemical conditions, makes treating urine by means of BES very challenging. The complexity of organic compounds can make the scale-up of the technology more difficult, as the need of longer retention times translates into larger reactor volumes. Reaching the optimum between COD removal efficiency and COD removal rate will be crucial to improve the general applicability of BESs.

Studies conducted with diluted urine have shown more promising results, but diluting urine undermines the purpose of urine separation. Moreover, one of the advantages of urine is its high conductivity, because high conductivities decrease the resistance of the electrolyte to the transport of ions, making a (B)ES more energy efficient.

To determine the true capabilities of BES as a technology for the recovery of TAN from urine, further research into the factors limiting the biodegradation of organic compounds in urine, (probable) toxicity, and strategies to improve Coulombic efficiencies (e.g. different anode overpotentials and substrate concentrations/urine dilutions) is of key importance. Knowledge into these aspects will determine the applicability of BES to nitrogen-rich wastewaters in general.

6.2.2 TAN recovery from urine in (B)ESs: General upscaling challenges

In the previous section we focused on the challenges for the recovery of TAN from urine in bioelectrochemical systems. In this section, we will address general challenges experienced in both electrochemical and bioelectrochemical systems for the recovery of TAN from urine.

Struvite precipitation and scaling issues

The recovery of ammonia by a BES has already been studied at a pilot scale [168]. In this study they tested a complete treatment concept for urine, in which phosphorous (P) is recovered via struvite precipitation and the TAN by a bioelectrochemical system coupled to a gas-permeable hydrophobic membrane unit [168]. Recovering P from urine prior to introducing it to a (B)ES has the advantage of not only recovering a fertilizer product, but also removing phosphates, which might result in scaling and unwanted precipitation in the (B)ES [202]. For that reason, in all the studies presented in this thesis the urine used was pre-treated via struvite precipitation.

Part of the precipitation (including minerals such as hydroxyapatite ($Ca_{10}(PO_4)_6OH_2$) or calcite ($CaCO_3$)) occurs spontaneously after the pH increases due to urea hydrolysis, therefore some studies only filter the hydrolyzed urine (after a storage period) or trigger urea hydrolysis by adding urease [88]. As magnesium is limiting, however, spontaneous precipitation can only remove around 50% of the phosphate [84, 88]. To prevent scaling in the equipment, it would be ideal to remove the remaining phosphates, which can be done by adding a suitable magnesium salt.

More than 90% of the phosphate from urine can be recovered by struvite precipitation [163, 203]. This pre-treatment step makes the (B)ES treatment of urine more energy demanding, but also adds potential benefits, such as reduction of the P load to WWTPs and the production of a P-rich fertilizer, as shown in the LCA analysis of the complete treatment concept [204]. A specific remark for BES about the struvite precipitation process is that COD can be lost: in the pilot-scale study, around 25% of the COD in the urine was biologically degraded within the struvite reactor [168]. This reduces the amount of organic matter available for current generation.

Apart from the removal of phosphates, a softening method might be needed to prevent the scaling of the cell due to calcium and magnesium ions in urine. This was done in the pilot-plant mentioned previously by an ion-exchange column [168]. In our studies, the urine was not softened, which resulted in precipitation of calcium carbonates on the cathode side of the membrane after long term operation (around 6 months) (data not shown). Luther et al (2015) also reported white precipitates on both the cathode and the cathode side of the membrane, and hypothesized it might have been calcium carbonate [88]. The extent of this issue has not been reported in any of the previous studies concerning electrochemical or bioelectrochemical treatment of urine, so further studies are needed to assess the extent of scaling and the need of a softening pre-treatment step.

The phosphorous removal and softening pre-treatment steps will be crucial to prevent precipitation, scaling or blockages throughout the treatment system, and should be considered when upscaling the technology.

Final product recovery

The recovery of TAN as a final product still remains a challenging issue in general. Some of the studies in Tables 6.1 and 6.2 show substantially lower recovery efficiencies compared to removal efficiencies. That means that the nitrogen is removed from the wastewater, yet not recovered from the catholyte, as intended. This is mainly due to inefficiencies of the recovery method (e.g. low stripping efficiency, low absorption capacity, small TMCS membrane surface area, etc.) or NH_3 losses. In our study from Chapter 3, we hypothesize that NH_3 might have been lost due to its reaction with chlorine due to chloride oxidation (an unwanted reaction in our system). This was based on the measurement of chloride and the anode potential. Recently, the formation of chloramines from urine was confirmed in a very similar system for the recovery of TAN from urine [180]. The formation of these by-products needs further assessment, but the use of an HRES can circumvent this issue [169].

Pharmaceuticals and pathogens

From all domestic wastewater streams, urine is the main source of pharmaceuticals [15, 205]. The fate of these pharmaceuticals and their metabolites is important, because many of them are persistent and can have negative effects on the environment and human health [206]. Furthermore, urine also contains pathogens, mainly due to fecal cross-contamination [207].

Two recent studies evaluated the presence of pharmaceuticals and pathogens in the liquid ammonium salt solutions obtained from the electrochemical treatment of urine, coupled to membrane stripping or conventional stripping-absorption [180, 183]. Although the solution from the conventional stripping contained pathogens spiked in the urine influent [183], the solution from the membrane stripping did not contain either pathogens or pharmaceuticals [180, 183].

The urine effluent, however, might need further post-treatment if the intention of the up-scaled system is to discharge directly to the environment.

6.3 Future perspectives and recommendations

Even though MFCs would be the most attractive option in the context of decentralized systems due to their electricity generation, their implementation is far from application compared to MECs. So far, MECs have shown to produce much higher current densities than MFCs (maximum of 23 compared to 0.5 A m^{-2} [62]). As current density is the driving force for the recovery of TAN, high current densities are needed for the adequate recovery of TAN. The use of MECs for the recovery of TAN from urine, however, also needs further

investigation in order to bring the technology closer to application, as mentioned in the previous section.

Until further investigation into the cause for low current densities in BESs is addressed, ESs are considered as better candidates for upscaling of this technology. The advantages of ESs over BESs are the higher applied current densities, the stability and robustness to changes in influent and the controlled current density. Given that the COD/TAN ratio is irrelevant to ES, the current density and TAN loading rate can be controlled independently, so the system can be set to work at the optimum load ratio. As the current density is not dependent on the consumption of COD by microorganisms, the system is easier to control. This is advantageous to a certain extent, as very high current densities (anode potentials) can result in the production of chlorinated compounds in wastewaters with high chloride concentrations, such as urine (*Chapters 3 and 4*).

From the options explored in this thesis, the HRES (*Chapter 4*) seems the most promising technology for future implementation. The reason for this is its lower energy input compared to an EC, the high removal efficiencies and the lower risk for the formation of chlorine, chlorinated byproducts and adsorbable organic halides (AOX).

At the time the research on the HRES was performed, it was concluded that in order to bring the technology closer to application, the energy demand of the system needed to be lowered by optimizing the cell design, the hydrogen oxidation and evolution catalysts and the pH profile. These aspects were taken into account in a following publication from Kuntke et al (2018) [181]. In their study, the design of the HRES prototype was improved by adding a third compartment, called the 'concentrate' compartment. This compartment was placed in between the anode and the cathode compartments and separated from them by a cation-exchange membrane (anode side) and an anion-exchange membrane (cathode side). The improved system design increased the energy efficiency and treatment capacity of the HRES considerably (Table 6.2). The better compression of the gas diffusion electrode allowed for its better contact with the H_2 gas, reducing the anode overpotential. Furthermore, the transport losses were reduced by the introduction of the third compartment with an anion exchange membrane [181, 208].

The post-treatment of the effluent from the HRES remains open for future investigation. The high concentration of organic compounds remaining in the effluent (≈ 4 g L^{-1}) would make the stream a good candidate for removal by BES. In the case of an MEC, the hydrogen produced in the cathode could be used as part of the inflow to the HRES. However, post-treatment by a BES will also depend on the effluent pH and TAN concentration. The effluent pH in the HRES prototype was too low (2.5 – 5) to be considered a good candidate for BES treatment, but the effluent from the up-scaled HRES had a pH closer to neutral (6.4-

7.3 [181]). This pH, however, might still be problematic for BES post-treatment without the addition of buffer or pH control. The biofilm might get inhibited as the anolyte gets acidified during operation. Future research in this aspect might be necessary.

Based on the research conducted for this thesis and the previous discussion, the following recommendations are proposed in order to bring the (B)ESs for TAN recovery closer to application:

Operation:

- The operation on the optimum range in regards to TAN removal efficiency and energy input (load ratio)
- The use of wastewater with a TAN fraction compared to the total cations (C_{TAN}/ $C_{cations}$) higher than 0.4
- The integration of a pre-treatment step to remove solid particles and compounds that might precipitate in the (B)ES, such as phosphates, calcium and magnesium.

Materials:

- The use of less expensive materials (for example different membranes or Pt-free catalysts)

Subjects for further investigation:

- Factors limiting the biodegradation of organic compounds in urine (possible toxicity of compounds found in urine)
- The adequate design parameters to improve coulombic efficiencies in BES (e.g. HRT or substrate concentration, anode overpotentials) and the study of alternative electron donors, such as H_2 [209]
- The fate of micropollutants and pathogens in urine and probable effluent post-treatment

References

1. Falkowski PG. Evolution of the nitrogen cycle and its influence on the biological sequestration of CO2 in the ocean. *Nature* 1997, *387*, 272–275.
2. Campbell NA, Reece JB. *Biology.* 7th edition. San Francisco, CA: Pearson/Benjamin Cummings. 2005.
3. Erisman JW, Sutton MA, Galloway J, Klimont Z, Winiwarter W. How a century of ammonia synthesis changed the world. *Nat. Geosci.* 2008, *1* (10), 636–639.
4. Smil V. Nitrogen cycle and world food production. *World Agric.* 2011, *2*, 9–13.
5. Galloway JN, Townsend AR, Erisman JW, Bekunda M, Cai Z, Freney JR, Martinelli LA, Seitzinger SP, Sutton MA. Transformation of the nitrogen cycle: recent trends, questions, and potential solutions. *Science* 2008, *320* (5878), 889–892.
6. Giddey S, Badwal SPS, Munnings C, Dolan M. Ammonia as a renewable energy transportation media. *ACS Sustain. Chem. Eng.* 2017, *5* (11), 10231–10239.
7. Wang L, Xia M, Wang H, Huang K, Qian C, Maravelias CT, Ozin GA. Greening ammonia toward the solar ammonia refinery. *Joule* 2018, *2* (6), 1055–1074.
8. Kitano M, Inoue Y, Yamazaki Y, Hayashi F, Kanbara S, Matsuishi S, Yokoyama T, Kim SW, Hara M, Hosono H. Ammonia synthesis using a stable electride as an electron donor and reversible hydrogen store. *Nat. Chem.* 2012, *4* (11), 934–940.
9. Service RF. New recipe produces ammonia from air, water, and sunlight. *Science* 2014, *345* (6197), 610 LP – 610.
10. Song Y, Johnson D, Peng R, Hensley DK, Bonnesen P V, Liang L, Huang J, Yang F, Zhang F, Qiao R, et al. A physical catalyst for the electrolysis of nitrogen to ammonia. *Sci. Adv.* 2018, *4* (4), e1700336.
11. Gong Y, Wu J, Kitano M, Wang J, Ye T-N, Li J, Kobayashi Y, Kishida K, Abe H, Niwa Y, et al. Ternary intermetallic LaCoSi as a catalyst for N2 activation. *Nat. Catal.* 2018, *1* (3), 178–185.
12. Kitano M, Kanbara S, Inoue Y, Kuganathan N, Sushko P V, Yokoyama T, Hara M, Hosono H. Electride support boosts nitrogen dissociation over ruthenium catalyst and shifts the bottleneck in ammonia synthesis. *Nat. Commun.* 2015, *6*, 6731.
13. Shi MM, Bao D, Wulan BR, Li YH, Zhang YF, Yan JM, Jiang Q. Au sub-nanoclusters on TiO2 toward highly efficient and selective electrocatalyst for N2 conversion to NH3 at ambient conditions. *Adv. Mater.* 2017, *29* (17), 2–7.
14. National Institute for Public Health and the Environment (RIVM). *Greenhouse gas emissions in the netherlands 1990-2016. national inventory report 2018*; 2018.
15. Kujawa-Roeleveld K, Zeeman G. Anaerobic treatment in decentralised and source-separation-based sanitation concepts. *Rev. Environ. Sci. Bio/Technology* 2006, *5* (1), 115–139.
16. Gruber N, Galloway JN. An earth-system perspective of the global nitrogen cycle. *Nature* 2008, *451* (7176), 293–296.
17. Zhang X, Davidson EA, Mauzerall DL, Searchinger TD, Dumas P, Shen Y. Managing nitrogen for sustainable development. *Nature* 2015, *528*, 51–59.

18. McAllister CH, Beatty PH, Good AG. Engineering nitrogen use efficient crop plants: the current status. *Plant Biotechnol. J.* 2012, *10* (9), 1011–1025.
19. Lu C, Tian H. Global nitrogen and phosphorus fertilizer use for agriculture production in the past half century: shifted hot spots and nutrient imbalance. *Earth Syst. Sci. Data* 2017, *9* (1), 181–192.
20. Firmansyah I, Spiller M, de Ruijter FJ, Carsjens GJ, Zeeman G. Assessment of nitrogen and phosphorus flows in agricultural and urban systems in a small island under limited data availability. *Sci. Total Environ.* 2017, *574*, 1521–1532.
21. Mrdjen I, Fennessy S, Schaal A, Dennis R, Slonczewski JL, Lee S, Lee J. Tile drainage and anthropogenic land use contribute to harmful algal blooms and microbiota shifts in inland water bodies. *Environ. Sci. Technol.* 2018, *52* (15), 8215–8223.
22. Mulder A. The quest for sustainable nitrogen removal technologies. *Water Sci. Technol.* 2003, *48* (1), 67–75.
23. Matassa S, Batstone DJ, Hülsen T, Schnoor J, Verstraete W. Can direct conversion of used nitrogen to new feed and protein help feed the world? *Environ. Sci. Technol.* 2015, *49* (9), 5247–5254.
24. Rijksinstituut voor Volksgezondheid en Milieu (RIVM). Emissieregistratie: Belasting van oppervlaktewater per doelgroep 1990-2017. www.emissieregistratie.nl (accessed Feb 22, 2019).
25. Centraal Bureau voor de Statistiek (CBS). Zuivering van stedelijk afvalwater; per provincie en stroomgebieddistrict. https://opendata.cbs.nl/statline/#/CBS/nl/ (accessed Mar 17, 2019).
26. *Council directive 91/271/eec of 21 may 1991 concerning urban waste-water treatment*. *Official Journal of the European Communities*, 1991, 40–52.
27. Wilsenach JA, Maurer M, Larsen TA, van Loosdrecht MCM. From waste treatment to integrated resource management. *Water Sci. Technol.* 2003, *48* (1), 1–9.
28. Rosso D, Larson LE, Stenstrom MK. Aeration of large-scale municipal wastewater treatment plants: state of the art. *Water Sci. Technol.* 2008, *57* (7), 973–978.
29. Stoica A, Sandberg M, Holby O. Energy use and recovery strategies within wastewater treatment and sludge handling at pulp and paper mills. *Bioresour. Technol.* 2009, *100* (14), 3497–3505.
30. Longo S, D'Antoni BM, Bongards M, Chaparro A, Cronrath A, Fatone F, Lema JM, Mauricio-Iglesias M, Soares A, Hospido A. Monitoring and diagnosis of energy consumption in wastewater treatment plants. a state of the art and proposals for improvement. *Appl. Energy* 2016, *179*, 1251–1268.
31. Maktabifard M, Zaborowska E, Makinia J. Achieving energy neutrality in wastewater treatment plants through energy savings and enhancing renewable energy production. *Rev. Environ. Sci. Biotechnol.* 2018, *17* (4), 655–689.
32. Smith K, Liu S. Energy for conventional water supply and wastewater treatment in urban China: a review. *Glob. Challenges* 2017, *1* (5), 1600016.

33. Brandt M, Middleton R, Wheale G, Schulting F. Energy efficiency in the water industry, a global research project. *Water Pract. Technol.* 2011, *6* (2).
34. Escapa A, San-Martín MI, Morán A. Potential use of microbial electrolysis cells in domestic wastewater treatment plants for energy recovery. *Front. Energy Res.* 2014, *2* (June), 1–10.
35. Logan BE, Call D, Cheng S, Hamelers HVM, Sleutels THJA, Jeremiasse AW, Rozendal RA. Microbial electrolysis cells for high yield hydrogen gas production from organic matter. *Environ. Sci. Technol.* 2008, *42* (23), 8630–8640.
36. Kampschreur MJ, Temmink H, Kleerebezem R, Jetten MSM, van Loosdrecht MCM. Nitrous oxide emission during wastewater treatment. *Water Res.* 2009, *43* (17), 4093–4103.
37. Daelman MRJ, Van Voorthuizen EM, Van Dongen LGJM, Volcke EIP, Van Loosdrecht MCM. Methane and nitrous oxide emissions from municipal wastewater treatment - results from a long-term study. *Water Sci. Technol.* 2013, *67* (10), 2350–2355.
38. van Eekert M, Weijma J, Verdoes N, de Buisonjé F, Reitsma B, van den Bulk J, van Gastel J. *Explorative research on innovative nitrogen recovery*; Rapport / STOWA : 2012-51; Stichting Toegepast Onderzoek Waterbeheer (STOWA), 2012.
39. Maurer M, Pronk W, Larsen TA. Treatment processes for source-separated urine. *Water Res.* 2006, *40* (17), 3151–3166.
40. Desloover J, Abate Woldeyohannis A, Verstraete W, Boon N, Rabaey K. Electrochemical resource recovery from digestate to prevent ammonia toxicity during anaerobic digestion. *Environ. Sci. Technol.* 2012, *46* (21), 12209–12216.
41. Lei X, Sugiura N, Feng C, Maekawa T. Pretreatment of anaerobic digestion effluent with ammonia stripping and biogas purification. *J. Hazard. Mater.* 2007, *145* (3), 391–397.
42. Guštin S, Marinšek-Logar R. Effect of pH, temperature and air flow rate on the continuous ammonia stripping of the anaerobic digestion effluent. *Process Saf. Environ. Prot.* 2011, *89* (1), 61–66.
43. Wu X, Modin O. Ammonium recovery from reject water combined with hydrogen production in a bioelectrochemical reactor. *Bioresour. Technol.* 2013, *146*, 530–536.
44. Tao W, Ukwuani AT. Coupling thermal stripping and acid absorption for ammonia recovery from dairy manure: ammonia volatilization kinetics and effects of temperature, pH and dissolved solids content. *Chem. Eng. J.* 2015, *280*, 188–196.
45. Bonmatí A, Flotats X. Air stripping of ammonia from pig slurry: characterisation and feasibility as a pre- or post-treatment to mesophilic anaerobic digestion. *Waste Manag.* 2003, *23* (3), 261–272.
46. García-González MC, Vanotti MB, Szogi AA. Recovery of ammonia from swine manure using gas-permeable membranes: effect of aeration. *J. Environ. Manage.* 2015, *152*, 19–26.
47. Dube PJ, Vanotti MB, Szogi AA, García-González MC. Enhancing recovery of ammonia from swine manure anaerobic digester effluent using gas-permeable membrane technology. *Waste Manag.* 2016, *49*, 372–377.
48. Sotres A, Cerrillo M, Viñas M, Bonmatí A. Nitrogen recovery from pig slurry in a two-chambered bioelectrochemical system. *Bioresour. Technol.* 2015, *194*, 373–382.

49. Ippersiel D, Mondor M, Lamarche F, Tremblay F, Dubreuil J, Masse L. Nitrogen potential recovery and concentration of ammonia from swine manure using electrodialysis coupled with air stripping. *J. Environ. Manage.* 2012, *95*, S165–S169.
50. Qin M, Molitor H, Brazil B, Novak JT, He Z. Recovery of nitrogen and water from landfill leachate by a microbial electrolysis cell–forward osmosis system. *Bioresour. Technol.* 2016, *200*, 485–492.
51. van der Hoek J, Duijff R, Reinstra O. Nitrogen recovery from wastewater: possibilities, competition with other resources, and adaptation pathways. *Sustainability* 2018, *10* (12), 4605.
52. Volpin F, Chekli L, Phuntsho S, Cho J, Ghaffour N, Vrouwenvelder JS, Kyong Shon H. Simultaneous phosphorous and nitrogen recovery from source-separated urine: a novel application for fertiliser drawn forward osmosis. *Chemosphere* 2018, *203*, 482–489.
53. Mondor M, Masse L, Ippersiel D, Lamarche F, Massé DI. Use of electrodialysis and reverse osmosis for the recovery and concentration of ammonia from swine manure. *Bioresour. Technol.* 2008, *99* (15), 7363–7368.
54. Kuntke P. Nutrient and energy recovery from urine. PhD thesis, Wageningen University, Wageningen, 2013.
55. Ward AJ, Arola K, Thompson Brewster E, Mehta CM, Batstone DJ. Nutrient recovery from wastewater through pilot scale electrodialysis. *Water Res.* 2018.
56. Hedström A. Ion exchange of ammonium in zeolites: a literature review. *J. Environ. Eng.* 2001, *127* (8), 673–681.
57. Lind B-B, Ban Z, Bydén S. Nutrient recovery from human urine by struvite crystallization with ammonia adsorption on zeolite and wollastonite. *Bioresour. Technol.* 2000, *73*, 169–174.
58. Maurer M, Schwegler P, Larsen TA. Nutrients in urine: energetic aspects of removal and recovery. *Water Sci. Technol.* 2003, *48* (1), 37–46.
59. Larsen TA, Udert KM, Lienert J. *Source separation and decentralization for wastewater management*. *Water Intelligence Online*, 2013, *12*.
60. Doyle JD, Parsons SA. Struvite formation, control and recovery. *Water Res.* 2002, *36*, 3925–3940.
61. Kuntke P, Geleji M, Bruning H, Zeeman G, Hamelers HVM, Buisman CJN. Effects of ammonium concentration and charge exchange on ammonium recovery from high strength wastewater using a microbial fuel cell. *Bioresour. Technol.* 2011, *102* (6), 4376–4382.
62. Kuntke P, Sleutels THJA, Rodríguez Arredondo M, Georg S, Barbosa SG, ter Heijne A, Hamelers HVM, Buisman CJN. (Bio)electrochemical ammonia recovery: progress and perspectives. *Appl. Microbiol. Biotechnol.* 2018, *102* (9), 3865–3878.
63. Logan BE, Hamelers HVM, Rozendal RA, Schröder U, Keller J, Freguia S, Aelterman P, Verstraete W, Rabaey K. Microbial fuel cells: methodology and technology. *Environ. Sci. Technol.* 2006, *40* (17), 5181–5192.

64. Gildemyn S, Verbeeck K, Slabbinck R, Andersen SJ, Prévoteau A, Rabaey K. Integrated production, extraction, and concentration of acetic acid from CO2 through microbial electrosynthesis. *Environ. Sci. Technol. Lett.* 2015, *2* (11), 325–328.
65. Van Eerten-Jansen MCAA, Heijne A Ter, Buisman CJN, Hamelers HVM. Microbial electrolysis cells for production of methane from CO2: long-term performance and perspectives. *Int. J. Energy Res.* 2012, *36* (6), 809–819.
66. Rabaey K, Rodríguez J, Blackall LL, Keller J, Gross P, Batstone D, Verstraete W, Nealson KH. Microbial ecology meets electrochemistry: electricity-driven and driving communities. *ISME J.* 2007, *1* (1), 9–18.
67. Zhang Y, Angelidaki I. Microbial electrolysis cells turning to be versatile technology: recent advances and future challenges. *Water Res.* 2014, *56*, 11–25.
68. Radjenovic J, Sedlak DL. Challenges and opportunities for electrochemical processes as next-generation technologies for the treatment of contaminated water. *Environ. Sci. Technol.* 2015, *49* (19), 11292–11302.
69. Kuntke P, Śmiech KM, Bruning H, Zeeman G, Saakes M, Sleutels THJA, Hamelers HVM, Buisman CJN. Ammonium recovery and energy production from urine by a microbial fuel cell. *Water Res.* 2012, *46* (8), 2627–2636.
70. Rozendal RA, Hamelers HVM, Rabaey K, Keller J, Buisman CJN. Towards practical implementation of bioelectrochemical wastewater treatment. *Trends Biotechnol.* 2008, *26* (8), 450–459.
71. Bagastyo AY, Radjenovic J, Mu Y, Rozendal RA, Batstone DJ, Rabaey K. Electrochemical oxidation of reverse osmosis concentrate on mixed metal oxide (MMO) titanium coated electrodes. *Water Res.* 2011, *45* (16), 4951–4959.
72. Sleutels THJA, Hamelers HVM, Rozendal RA, Buisman CJN. Ion transport resistance in microbial electrolysis cells with anion and cation exchange membranes. *Int. J. Hydrog. Energ.* 2009, *34* (9), 3612–3620.
73. Sleutels THJA, Ter Heijne A, Buisman CJN, Hamelers HVM. Bioelectrochemical systems: an outlook for practical applications. *ChemSusChem* 2012, *5* (6), 1012–1019.
74. Rabaey K, Verstraete W. Microbial fuel cells: novel biotechnology for energy generation. *Trends Biotechnol.* 2005, *23* (6), 291–298.
75. Sleutels THJA, Hoogland BJ, Kuntke P, ter Heijne A, Buisman CJN, Hamelers HVM. Gas-permeable hydrophobic membranes enable transport of CO2 and NH3 to improve performance of bioelectrochemical systems. *Environ. Sci. Water Res. Technol.* 2016, *2* (4), 743–748.
76. Zöllig H, Remmele A, Fritzsche C, Morgenroth E, Udert KM. Formation of chlorination byproducts and their emission pathways in chlorine mediated electro-oxidation of urine on active and nonactive type anodes. *Environ. Sci. Technol.* 2015, *49* (18), 11062–11069.
77. Ledezma P, Kuntke P, Buisman CJN, Keller J, Freguia S. Source-separated urine opens golden opportunities for microbial electrochemical technologies. *Trends Biotechnol.* 2015, *33* (4), 214–220.

78. Vinneras B, Jönsson H. The performance and potential of faecal separation and urine diversion to recycle plant nutrients in household wastewater. *Bioresour. Technol.* 2002, *84*, 275–282.
79. Rossi L, Lienert J, Larsen TA. Real-life efficiency of urine source separation. *J. Environ. Manage.* 2009, *90* (5), 1909–1917.
80. Rose C, Parker A, Jefferson B, Cartmell E. The characterization of feces and urine: a review of the literature to inform advanced treatment technology. *Crit. Rev. Environ. Sci. Technol.* 2015, *45* (17), 1827–1879.
81. Putnam DF. *Composition and concentrative properties of human urine*; National Aeronautics and Space Administration (NASA): Washington, D.C., 1971.
82. Tuantet K, Janssen M, Temmink H, Zeeman G, Wijffels R, Buisman C. Microalgae growth on concentrated human urine. *J. Appl. Phycol.* 2014, *26* (1), 287–297.
83. Kirchmann H, Pettersson S. Human urine - chemical composition and fertilizer use efficiency. *Fertil. Res.* 1995, *40*, 149–154.
84. Udert KM, Larsen TA, Biebow M, Gujer W. Urea hydrolysis and precipitation dynamics in a urine-collecting system. *Water Res.* 2003, *37* (11), 2571–2582.
85. Viskari E, Grobler G, Karimäki K, Gorbatova A, Vilpas R, Lehtoranta S. Nitrogen recovery with source separation of human urine-preliminary results of its fertiliser potential and use in agriculture. *Front. Sustain. Food Syst.* 2018, *2* (June), 1–14.
86. Wilsenach JA, van Loosdrecht MCM. Integration of processes to treat wastewater and source-separated urine. *J. Environ. Eng.* 2006, *132* (3).
87. Kuntke P, Sleutels THJA, Saakes M, Buisman CJN. Hydrogen production and ammonium recovery from urine by a microbial electrolysis cell. *Int. J. Hydrog. Energ.* 2014, *39* (10), 4771–4778.
88. Luther AK, Desloover J, Fennell DE, Rabaey K. Electrochemically driven extraction and recovery of ammonia from human urine. *Water Res.* 2015, *87*, 367–377.
89. Rodríguez Arredondo M, Kuntke P, Jeremiasse AW, Sleutels THJA, Buisman CJN, ter Heijne A. Bioelectrochemical systems for nitrogen removal and recovery from wastewater. *Environ. Sci. Water Res. Technol.* 2015, *1* (1), 22–33.
90. United States Census Bureau. World Population. http://www.census.gov/population/international/data/worldpop/table_population.php (accessed May 15, 2014).
91. UN. World population projected to reach 9.6 billion by 2050 with most growth in developing regions, especially Africa – says UN. http://esa.un.org/unpd/wpp/Documentation/pdf/WPP2012_Press_Release.pdf (accessed May 9, 2014).
92. Rockström J, Steffen W, Noone K, Persson A, Chapin FS, Lambin EF, Lenton TM, Scheffer M, Folke C, Schellnhuber HJ, et al. A safe operating space for humanity. *Nature* 2009, *461* (7263), 472–475.
93. Madigan MT, Martinko JM, Parker J. *Brock biology of microorganisms* 9 edition. Upper Saddle River: Prentice Hall. 2000.

94. Leach AM, Galloway JN, Bleeker A, Erisman JW, Kohn R, Kitzes J. A nitrogen footprint model to help consumers understand their role in nitrogen losses to the environment. *Environ. Dev.* 2012, *1* (1), 40–66.
95. Cheng S, Xing D, Call DF, Logan BE. Direct biological conversion of electrical current into methane by electromethanogenesis. *Environ. Sci. Technol.* 2009, *43* (10), 3953–3958.
96. Rozendal RA, Leone E, Keller J, Rabaey K. Efficient hydrogen peroxide generation from organic matter in a bioelectrochemical system. *Electrochem. commun.* 2009, *11* (9), 1752–1755.
97. Steinbusch KJJ, Hamelers HVM, Schaap JD, Kampman C, Buisman CJN. Bioelectrochemical ethanol production through mediated acetate reduction by mixed cultures. *Environ. Sci. Technol.* 2009, *44* (1), 513–517.
98. Van Eerten-Jansen MCAA, Ter Heijne A, Grootscholten TIM, Steinbusch KJJ, Sleutels THJA, Hamelers HVM, Buisman CJN. Correction to bioelectrochemical production of caproate and caprylate from acetate by mixed cultures. *ACS Sustain. Chem. Eng.* 2013, *1* (8), 1069.
99. Kelly PT, He Z. Nutrients removal and recovery in bioelectrochemical systems: a review. *Bioresour. Technol.* 2014, *153*, 351–360.
100. Barnard JL. Elimination of eutrophication through resource recovery. *International Conference on Nutrient Recovery from Wastewater Streams*, 2009, 1–22.
101. Tchobanoglous G, Burton FL, Metcalf, Eddy I. *Wastewater engineering : treatment and reuse*. In *McGraw-Hill series in civil and environmental engineering* Boston: McGraw-Hill. 2003.
102. Jetten MSM, Cirpus I, Kartal B, van Niftrik L, van de Pas-Schoonen KT, Sliekers O, Haaijer S, van der Star W, Schmid M, van de Vossenberg J, et al. 1994-2004: 10 years of research on the anaerobic oxidation of ammonium. *Biochem. Soc. Trans.* 2005, *33*, 119–123.
103. van Dongen U, Jetten MSM, van Loosdrecht MCM. The sharon®-anammox® process for treatment of ammonium rich wastewater. *Water Sci. Technol.* 2001, *44* (1), 153–160.
104. van Dongen LGJM, Jetten MSM, van Loosdrecht MCM, Publishing IWA. *The combined sharon/anammox process. a sustainable method for n-removal from sludge water*; STOWA: Delft, 2001.
105. Jetten MSM, Wagner M, Fuerst J, van Loosdrecht M, Kuenen G, Strous M. Microbiology and application of the anaerobic ammonium oxidation ('anammox') process. *Curr. Opin. Biotechnol.* 2001, *12*, 283–288.
106. Scherson YD, Wells GF, Woo S-G, Lee J, Park J, Cantwell BJ, Criddle CS. Nitrogen removal with energy recovery through n2o decomposition. *Energy Environ. Sci.* 2013, *6* (1), 241–248.
107. ter Heijne A, Hamelers HVM, de Wilde V, Rozendal RA, Buisman CJN. A bipolar membrane combined with ferric iron reduction as an efficient cathode system in microbial fuel cells. *Environ. Sci. Technol.* 2006, *40* (17), 5200–5205.
108. Ter Heijne A, Liu F, van der Weijden R, Weijma J, Buisman CJN, Hamelers HVM. Copper recovery combined with electricity production in a microbial fuel cell. *Environ. Sci. Technol.* 2010, *44* (11), 4376–4381.

109. Zhao F, Harnisch F, Schröder U, Scholz F, Bogdanoff P, Herrmann I. Challenges and constraints of using oxygen cathodes in microbial fuel cells. *Environ. Sci. Technol.* 2006, *40* (17), 5193–5199.
110. Hamelers HVM, Ter Heijne A, Sleutels THJA, Jeremiasse AW, Strik DPBTB, Buisman CJN. New applications and performance of bioelectrochemical systems. *Appl. Microbiol. Biotechnol.* 2010, *85* (6), 1673–1685.
111. Liu H, Grot S, Logan BE. Electrochemically assisted microbial production of hydrogen from acetate. *Environ. Sci. Technol.* 2005, *39* (11), 4317–4320.
112. Diem K, Lentner C. *Scientific tables.* 7th edition. Basle: Ciba-Geigy Limited. 1970.
113. Wilsenach J, van Loosdrecht M. *Separate urine collection and treatment: options for sustainable wastewater systems and mineral recovery*; Stichting Toegepast Onderzoek Waterbeheer (STOWA), 2002.
114. He Z, Kan J, Wang Y, Huang Y, Mansfeld F, Nealson KH. Electricity production coupled to ammonium in a microbial fuel cell. *Environ. Sci. Technol.* 2009, *43* (9), 3391–3397.
115. Kim JR, Zuo Y, Regan JM, Logan BE. Analysis of ammonia loss mechanisms in microbial fuel cells treating animal wastewater. *Biotechnol. Bioeng.* 2008, *99* (5), 1120–1127.
116. Zang G-LG-L, Sheng G-PG-P, Li W-WW-W, Tong Z-HZ-H, Zeng RJ, Shi C, Yu H-QH-Q. Nutrient removal and energy production in a urine treatment process using magnesium ammonium phosphate precipitation and a microbial fuel cell technique. *Phys. Chem. Chem. Phys.* 2012, *14* (6), 1978.
117. Clauwaert Rabaey, K., Aelterman, P., De Schamphelaire, L., Pham, T.H., Boeckx, P., Boon, N. and Verstraete, W. P. Biological denitrification in microbial fuel cells. *Environ. Sci. Technol.* 2007, *41* (9), 3354–3360.
118. Virdis B, Rabaey K., Yuan Z, Keller J. Microbial fuel cells for simultaneous carbon and nitrogen removal. *Water Res.* 2008, *42* (12), 3013–3024.
119. Virdis B, Rabaey K, Rozendal RA, Yuan Z, Keller J. Simultaneous nitrification, denitrification and carbon removal in microbial fuel cells. *Water Res.* 2010, *44* (9), 2970–2980.
120. Zhang F, He Z. Integrated organic and nitrogen removal with electricity generation in a tubular dual-cathode microbial fuel cell. *Process Biochem.* 2012, *47* (12), 2146–2151.
121. Yan H, Saito T, Regan JM. Nitrogen removal in a single-chamber microbial fuel cell with nitrifying biofilm enriched at the air cathode. *Water Res.* 2012, *46* (7), 2215–2224.
122. Haddadi S, Elbeshbishy E, Lee H-S. Implication of diffusion and significance of anodic ph in nitrogen-recovering microbial electrochemical cells. *Bioresour. Technol.* 2013, *142*, 562–569.
123. Rozendal RA, Hamelers HVM, Buisman CJN. Effects of membrane cation transport on ph and microbial fuel cell performance. *Environ. Sci. Technol.* 2006, *40* (17), 5206–5211.
124. Rozendal RA, Sleutels THJA, Hamelers HVM, Buisman CJN. Effect of the type of ion exchange membrane on performance, ion transport, and ph in biocatalyzed electrolysis of wastewater. *Water Sci. Technol.* 2008, *57* (11), 1757–1762.
125. Cord-Ruwisch R, Law Y, Cheng KY. Ammonium as a sustainable proton shuttle in bioelectrochemical systems. *Bioresour. Technol.* 2011, *102* (20), 9691–9696.

126. Cheng KY, Kaksonen AH, Cord-Ruwisch R. Ammonia recycling enables sustainable operation of bioelectrochemical systems. *Bioresour. Technol.* 2013, *143*, 25–31.
127. Larsen TA, Gujer W. Separate management of anthropogenic nutrient solutions (human urine). *Water Sci. Technol.* 1996, *34* (3–4), 87–94.
128. Mobley HLT, Hausinger RP. Microbial ureases - significance, regulation, and molecular characterization. *Microbiol. Rev.* 1989, *53* (1), 85–108.
129. Volcke E, Villez K, Van Hulle S, van Loosdrecht M, Vanrolleghem P. Wat met rejectiewater? *Afvalwaterwetenschap* 2004, *3* (4), 297–318.
130. Fuerte A, Valenzuela RX, Escudero MJ, Daza L. Ammonia as efficient fuel for sofc. *J. Power Sources* 2009, *192* (1), 170–174.
131. US Department of Energy. Hydrogen analysis resource center. http://hydrogen.pnl.gov/cocoon/morf/hydrogen/site_specific/fuel_heating_calculator?canprint=false (accessed May 12, 2014).
132. Hacker V, Kordesch K. Ammonia crackers. *Handbook of fuel cells- Fundamentals, technology and applications*, 2003, *3*, 121–127.
133. Centraal Bureau voor de Statistiek (CBS). Aardgas en elektriciteit, gemiddelde prijzen van eindverbruikers. http://statline.cbs.nl/StatWeb/publication/?VW=T&DM=SLNL&PA=81309NED&D1=1,3,5,8,11,15&D2=0&D3=l&D4=0-3,5-8,10-13,15-18,20-23,l&HD=120813-1059&HDR=T&STB=G2,G1,G3 (accessed May 14, 2014).
134. International Energy Agency (IEA). Hydrogen Production & Distribution. http://www.iea.org/techno/essentials5.pdf (accessed Jun 2, 2014).
135. Post JW. Blue energy: electricity production from salinity gradients by reverse electrodialysis. PhD thesis, Wageningen University, Wageningen, 2009.
136. Aiyuk S, Forrez I, Lieven DK, van Haandel A, Verstraete W. Anaerobic and complementary treatment of domestic sewage in regions with hot climates—a review. *Bioresour. Technol.* 2006, *97* (17), 2225–2241.
137. Kang Olmstead, K., Takacs, K. and Collins, J. SJ. *Municipal nutrient removal technologies reference document*; U.S. Environmental Protection Agency, 2008.
138. Sleutels THJA, Ter Heijne A, Buisman CJN, Hamelers HVM. Steady-state performance and chemical efficiency of microbial electrolysis cells. *Int. J. Hydrogen Energy* 2013, *38* (18), 7201–7208.
139. Dykstra JE, Biesheuvel PM, Bruning H, ter Heijne A. Theory of ion transport with fast acid-base equilibrations in bioelectrochemical systems. *Phys. Rev. E* 2014, *90* (1).
140. Janicek A, Fan Y, Liu H. Design of microbial fuel cells for practical application: a review and analysis of scale-up studies. *Biofuels* 2014, *5* (1), 79–92.
141. von Sperling M. Wastewater characteristics, treatment and disposal. *Biological Wastewater Treatment Series*, 2007, *1*.
142. Rozendal RA, Hamelers HVM, Molenkamp RJ, Buisman CJN. Performance of single chamber biocatalyzed electrolysis with different types of ion exchange membranes. *Water Res.* 2007, *41* (9), 1984–1994.

143. Kuntke P, Zamora P, Saakes M, Buisman CJN, Hamelers HVM. Gas-permeable hydrophobic tubular membranes for ammonia recovery in bio-electrochemical systems. *Environ. Sci. Water Res. Technol.* 2016, *2* (2), 261–265.
144. Długołęcki P, Anet B, Metz SJ, Nijmeijer K, Wessling M. Transport limitations in ion exchange membranes at low salt concentrations. *J. Membr. Sci.* 2010, *346* (1), 163–171.
145. Gildemyn S, Luther AK, Andersen SJ, Desloover J, Rabaey K. Electrochemically and bioelectrochemically induced ammonium recovery. *J. Vis. Exp.* 2015, No. 95.
146. Liu Y, Qin M, Luo S, He Z, Qiao R. Understanding ammonium transport in bioelectrochemical systems towards its recovery. *Sci. Rep.* 2016, *6* (1), 22547.
147. Dbira S, Bensalah N, Bedoui A, Cañizares P, Rodrigo MA. Treatment of synthetic urine by electrochemical oxidation using conductive-diamond anodes. *Environ. Sci. Pollut. R.* 2014, *22* (8), 6176–6184.
148. Kapałka A, Katsaounis A, Michels NL, Leonidova A, Souentie S, Comninellis C, Udert KM. Ammonia oxidation to nitrogen mediated by electrogenerated active chlorine on Ti/PtOx-IrO2. *Electrochem. Commun.* 2010, *12* (9), 1203–1205.
149. Zöllig H, Fritzsche C, Morgenroth E, Udert KM. Direct electrochemical oxidation of ammonia on graphite as a treatment option for stored source-separated urine. *Water Res.* 2015, *69*, 284–294.
150. Candido L, Gomes JACP. Evaluation of anode materials for the electro-oxidation of ammonia and ammonium ions. *Mater. Chem. Phys.* 2011, *129* (3), 1146–1151.
151. Kim KW, Kim YJ, Kim IT, Park GI, Lee EH. The electrolytic decomposition mechanism of ammonia to nitrogen at an iro2 anode. *Electrochim. Acta* 2005, *50* (22), 4356–4364.
152. Food and Agriculture Organization (FAO). *World fertilzer trends and outlook to 2018* 2018. http://www. fao.org/3/a-i4324e.pdf (accessed May 2, 2016).
153. Metson GS, Cordell D, Ridoutt B. Potential impact of dietary choices on phosphorus recycling and global phosphorus footprints: the case of the average australian city. *Front. Nutr.* 2016, *3* (August), 35.
154. Cordell D, Drangert J-O, White S. The story of phosphorus: global food security and food for thought. *Glob. Environ. Chang.* 2009, *19* (2), 292–305.
155. Worrell E, Phylipsen D, Einstein D, Martin N. Energy Use and Energy Intensity of the U.S. Chemical Industry. https://www.energystar.gov/sites/default/files/buildings/tools/industrial_LBNL-44314.pdf (accessed Jan 20, 2017).
156. International Energy Agency (IEA). Tracking Industrial Energy Efficiency and CO2 Emissions. https://www.iea.org/publications/freepublications/publication/tracking_emissions.pdf (accessed Jan 20, 2017).
157. Larsen TA, Gujer W. Separate management of anthropogenic nutrient solutions (human urine). *Water Sci. Technol.* 1996, *34* (3-4–4 pt 2), 87–94.
158. Ieropoulos I, Greenman J, Melhuish C. Urine utilisation by microbial fuel cells; energy fuel for the future. *Phys. Chem. Chem. Phys.* 2012, *14* (1), 94–98.

159. Ieropoulos IA, Ledezma P, Stinchcombe A, Papaharalabos G, Melhuish C, Greenman J. Waste to real energy: the first MFC powered mobile phone. *Phys. Chem. Chem. Phys.* 2013, *15* (37), 15312.
160. Sleutels THJA, Darus L, Hamelers HVM, Buisman CJN. Effect of operational parameters on coulombic efficiency in bioelectrochemical systems. *Bioresour. Technol.* 2011, *102* (24), 11172–11176.
161. Sleutels T, Molenaar S, Heijne A, Buisman C. Low substrate loading limits methanogenesis and leads to high coulombic efficiency in bioelectrochemical systems. *Microorganisms* 2016, *4* (7), 1–11.
162. Amstutz V, Katsaounis A, Kapałka A, Comninellis C, Udert KM. Effects of carbonate on the electrolytic removal of ammonia and urea from urine with thermally prepared iro2 electrodes. *J. Appl. Electrochem.* 2012, *42* (9), 787–795.
163. Zamora P, Georgieva T, Salcedo I, Elzinga N, Kuntke P, Buisman CJN. Long-term operation of a pilot-scale reactor for phosphorus recovery as struvite from source-separated urine. *J. Chem. Technol. Biotechnol.* 2017, *92* (5), 1035–1045.
164. Post JW, Hamelers HVM, Buisman CJN. Influence of multivalent ions on power production from mixing salt and fresh water with a reverse electrodialysis system. *J. Memb. Sci.* 2009, *330* (1–2), 65–72.
165. Tylus U, Jia Q, Hafiz H, Allen RJ, Barbiellini B, Bansil A, Mukerjee S. Engendering anion immunity in oxygen consuming cathodes based on Fe-Nx electrocatalysts: Spectroscopic and electrochemical advanced characterizations. *Appl. Catal. B Environ.* 2016, *198*, 318–324.
166. Herrera OE, Wilkinson DP, Mérida W. Anode and cathode overpotentials and temperature profiles in a PEMFC. *J. Power Sources* 2012, *198*, 132–142.
167. Christiaens MER, Gildemyn S, Matassa S, Ysebaert T, De Vrieze J, Rabaey K. Electrochemical ammonia recovery from source-separated urine for microbial protein production. *Environ. Sci. Technol.* 2017, *51* (22), 13143–13150.
168. Zamora P, Georgieva T, ter Heijne A, Sleutels THJA, Jeremiasse AW, Saakes M, Buisman CJN, Kuntke P. Ammonia recovery from urine in a scaled-up microbial electrolysis cell. *J. Power Sources* 2017, *356*, 491–499.
169. Kuntke P, Rodríguez Arredondo M, Widyakristi L, ter Heijne A, Sleutels THJA, Hamelers HVM, Buisman CJN. Hydrogen gas recycling for energy efficient ammonia recovery in electrochemical systems. *Environ. Sci. Technol.* 2017, *51* (5), 3110–3116.
170. Rodríguez Arredondo M, Kuntke P, ter Heijne A, Hamelers HVM, Buisman CJN. Load ratio determines the ammonia recovery and energy input of an electrochemical system. *Water Res.* 2017, *111*, 330–337.
171. Barbosa SG, Peixoto L, ter Heijne A, Kuntke P, Alves MM, Pereira MA. Investigating bacterial community changes and organic substrate degradation in microbial fuel cells operating on real human urine. *Environ. Sci. Water Res. Technol.* 2017, *3*, 897–904.
172. You J, Greenman J, Melhuish C, Ieropoulos I. Electricity generation and struvite recovery from human urine using microbial fuel cells. *J. Chem. Technol. Biotechnol.* 2016, *91* (3), 647–654.

173. Pletcher D, Li X. Prospects for alkaline zero gap water electrolysers for hydrogen production. *Int. J. Hydrogen Energy* 2011, *36* (23), 15089–15104.
174. Ledezma P, Jermakka J, Keller J, Freguia S. Recovering nitrogen as a solid without chemical dosing: bio-electroconcentration for recovery of nutrients from urine. *Environ. Sci. Technol. Lett.* 2017, *4* (3), 119–124.
175. Zehnder AJB, Huser BA, Brock TD, Wuhrmann K. Characterization of an acetate-decarboxylating, non-hydrogen-oxidizing methane bacterium. *Arch. Microbiol.* 1980, *124* (1), 1–11.
176. Qin M, Hynes EA, Abu-Reesh IM, He Z. Ammonium removal from synthetic wastewater promoted by current generation and water flux in an osmotic microbial fuel cell. *J. Clean. Prod.* 2017, *149*, 856–862.
177. Zhang Y, Angelidaki I. Submersible microbial desalination cell for simultaneous ammonia recovery and electricity production from anaerobic reactors containing high levels of ammonia. *Bioresour. Technol.* 2015, *177*, 233–239.
178. Zhang Y, Angelidaki I. Counteracting ammonia inhibition during anaerobic digestion by recovery using submersible microbial desalination cell. *Biotechnol. Bioeng.* 2015, *112* (7), 1478–1482.
179. Zhang Y, Angelidaki I. Recovery of ammonia and sulfate from waste streams and bioenergy production via bipolar bioelectrodialysis. *Water Res.* 2015, *85*, 177–184.
180. Tarpeh WA, Barazesh JM, Cath TY, Nelson KL. Electrochemical stripping to recover nitrogen from source-separated urine. *Environ. Sci. Technol.* 2018, *52* (3), 1453–1460.
181. Kuntke P, Rodrigues M, Sleutels T, Saakes M, Hamelers HVM, Buisman CJN. Energy-efficient ammonia recovery in an up-scaled hydrogen gas recycling electrochemical system. *ACS Sustain. Chem. Eng.* 2018, *6* (6), 7638–7644.
182. Hou D, Iddya A, Chen X, Wang M, Zhang W, Ding Y, Jassby D, Ren ZJ. Nickel-based membrane electrodes enable high-rate electrochemical ammonia recovery. *Environ. Sci. Technol.* 2018, *52* (15), 8930–8938.
183. Christiaens MER, Udert KM, Arends JBA, Huysman S, Vanhaecke L, McAdam E, Rabaey K. Membrane stripping enables effective electrochemical ammonia recovery from urine while retaining microorganisms and micropollutants. *Water Res.* 2019, *150*, 349–357.
184. Qin M, He Z. Self-supplied ammonium bicarbonate draw solute for achieving wastewater treatment and recovery in a microbial electrolysis cell-forward osmosis-coupled system. *Environ. Sci. Technol. Lett.* 2014, *1* (10), 437–441.
185. Zou S, Qin M, Moreau Y, He Z. Nutrient-energy-water recovery from synthetic sidestream centrate using a microbial electrolysis cell - forward osmosis hybrid system. *J. Clean. Prod.* 2017, *154*, 16–25.
186. Rodríguez Arredondo M, Kuntke P, ter Heijne A, Buisman CJN. The concept of load ratio applied to bioelectrochemical systems for ammonia recovery. *J. Chem. Technol. Biotechnol.* 2019, *94* (6), 2055–2061.

187. Barbosa SG, Peixoto L, Soares OSGP, Pereira MFR, Heijne A Ter, Kuntke P, Alves MM, Pereira MA. Influence of carbon anode properties on performance and microbiome of microbial electrolysis cells operated on urine. *Electrochim. Acta* 2018, *267*, 122–132.
188. Barbosa SG, Rodrigues T, Peixoto L, Kuntke P, Alves MM, Pereira MA, ter Heijne A. Anaerobic biological fermentation of urine as a strategy to enhance the performance of a microbial electrolysis cell (MEC). *Renew. Energy* 2019, *139*, 936–943.
189. Christiaens MER, De Vrieze J, Clinckemaillie L, Ganigué R, Rabaey K. Anaerobic ureolysis of source-separated urine for nh3 recovery enables direct removal of divalent ions at the toilet. *Water Res.* 2019, *148*, 97–105.
190. Nam JY, Kim HW, Shin HS. Ammonia inhibition of electricity generation in single-chambered microbial fuel cells. *J. Power Sources* 2010, *195* (19), 6428–6433.
191. Yenigün O, Demirel B. Ammonia inhibition in anaerobic digestion: A review. *Process Biochem.* 2013, *48* (5), 901–911.
192. Mahmoud M, Parameswaran P, Torres CI, Rittmann BE. Electrochemical techniques reveal that total ammonium stress increases electron flow to anode respiration in mixed-species bacterial anode biofilms. *Biotechnol. Bioeng.* 2017, *114* (6), 1151–1159.
193. Lin H, Wu X, Nelson C, Miller C, Zhu J. Electricity generation and nutrients removal from high-strength liquid manure by air-cathode microbial fuel cells. *J. Environ. Sci. Heal. Part A* 2016, *51* (3), 240–250.
194. Clauwaert P, Tolêdo R, van der Ha D, Crab R, Verstraete W, Hu H, Udert KM, Rabaey K. Combining biocatalyzed electrolysis with anaerobic digestion. *Water Sci. Technol.* 2008, *57* (4), 575–579.
195. Wang L, Xie B, Gao N, Min B, Liu H. Urea removal coupled with enhanced electricity generation in single-chambered microbial fuel cells. *Environ. Sci. Pollut. Res.* 2017, *24* (25), 20401–20408.
196. Kim HW, Nam JY, Shin HS. Ammonia inhibition and microbial adaptation in continuous single-chamber microbial fuel cells. *J. Power Sources* 2011, *196* (15), 6210–6213.
197. Tice RC, Kim Y. Influence of substrate concentration and feed frequency on ammonia inhibition in microbial fuel cells. *J. Power Sources* 2014, *271*, 360–365.
198. Müller T, Walter B, Wirtz A, Burkovski A. Ammonium toxicity in bacteria. *Curr. Microbiol.* 2006, *52* (5), 400–406.
199. Stein NE. A microbial fuel cell-based biosensor for the detection of toxic components in water. PhD thesis, Wageningen University, 2011.
200. Rabaey K, Clauwaert P, Aelterman P, Verstraete W. Tubular microbial fuel cells for efficient electricity generation. *Environ. Sci. Technol.* 2005, *39* (20), 8077–8082.
201. Lovley DR, Klug MJ. Methanogenesis from methanol and methylamines and acetogenesis from hydrogen and carbon dioxide in the sediments of a eutrophic lake. *Appl. Environ. Microbiol.* 1983, *45* (4), 1310–1315.
202. Cusick RD, Ullery ML, Dempsey BA, Logan BE. Electrochemical struvite precipitation from digestate with a fluidized bed cathode microbial electrolysis cell. *Water Res.* 2014, *54*, 297–306.

203. Barbosa SG, Peixoto L, Meulman B, Alves MM, Pereira MA. A design of experiments to assess phosphorous removal and crystal properties in struvite precipitation of source separated urine using different Mg sources. *Chem. Eng. J.* 2016, *298*, 146–153.
204. Igos E, Besson M, Navarrete Gutiérrez T, Bisinella de Faria AB, Benetto E, Barna L, Ahmadi A, Spérandio M. Assessment of environmental impacts and operational costs of the implementation of an innovative source-separated urine treatment. 2017, *126*, 50–59.
205. Lienert J, Bürki T, Escher BI. Reducing micropollutants with source control: substance flow analysis of 212 pharmaceuticals in faeces and urine. *Water Sci. Technol.* 2007, *56* (5), 87–96.
206. Butkovskyi A. Removal of micropollutants in source separated sanitation. PhD thesis, Wageningen University, Wageningen, 2015.
207. Bischel HN, Ozel BD, Strande L, Mcardell CS, Udert KM, Kohn T. Pathogens and pharmaceuticals in source-separated urine in eThekwini , South Africa. 2015, *85*, 57–65.
208. Sleutels THJA, ter Heijne A, Kuntke P, Buisman CJN, Hamelers HVM. Membrane selectivity determines energetic losses for ion transport in bioelectrochemical systems. *ChemistrySelect* 2017, *2* (12), 3462–3470.
209. Parameswaran P, Torres CI, Lee H-S, Krajmalnik-Brown R, Rittmann BE. Syntrophic interactions among anode respiring bacteria (ARB) and non-ARB in a biofilm anode: Electron balances. *Biotechnol. Bioeng.* 2009, *103* (3), 513–523.

Summary

Nitrogen removal from wastewaters is necessary to prevent the pollution of receiving water bodies. At the same time, nitrogen is an essential nutrient for plants, so it is used in the production of fertilizers. Both the conventional removal of nitrogen compounds from wastewater and their production are energy intensive. For this reason, recovering nitrogen directly from wastewater, instead of removing it, can result in reduced energy consumption associated with both its production and removal processes.

The use of electrochemical systems (ES) and bioelectrochemical systems (BES) for the recovery of ammonia from wastewaters has been investigated over the past few years. These systems have been proposed as a sustainable alternative to conventional processes because they have the potential to recover energy (in the form of electricity or H_2) from wastewaters while recovering ammonia.

From all the domestic wastewater streams, urine contains most of the nitrogen (around 80%), and represents only 1% of the volume. Urine can be collected by the use of urine-diverting toilets or waterless urinals, preventing the dilution of the nutrients with high volumes of potable water.

In this thesis, we evaluated the use of (bio)electrochemical systems for the recovery of total ammonia nitrogen (TAN) from urine. Our focus was on improving the understanding and performance of the system in terms of TAN recovery. This was needed to get the technology closer to application as, at the start of this research, the proof-of-principle had just been demonstrated, and the highest TAN recoveries were around 30%.

The feasibility of BES as a technology for energy-efficient TAN recovery was evaluated in **Chapter 2**. It was shown that BESs can become economically feasible if, on top of electricity or hydrogen production, the benefits of TAN removal are taken into account. According to our analysis, when TAN removal is taken into account, BESs can still be economic at high internal resistances (200 $m\Omega.m^2$), which makes it easier for the application of the system at a bigger scale.

The need to develop and test a method to effectively extract NH_3 from the catholyte solution was identified as one of the main limiting factors of the system. One of the main conclusions from **Chapter 2** was that it was crucial to couple an effective TAN stripping system to the BES to increase TAN recovery. This was addressed in **Chapter 3**, and followed up in **Chapters 4 and 5**. Finally, it was determined that to improve TAN recovery in BES, the interactions between the factors affecting the recovery of TAN in BES (such as current density, catholyte pH, TAN concentration, etc.) should be studied in more detail.

In **Chapter 3**, we demonstrated that an ES with an integrated gas-permeable hydrophobic membrane unit can effectively recover TAN from urine. Furthermore, the relationship between current density and TAN loading rate was studied in more detail. It was shown that the relationship between the applied current density and the TAN loading, here called the load ratio, is essential to assess the TAN removal efficiency and energy input of (B)ESs. The load ratio is useful to find the conditions in which a (B)ES for the recovery of TAN can be operated optimally, but it does not take into account other parameters essential to assess the performance of (B)ESs. These limitations are discussed throughout the thesis and in **Chapter 6.**

In **Chapter 4**, a hydrogen-recycling electrochemical system (HRES) was developed *to* minimize the energy input of electrochemical systems for the recovery of TAN. In this technology, the hydrogen gas produced at the cathode is reused as the electron donor in the anode, allowing for ammonia recovery at high rates and relatively low energy input. This technology can be applied to recover TAN from wastewaters that do not contain enough organic matter to be treated in a BES. Furthermore, it lowers the risk of chloride oxidation, which typically occurs in electrochemical systems treating wastewaters with high concentrations of chloride, such as urine. Chloride oxidation can result in the formation of harmful compounds such as chlorine gas, chlorination byproducts and adsorbable organic halides (AOX). At a load ratio of 1.2-1.3, the system accomplished TAN removal efficiencies of 73-82% and recoveries of 60-73%. Additional hydrogen needed to be supplied by a supporting electrolyzer, which accounted for 4-9% of the total energy demand of the system.

Finally, in **Chapter 5**, we tested the concept of load ratio in a BES. The load ratio can be manipulated either by changing the current density or the TAN loading rate. In a BES the current density cannot be controlled as easily as in an electrochemical system, because it depends on the oxidation of organic matter by microorganisms. At the same time, manipulating the TAN loading rate would directly affect the organic loading rate, and therefore the current density. We ran the BES coupled to a gas-permeable hydrophobic membrane on synthetic urine and urine. Both influents were fed at different dilutions, flow rates and certain modifications (such as removing TAN from urine prior to feeding it to the cell) in order to obtain a variety of load ratios. We found out that there was a clear increasing trend in TAN removal efficiency with respect to load ratio for both human and synthetic urine. We did not obtain load ratios higher than 0.8, which means that the current was not enough to transport all the TAN across the membrane. This resulted in overall low removal efficiencies (2 to 47%, with 3 exceptions from 52- 61%).

In **Chapter 6**, we discuss what may cause these low current densities. In this last chapter, we also focus on the reasons why (B)ESs have not been applied at larger scales yet, and

give future perspectives and recommendations to bring this promising technology closer to application.

List of publications

Rodríguez Arredondo M, Kuntke P, Jeremiasse AW, Sleutels THJA, Buisman CJN, ter Heijne A. Bioelectrochemical systems for nitrogen removal and recovery from wastewater. *Environ. Sci. Water Res. Technol.* 2015, *1* (1), 22–33.

Rodríguez Arredondo M, Kuntke P, ter Heijne A, Hamelers HVM, Buisman CJN. Load ratio determines the ammonia recovery and energy input of an electrochemical system. *Water Res.* 2017, *111*, 330–337.

Kuntke P, **Rodríguez Arredondo M**, Widyakristi L, ter Heijne A, Sleutels THJA, Hamelers HVM, Buisman CJN. Hydrogen gas recycling for energy efficient ammonia recovery in electrochemical systems. *Environ. Sci. Technol.* 2017, *51* (5), 3110–3116.

Kuntke P, Sleutels THJA, **Rodríguez Arredondo M**, Georg S, Barbosa SG, ter Heijne A, Hamelers HVM, Buisman CJN. (Bio)electrochemical ammonia recovery: progress and perspectives. *Appl. Microbiol. Biotechnol.* 2018, *102* (9), 3865–3878.

Rodríguez Arredondo M, Kuntke P, ter Heijne A, Buisman CJN. The concept of load ratio applied to bioelectrochemical systems for ammonia recovery. *J. Chem. Technol. Biotechnol.* 2019, *94* (6), 2055–2061.

Acknowledgements

This is it. The end of an era! I wouldn't have finished this long journey without the contribution of many people who were there for me in one way or another. I would like to thank all of you on these pages, so... here we go!

I would like to thank my supervisors, Philipp and Annemiek, for letting me be part of their team. **Philipp**, I probably have said this before but I think I would never finish writing all the things I thank you for. You were always there, you had a lot of patience when I was learning, when I was stubborn (so, very often!) and when I was struggling. I always felt your support. I truly appreciated you showing up in the lab and helping with practical things, too! **Annemiek**, thank you for always showing me the bright side when things got difficult, for your patience, your understanding and your support throughout this journey. Thank you for the countless writing suggestions, encouraging words, and for caring for my development not only as a scientist but as a person. I really enjoyed the short trip in your bakfiets! :D

I would like to thank **Cees**, my promotor, for giving me the opportunity to start this project. Thank you for your clear suggestions in papers and presentations, and for your practical insight and broad vision during our meetings. I will always be very grateful to you for letting Mark come to Leeuwarden.

There are many other people that were also part of this project in one way or another, and that made it a lot nicer. **Michel**, your endless energy and enthusiasm is super contagious. Your approach to science makes us PhDs remember the fun part of being in the lab! Thank you for all the knowledge you shared, the papers you sent and the schemes you drew. Thank you also for always brightening up my day. **Tom**, I really enjoyed working with you. Thank you for pushing for the papers to be published soon! :D Thank you for the funny e-mails, music, talks and for making me feel like I could always talk to you. I really appreciate that. **Bert**, I really enjoyed working with you, too. You helped re-direct the project when it was needed. Thank you for the model idea, for your interest in my data, for being enthusiastic about the project and for asking questions that pushed me to look at my work from a different angle. Thank you also for reminding me to go back to the basics and for your feedback on the presentations I gave, which made my work better.

I would also like to thank the **Resource Recovery theme members** and the **Value*from*Urine members** for your interest and critical look into my work. I enjoyed our meetings and trips a lot. A special thanks to **Sónia**, who came from Portugal in the very beginning, for being so nice to work with ☺. To **Martijn**, thank you for your practical ideas for the stripping-absorption column and for being so understanding when I got pregnant

with Elías, but especially thanks for putting up with pregnant-me on that plane to Madrid! **Patricia**, disfruté mucho el tiempo que estuviste en Leeuwarden. Gracias por estar ahí en todo momento y compartir las frustraciones de trabajar con bichos que hacen lo que se les pega la gana!

Rakesh, Fátima, Lucía Zwart and Ruben, thank you for your hard work and for not complaining once about working with urine :D. I learned a lot by supervising you. I would also like to thank **Olga, Marzena, Laksmi** and other students with whom I worked for their effort and enthusiasm. **Mariana Rodrigues** (you will finally stop receiving my e-mails! Woohoo!) and **Steffen**, thanks for the help at the very end of this journey. I really like you both! You guys will do great in your own urine/ES/BES adventure, and you know I am there for you.

My work would have never been accomplished without the help of a great staff. Thanks to the **whole analytical team at Wetsus** for dealing with my numerous samples and different analyses. Special thanks to **Mieke** and **Marianne** who dealt with most of them! Also thanks to **Janneke** and **Jelmer** for your help with the SEM and XRD. **Arie**, thank you for helping me out analyzing samples with the SEM; but most importantly thanks for your super positive attitude. I still miss hearing you whistle in the corridors and lab. Thanks to **all the awesome technicians in the Wetsus lab**! You guys do amazing work. A special thanks goes to **Harm**! Harm, you were there with me since I was doing my MSc thesis in the WAC, helping me with all sorts of wastewater issues at all times, and later on during the PhD with all urine-matters. Thank you for your prompt help, your ideas, and for making the Value*from*Urine setup (The Legendary Peeing Ken) come true!

Thank you, **Wetsus secretaries**, for all the times you helped me with numerous tasks. Special thanks to **Helena van der Werff, Linda, Trienke** and **Anke** for all the administrative work you helped me with during all these years (students, trips, workshops and congresses, booking of rooms and computers, etc.!). **Liesbeth and Gea**, thank you for helping me with all that paper work in Wageningen, too.

Rienk! I would have never been able to write the thesis without your IT skills. Thank you for always coming right away whenever there was an issue. **Janneke Tempel and Geke**: I cannot thank you enough for making the "breastfeeding room" happen. To **Jan, Claudia and Lucy**, thanks for helping me with all the declarations and for putting up with me not filling the Timewriter on time! To **Riet** and **Gerben**, you made the canteen a great place. Gerben, I will miss arriving to get some coffee and listening to your music playing in the kitchen :D. I will miss your ever positive vibes and great smile even more! **Johannes Boonstra**, thank you for making Wetsus a great place, and for your endless jokes and funny e-mails that always made me smile.

To all my Wetsus colleagues: thank you for all the amazing moments! The fact that I started my journey at Wetsus as an MSc student meant that I saw way too many people coming and going. Sorry if you are reading this and I forget to mention you!

I always happened to be in offices full with awesome people, both in the old and in the new building. Thanks to **Pau, Patrick, Jouke, Sam, Fei, Lina, Rebeca, Héctor, Prashanth, Gosia, Diego, Emanuel and Kaustub** for the countless coffees, talks, random pranks, jokes, and dinners.

A super special thanks goes to Anna and Joeri. **Anna**, qué bonito es tenerte como amiga ☺. Gracias por todos los abrazos, las conversaciones (profundas y simples), las risas (y las lágrimas), los buenos momentos y el viaje a Bath! Gracias por siempre estar ahí, incluso ahora a pesar de la distancia. **Joeri**, hola supermercado! Thanks for all the laughter and for being the only one willing to watch ballet and contemporary dance with me!

Jouke, Rik, Sam, and Tim Donkers: thanks for the awesome dinners we had! Rik, sorry you had to eat vegetarian so many times :D. Thank you for all the nice talks, for sharing with me and for making me feel like someone understands some aspects of my life that not many people can relate to. I am very glad to have you as a friend, and I love seeing you so happy with Raquel ☺. Sam, keep trying to change the world (one farm at a time!). I might still want to have another kid…don't kill me! In a more serious note: thanks for the motorcycle rides, DGTL, Amsterdam parties, e-mails sharing good music, the short period of watching movies, and the dinners at your place with Tim, Sebastián and Casper. It will always be amazing to me how much energy you have, how hard you can work and how passionate (and stubborn!) you can be. Keep enjoying life! Tim, even though you left Wetsus a very long time ago I still miss you! I really admire you for having the courage of going after what you want.

To **Martina, Christina, Alexandra and Philipp**, thanks a lot for letting me be part of the cozy pizza nights! I had a great time and certainly miss those.

To **Roel and Jan de Groot**, thanks for always being the last ones standing up, and for the times you made sure I (or Mark) went back home safe! Roel, thanks for all the BBQs and dinners at your place, for the sailing trip and for being one of the best Halloween-party hosts ever (together with Dries)!

Jaap, with you I have nice memories since the MSc times. Thanks for your always bright mood and for the nice drinks and dinners! **Sebastián**, mi colombiano favorito! Todavía me alegra que hayas regresado a hacer tu PhD en Wetsus. Gracias por tantas buenas pláticas, fiestas y bailes aquí y en Wageningen ☺. **Terica**, it was super nice being a paranymph

together with you. Thank you for the nice cocktails, talks, gossip and for spoiling Elías :D. **Rebeca and Karine (chica!)**, thanks for always being up to dancing and for enjoying the latin music with me! **Héctor and Paulina**, ustedes también contribuyeron a que no me sintiera tan sola en mi "latinez". Además de la música compartimos muy buenas pláticas, bromas y comida…ya toca juntarnos de nuevo!

I would also like to thank **Aga, Bob, Brahzil, Casper, Fabian, Gerwin, Janneke Dickhout, Jan Willem, Jordi, Jorrit, Juanma, Karolina, Louis, Marianne, Michele, Monir, Natascha, Olivier, Pawel, Philipp Wilfert, Raquel, Sandra, Slawek, Vytautas, Yang, Ricardo, Victor Ajao** and **Víctor Torres**, for being there for a good talk, laugh, dance, party, or for helping me out at some point. Cooperation and joy for the win!

A big thank you to all the **ETE people** for the "gezelligheid" when I visited! A special thanks to the whole **Biorecovery group** for the great meetings, talks, drinks and international dishes. I would like to particularly thank Koen, Sanne and Yvonne for the fun in Wageningen (and elsewhere!). **Koen**, the Bath trip and the legendary A1 course were way too much fun. Thanks for all (aaaallll) the beers and the good times! **Sanne**, thanks for the parties, the dancing and for letting me stay at your place! **Yvonne**, I always enjoyed the conversations (and drinks) we had. Thank you for the post cards, the words of encouragement but especially thanks for your friendship!

I would like to give a very special thanks to two women who have shared with me the experience of being a mom very closely. **Lucía**, hermana, la matriarca de mi familia mexicana en Holanda :D. Eres una súper mamá! Gracias por escucharme siempre, por regañarme cuando me toca, pero más que nada por siempre recordarme que no estoy sola. Gracias por estar ahí en todo momento. En verdad no sé qué hubiera hecho sin tu ayuda. Gracias también por confiar en mí y por aguantar las malas bromas de Elías :D. Muchas gracias también a Johannes, Mateo, Lisa, Emma y Olivia por ser tan lindos con Elías! **Alma**, sin saberlo llegaste a mi vida justo en el momento en que más lo necesitaba (aunque suene a canción romántica!). Estoy muy feliz de haberte encontrado. En el poco tiempo de conocernos ya hemos compartido muchísimas cosas, y te agradezco mucho por eso. Gracias por todo tu apoyo, las pláticas, el super concierto de Muse, el viaje a Utrecht y las mil comidas y cenas. Muchas gracias también a Kris y a Kaly por todos los lindos momentos!

Jeremy and Jess, thank you for being such cool parents and for having such awesome kids! I love every time I see our kids play together. I am very glad to have met you!

A los BIs, gracias por todas las posadas, bodas y pachangas en general. A pesar de que sólo nos vemos una vez al año es como si el tiempo no pasara! Los extraño siempre. **Abril**,

gracias por compartir tanto conmigo a pesar de la distancia y por el viaje legendario a Bruselas (mejor no empiezo con los chistes locales porque nunca termino!). **Fresa y Betty**, gracias por las carcajadas en el viaje a Praga, Budapest y Barcelona. Fresa, muchas gracias por dejarme ser parte de cuando le pediste la mano a Bárbara…me encantó! **Amado**, qué te traes, %*&#?! Ya escribí y borré muchas veces lo que te quería decir porque todo incluye un 'lenguaje inapropiado para este medio'. Me remitiré a lo decente, pues. Gracias por todas las horas de tren para venir a visitarme, por las buenas fiestas en Eindhoven, por los muchos tragos y bailes, por los memes, la música y las carcajadas, por el viaje con Fresa, Betty y compañía y por introducirme a Macumba! A **Mariangel**, gracias por visitarme, escucharme, hacerme reír con tus bromas crueles :D, por el chisme y las fiestas con Balas, y por darle clases de yoga y leerle cuentos a Elías.

A **Anabel, Chuc e Iñaki**, qué buenas fiestas, caray! Hay que recordar no ir al OXXO en domingo :D. Anabel, amiga, gracias por siempre estar ahí para escucharme, por regañarme, por siempre atacarte de la risa conmigo y por visitarme aun viviendo en otro continente! Te quiero! Iñaki, gracias por los fritos con salsa, las enchiladas, las películas, las largas conversaciones y muchísimo más que no acabaría de escribir aquí ☺. **Hernán (Treviño)**, nuestras sesiones de recorte son sanadoras, aunque ya perdí la cuenta de los tickets al infierno que tenemos acumulados. Cernán y Marranilla 4eva!

Thanks to **my lovely paranymphs**, Adam and Jouke, for agreeing to stand next to me for one boring hour :D . **Adam**, what can I say? You have been there since the very beginning. We had SO. MUCH. FUN! Thank you for the countless laughs, the numerous drinks and dinners, the crazy dancing and the great music. Thank you for all the deep conversations and for understanding my frustrations. You've been gone for only 2 months and I already miss you! **Jouke**, as cheesy as it may sound, one of the best things that happened to me during this PhD was meeting you. You are an awesome friend. I truly enjoyed our lunch walks, taking courses and organizing things together, but mostly the dinners in the Pieter de Swartstraat, making pizza, camping (and partying!) at Oerol and Texel, sailing, dancing and laughing (a lot!). I will never forget you sneakily decorated my place with Lucía to cheer me up when I came back from México. Love you, my friend!

Aan de familie Roghair, dank jullie wel voor alle "Family Fun" en jullie steun. Ik kijk uit naar nog meer verjaardagsfeestjes, Sinterklaasvieringen en familieweekendjes.

A la **familia Rodríguez** y a la **familia Arredondo**, gracias por siempre estar al pendiente de mí y de mi familia, y por los buenos momentos cuando voy a Monterrey! Los quiero mucho. Gracias a mi prima **Natalia**, que vino a visitarme a Leeuwarden. Me encantó viajar junto contigo!

A **mis papás:** nunca hubiera llegado a donde estoy si no fuera por ustedes. No tengo palabras para expresar cuánto los quiero y los admiro. La vida no podría haberme ofrecido mejores papás. Yo sé que el haber decidido iniciar el doctorado tan lejos fue muy difícil para todos, y a pesar de eso ustedes apoyaron mi decisión y todo mi camino. Gracias por su amor, su apoyo incondicional, su comprensión y por estar ahí para mí siempre. A **mis hermanos**, Hernán y Luisa, los quiero muchísimo! Gracias por las carcajadas y por aguantarme, y perdón por no poder estar ahí para ustedes lo suficiente. Gracias por ser tan buenos tíos!

To **Mark**, I love you. Thanks for putting up with me 24/7 (an admirable job on its own!), and for always waking up with a smile, rain or shine. With 2 PhDs to finish and a son to raise we did not have it easy, but we finally made it. Thanks for all your support, for your practical help with my thesis and for being a great dad to our son. A **Elías**, mi bebé (por siempre!), espero que algún día leas esto y estés orgulloso de mí. Te quiero con todo mi corazón!

Netherlands Research School for the
Socio-Economic and Natural Sciences of the Environment

D I P L O M A

For specialised PhD training

The Netherlands Research School for the
Socio-Economic and Natural Sciences of the Environment
(SENSE) declares that

Mariana Rodríguez Arredondo

born on 2 April 1987, Monterrey, Mexico

has successfully fulfilled all requirements of the
Educational Programme of SENSE.

Leeuwarden, 4 October 2019

The Chairman of the SENSE board

Prof. dr. Martin Wassen

the SENSE Director of Education

Dr. Ad van Dommelen

The SENSE Research School has been accredited by the Royal Netherlands Academy of Arts and Sciences (KNAW)

KONINKLIJKE NEDERLANDSE
AKADEMIE VAN WETENSCHAPPEN

The SENSE Research School declares that **Mariana Rodríguez Arredondo** has successfully fulfilled all requirements of the Educational PhD Programme of SENSE with a work load of 38.5 EC, including the following activities:

SENSE PhD Courses

- Environmental research in context (2013)
- Research in context activity: 'Co-organizing and chairing organizing committee of 7th European Summer School of Electrochemical Engineering (Leeuwarden, Netherlands – 22-26 June 2015)'

Other PhD and Advanced MSc Courses

- Bath Electrochemistry Winter School, University of Bath (2013)
- Workshop OLI stream analyzer, Wageningen University (2013)
- Masterclass Biobased innovation, Wageningen University (2013)
- PhD competence assessment, Wageningen Graduate Schools (2014)
- Pitch presentation training, Wageningen Graduate Schools (2014)
- Supervision of thesis students by PhD students, Wetsus (2014)
- Image editing and graphical abstract, Wetsus (2014)
- Techniques for writing and presenting a scientific paper, Wageningen Graduate Schools (2016)
- Career perspectives, Wetsus (2017)

Selection of Management and Didactic Skills Training

- Supervising two MSc students with internship (2014-2015), one MSc student with thesis (2015), and one BSc student with thesis (2017)
- Co-organizing the Wetsus Waterseed Recruitment Challenge (2015)
- Co-organizing the workshop 'Up-scaling of Bioelectrochemical Systems towards application' 10-11 March 2016, Leeuwarden, The Netherlands

Selection of Oral Presentations

- *Nutrient recovery from urine via struvite precipitation and ammonium recovery by a microbial fuel cell*. Applications of Bio-Electrochemical Systems in effluents, 14 February 2014, Seville, Spain
- *Ammonium transport, removal and recovery in current-driven processes.* 3rd European Meeting of the International Society for Microbial Electrochemistry and Technology (ISMET), 26-28 September 2016, Rome, Italy

SENSE Coordinator PhD Education

Dr. ir. Peter Vermeulen

This work was performed in the cooperation framework of Wetsus, European Centre of Excellence for Sustainable Water Technology (www.wetsus.eu). Wetsus is co-funded by the Dutch Ministry of Economic Affairs and Ministry of Infrastructure and Environment, the European Union Regional Development Fund, the Province of Fryslân, and the Northern Netherlands provinces. This work has also received funding from the European Union's Seventh Programme for research, technological development and demonstration under grant agreement No. 308535. The author would like to thank the partners of the Value*from*Urine consortium and the participants of the research theme "Resource Recovery" for the fruitful discussions and their financial support.

Financial support from both Wageningen University and Wetsus for printing this thesis is gratefully acknowledged.

Cover painting by Mariana Rodríguez Arredondo
Thesis design by Bregje Jaspers (ProefschriftOntwerp.nl)
Printed by ProefschriftMaken/Digiforce on FSC-certified paper